NUREG/CR--5215

TI90 001480

A Standard Problem for HECTR–MAAP Comparison: In–Cavity Oxidation

Manuscript Completed: August 1989
Date Published: October 1989

Prepared by
C. C. Wong

Sandia National Laboratories
Albuquerque, NM 87185

Prepared for
Division of Systems Research
Office of Nuclear Regulatory Research
U.S. Nuclear Regulatory Commission
Washington, DC 20555
NRC FIN A1246

ABSTRACT

To assist in the resolution of differences between the NRC and IDCOR on the hydrogen combustion issue, a standard problem has been defined to compare the results of HECTR and MAAP analyses of hydrogen transport and combustion in a nuclear reactor containment. The first part of this problem, which addresses the question of deflagration in the upper and lower compartments , was presented in NUREG/CR-4993 . The second part of this problem has been completed and is discussed in this report. This part addresses the issue of in-cavity oxidation of combustible gases produced by core-concrete interactions and the natural circulation between the reactor cavity and the lower compartment. HECTR analyses of the problem show that it is overly optimistic to assume a complete oxidation in the reactor cavity because a variety of phenomena, such as steam inerting and oxygen transport by natural convection, may influence the degree of in-cavity oxidation that takes place. An incomplete in-cavity oxidation will lead to accumulation and combustion of hydrogen and carbon monoxide in the lower and upper compartments in the reactor containment. This deflagration generates a peak pressure of 384.2 kPa (55.72 psia) at 7.36 hours.

CONTENTS

LIST OF FIGURES

LIST OF FIGURES
(continued)

LIST OF FIGURES
(continued)

LIST OF TABLES

ACKNOWLEDGMENTS

This work was supported by the U. S. Nuclear Regulatory Commission under the direction of Dr. Patricia Worthington. Her interest and concern about the hydrogen combustion issue led to the development of this standard problem. Many thanks to Bob Palla of NRC for numerous discussions related to this subject, to Marty Plys of Fauske and Associates for providing information about the combustion model in MAAP, and also to Dave Bradley of Sandia National Laboratories for performing the CORCON calculations. The author also acknowledges Marshall Berman, Susan Dingman, and Douglas Stamps of Sandia National Laboratories for their review of and comments on this report.

EXECUTIVE SUMMARY

Sandia National Laboratories, with the support of the U. S. Nuclear Regulatory Commission, developed the HECTR code to analyze the transport and combustion of hydrogen during reactor accidents. IDCOR developed the MAAP code to perform similar analyses. Both of these codes are lumped-parameter codes, but they differ in the way that various phenomena are modeled, especially in the areas of (1) ignition criteria, (2) flame propagation criteria, (3) burn time, (4) combustion completeness, (5) continuous in-cavity oxidation of combustible gases from core-concrete interactions, and (6) natural circulation. In order to assist in the resolution of differences between the NRC and IDCOR on the hydrogen combustion issue, a standard problem was defined to compare the results of HECTR and MAAP analyses of hydrogen transport and combustion in a nuclear reactor containment. This standard problem is an S2HF accident sequence in a PWR ice-condenser containment. The objective of this comparison is to determine the impact of the modeling differences for risk assessment.

There are two parts to this standard problem. The first part, which addresses the question of deflagration in the upper and lower compartments, was presented in an earlier report, "A Standard Problem for HECTR-MAAP Comparison: Incomplete Burning." The second part, which concentrates on the questions of natural circulation between the reactor cavity and lower compartment and continuous oxidation of combustible gases in the reactor cavity, is discussed in this report.

For the second part of the standard problem, the oxidation of combustible gases in the reactor cavity is a complex process that requires detailed study of the combustion phenomenon at temperatures above 1000 K. In the past, accident analysts studying containment responses with respect to hydrogen combustion either neglected the in-cavity oxidation process by assuming no reaction or simplified the process by assuming a complete reaction as in the IDCOR analysis. HECTR analysis of the standard problem shows that it is overly optimistic to assume a complete in-cavity oxidation because a variety of phenomena, like oxygen transport and steam inerting, may influence the degree of in-cavity oxidation. Accumulation and subsequent combustion of hydrogen and carbon monoxide in the upper and lower compartments generate a peak pressure of 384 kPa (56 psia) at 7.4 hours that IDCOR analysis (MAAP) did not predict. The calculated peak pressure by MAAP was 336 kPa (48.73 psia) at 18.0 hours and was caused by steam overpressurization.

The HECTR analysis also shows that neglecting any oxidation in the reactor cavity may not be a conservative assumption in terms of the pressure loading on containment. Pressure generated from the global burn in the lower and upper compartments could be higher for the case with partial in-cavity oxidation than for the case with no in-cavity oxidation under similar conditions as in the standard problem. In those severe accidents in which the deliberate ignition system is functioning, the peak-to-initial pressure ratios from combustion are almost the same, since the ignition criteria for these cases in HECTR are set at 7% hydrogen concentration. However, a higher pressure is predicted because the initial containment pressure before ignition is higher. The partial oxidation of combustible gases in the cavity increases the baseline pressure in the containment. Then when ignition occurs in the lower compartment, it raises the total peak pressure and makes it higher.

It can be concluded from other observations of the HECTR results that it is very important to model the lower compartment with an adequate number of control volumes. Using five control volumes to represent the lower compartment, HECTR results show that the lower compartment is not well mixed and that the natural convective current into the cavity is lower than the prediction when one control volume represents the lower compartment. In disagreement with the single volume model, the five-control-volume model predicts an incomplete in-cavity oxidation. This leads to an accumulation and subsequent combustion of combustible gases in the upper and lower compartment and generates a higher peak pressure.

1. INTRODUCTION

Sandia National Laboratories developed the HECTR (Hydrogen Event: Containment Transient Responses) code primarily to analyze the transport and combustion of hydrogen during reactor accidents [1, 2]. IDCOR (Industry Degraded Core Rulemaking Program) uses the MAAP (Modular Accident Analysis Program) code [3] to perform similar analyses. Both of these codes are lumped-parameter codes, but they differ in the way that various phenomena are modelled, especially in the areas of (1) ignition criteria, (2) flame propagation criteria, (3) burn time, (4) combustion completeness, (5) continuous oxidation of hydrogen and carbon monoxide in the reactor cavity, and (6) natural circulation. These differences will give different predictions of pressure and temperature loadings imposed on the containment and equipment by the accumulation and combustion of hydrogen during a severe accident. We are trying to determine the impact of these differences and to assist the NRC in determining the acceptability of the models for performing risk assessments.

The listed modeling differences are particularly pronounced in multicompartment systems such as the Ice-Condenser (IC) and Mark III containments. HECTR calculations tend to allow higher concentrations of hydrogen to develop, which leads to the prediction of higher containment pressures and temperatures. HECTR also permits flames to propagate into the IC upper plenum region, where potentially detonable mixtures can develop for some accident scenarios (e.g., TMLB'). Flame propagation into the upper compartment is also possible in the HECTR model, and the global burns which ensue generate much higher pressures than burns restricted to the lower compartment. MAAP code calculations generally do not predict these effects.

In order to resolve differences between the NRC and IDCOR on the hydrogen combustion issue, a standard problem was defined to compare HECTR and MAAP analyses of hydrogen transport and combustion in a nuclear reactor containment. The important phenomena to be addressed include: (1) natural circulation between the reactor cavity and lower compartment, (2) continuous oxidation of combustible gases in the reactor cavity, and (3) incomplete burning in the lower and upper compartments. The problem selected is an S2HF accident sequence in a PWR ice-condenser containment, Figure 1. The selection of the S2HF accident sequence is for code comparison only.

In this topical report, two of these phenomena, natural convection and continuous in-cavity oxidation of combustible gases with respect to containment failure during a core-melt accident, will be discussed. The first part of the standard problem which addresses the incomplete burning of hydrogen in the

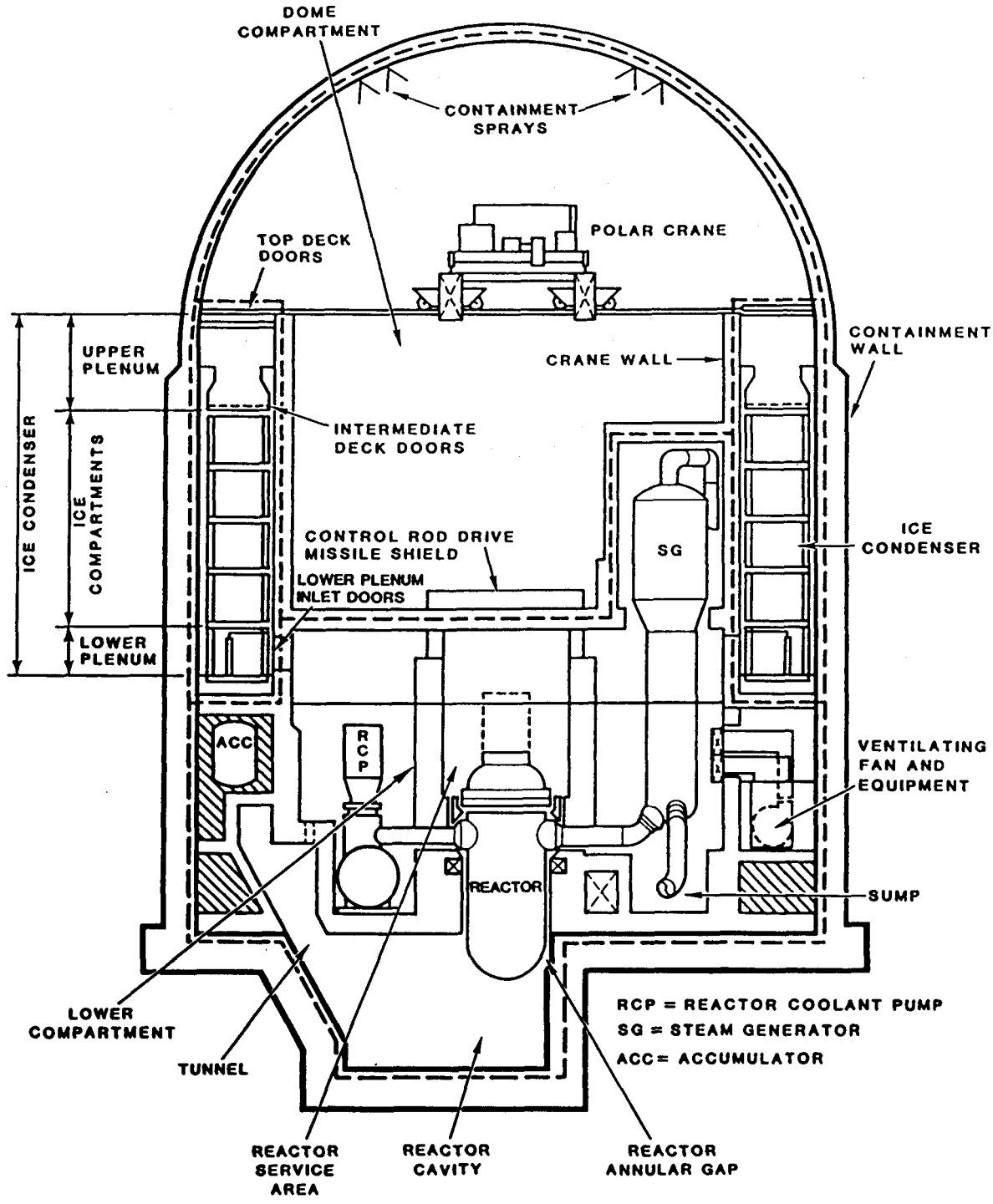

Figure 1. Simplified Diagram of Ice-Condenser Containment.

upper and lower compartment, has been completed and presented in a different topical report [4].

Analyses of the second part of the standard problem show that HECTR and MAAP gave different predictions of gas transport between the reactor cavity and lower compartment and also the in-cavity oxidation process. MAAP predicts that a complete oxidation of combustible gases would occur in the reactor cavity, hence no combustible gases would accumulate in the upper or lower containment in the early part of the transient. Pressures exceeding the estimated failure pressure for the containment occurs at a much later time (about 26 hours) because of steam-overpressure. On the contrary, HECTR predicts that the in-cavity oxidation process is limited by the rate at which oxygen is transported into the reactor cavity region. An incomplete in-cavity oxidation will occur and this results in accumulation and subsequent combustion of hydrogen and carbon monoxide in the upper and lower compartment. This deflagration generates a much higher peak pressure than the MAAP analysis at an earlier time.

2. DESCRIPTION OF THE HECTR-MAAP STANDARD PROBLEM

The S2HF accident scenario involves a small break (0.5 to 2-in. diameter) loss-of-coolant accident with failure of emergency coolant and containment-spray recirculation. All of the water inventory from the sprays (which are only operated in the injection mode) is trapped in the upper compartment due to the failure to remove upper-to-lower-compartment drain plugs. This failure causes the reactor cavity to remain dry throughout the transient. Incomplete hydrogen burns resulting from hydrogen released prior to reactor vessel failure that are initiated by the deliberate ignition system will occur in the lower and upper compartments. When the reactor vessel fails, the molten fuel slumps onto the floor of the cavity and results in core-concrete interactions. These interactions generate a substantial amount of combustible gases which may oxidize continuously in the reactor cavity. The stability of this continuous in-cavity oxidation strongly depends on the amount of oxygen present in the reactor cavity and the concentrations of steam, CO_2 and other diluents. A complete in-cavity oxidation will prevent any accumulation of combustible gases in the lower and upper compartments and minimize the threat to containment integrity due to combustion.

Because our main objective is to assess the importance of modeling differences of hydrogen transport and combustion in the HECTR and MAAP codes, the sources (either steam or any noncondensible gases) and initial conditions predicted by the MAAP code were put into HECTR to study the containment response. Moreover, for better comparison of both computer codes, we redefined the standard problem into a two-part transient problem in October 1985 [5]. The first part of the transient problem will study hydrogen behavior during the period of in-vessel hydrogen production (from the metal-water reaction) and the second part will cover hydrogen behavior during the period of ex-vessel hydrogen production (from core-concrete interactions). By setting up the standard problem this way, any discrepancies of the results between HECTR and MAAP in the first part of the problem will not affect the second part.

The first part of the standard problem, which addressed the incomplete burn in the lower and upper compartments during the early part of the accident, has been completed and presented in a different report [4]. This report concentrates on the second part of the problem, which begins shortly after the vessel breach. After the vessel breach, the molten core slumps onto the floor of the dry cavity; the hot molten fuel will interact with the concrete and generate a substantial amount of hydrogen, steam, carbon monoxide, and carbon dioxide. Since these hot gases are released at such a high temperature, the combustible gases are assumed to autoignite and oxidize to form combustion products according to the IDCOR analysis [6]. Hence, this will prevent any accumulation of combustible gases in the lower and

upper compartments and minimize any threat to containment integrity due to potential hydrogen/carbon monoxide combustion. Questions to be addressed in the second part of the standard problem are: (1) whether the gas mixture in the reactor cavity is hot enough to sustain the in-cavity oxidation process, (2) whether the natural convective flow into the cavity region will supply sufficient oxygen for a complete in-cavity oxidation, and (3) whether the steam content is large enough to preclude any in-cavity oxidation.

MAAP analysis of the S2HF drain-closed accident in a PWR ice-condenser containment [6] shows that after the vessel breach at 2.34 hours, the molten corium falls onto the floor of the dry cavity. Immediate concrete ablation occurs due to "jet" attack during the corium blowdown. Following the corium blowdown, water from the cold leg accumulator and remaining vessel inventory is discharged into the cavity through the breach location. The discharged water quenches the molten corium in the reactor cavity. This prevents any further core-concrete interactions and generation of noncondensible gases.

For a period of about 2.14 hours, the condition in the reactor cavity is very stable; there is no core-concrete interaction and no generation of noncondensible gases. Gradually the corium begins to heat up again and all the water boils away by the decay heating from the molten corium in the cavity. At 4.86 hours, the molten corium thermally attacks the concrete basemat generating substantial amounts of steam and carbon dioxide. No combustible gas is generated until 5.2 hours because the corium is not hot enough to initiate any molten metal-steam or molten metal-carbon dioxide reactions. MAAP predictions of the release rates of hydrogen, steam, carbon monoxide, and carbon dioxide from core-concrete interactions are plotted in Figures 2 to 5.

The release rates and thermal conditions of the noncondensible gases produced from the core-concrete interactions are two of the required boundary conditions provided by the MAAP code for HECTR analysis of the second part of the standard problem. Two other boundary conditions, heat transfer from the corium to the wall by radiation and heat transfer from the corium to the bulk gas environment in the cavity by convection are equally important in this analysis, as shown in Figures 6 and 7.

Since HECTR uses the initial and boundary conditions generated by the MAAP code, the following HECTR results do not represent our best estimate of the pressure and temperature responses of an ice-condenser containment during an S2HF accident. These HECTR analyses are only designed to better understand differences in the combustion models between two computer codes.

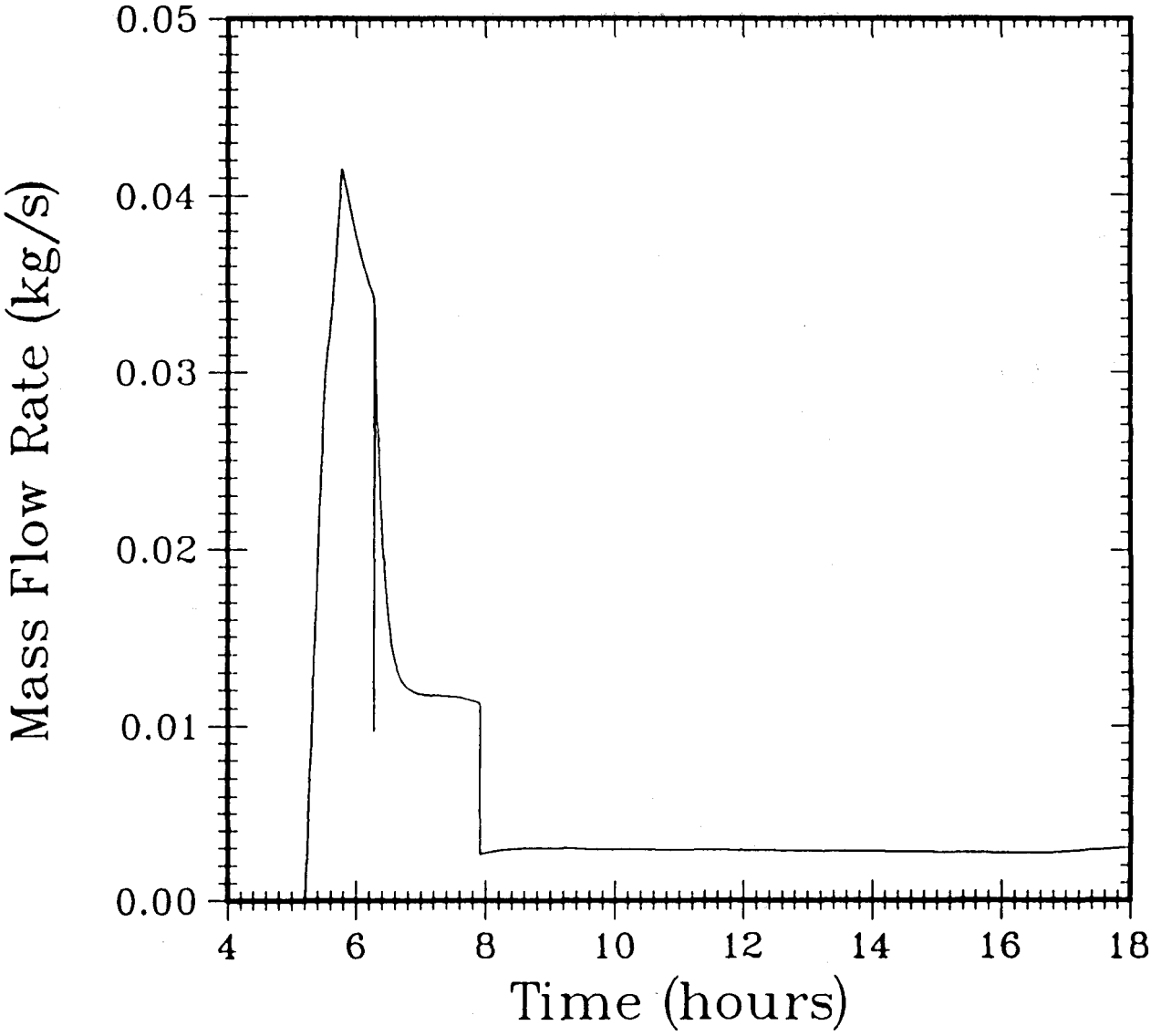

Figure 2. Hydrogen Release Rate from Core-Concrete Interactions Predicted by MAAP

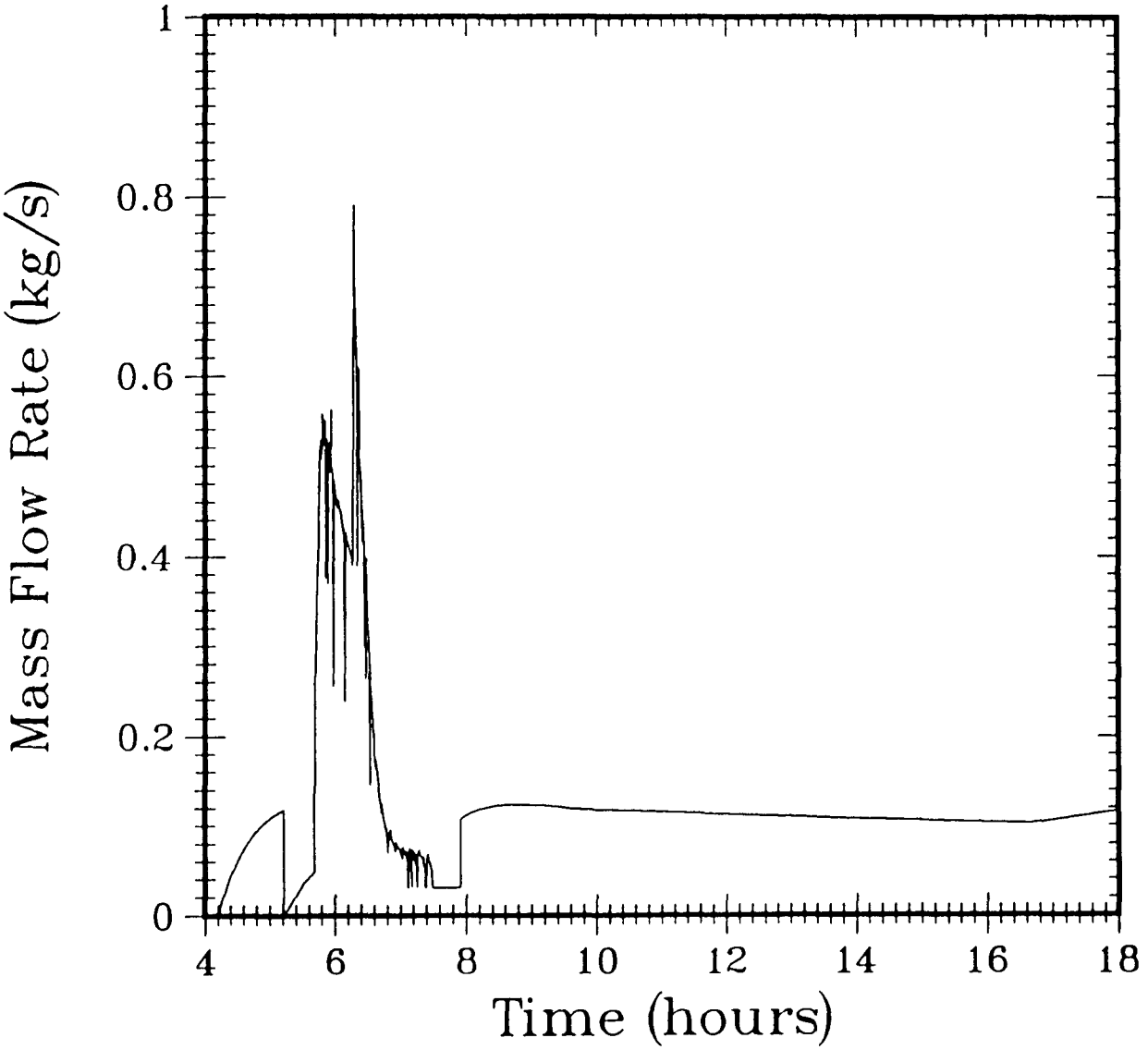

Figure 3. Steam Release Rate from Core-Concrete Interactions Predicted by MAAP

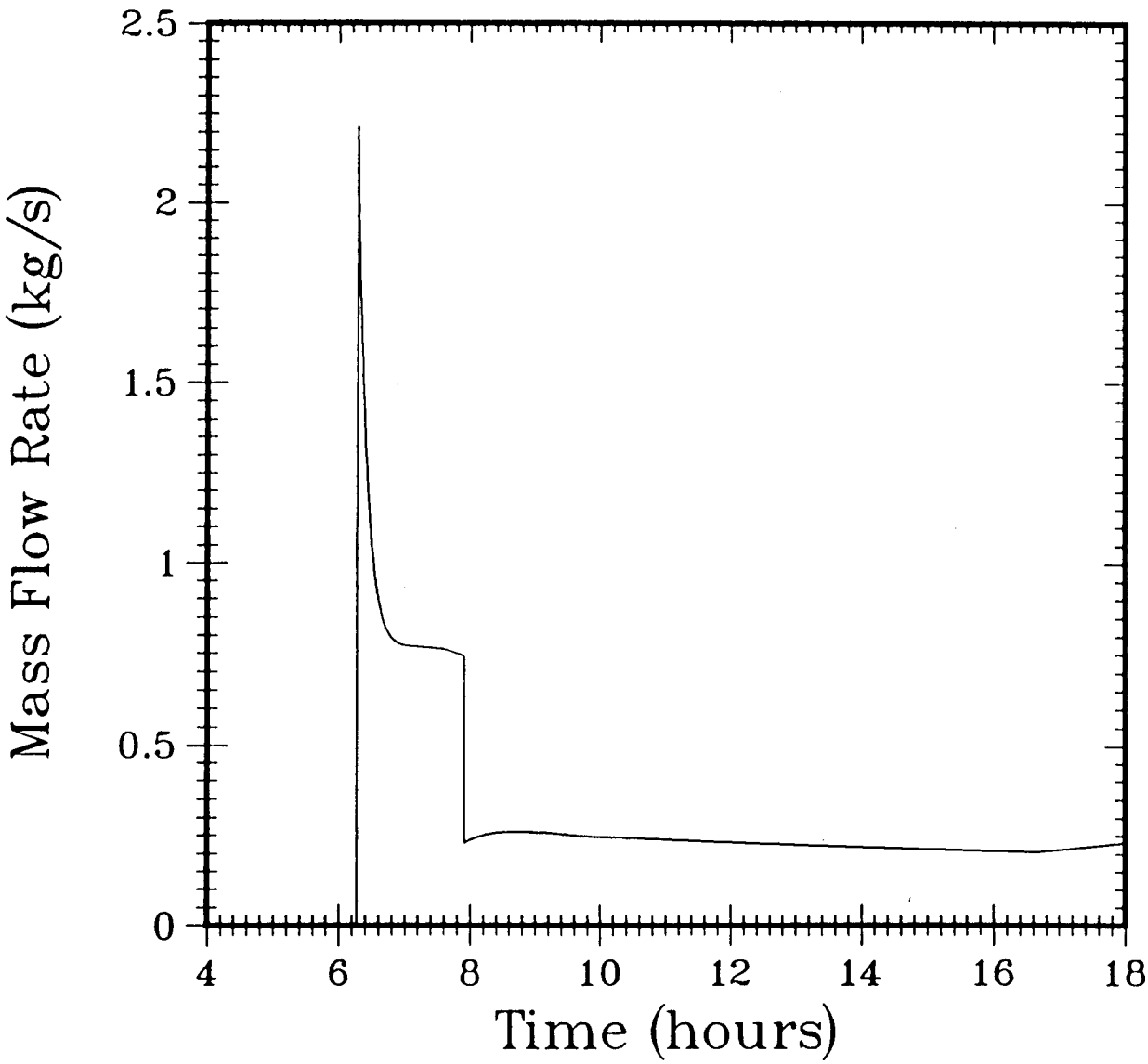

Figure 4. Carbon Monoxide Release Rate from Core-Concrete Interactions Predicted by MAAP

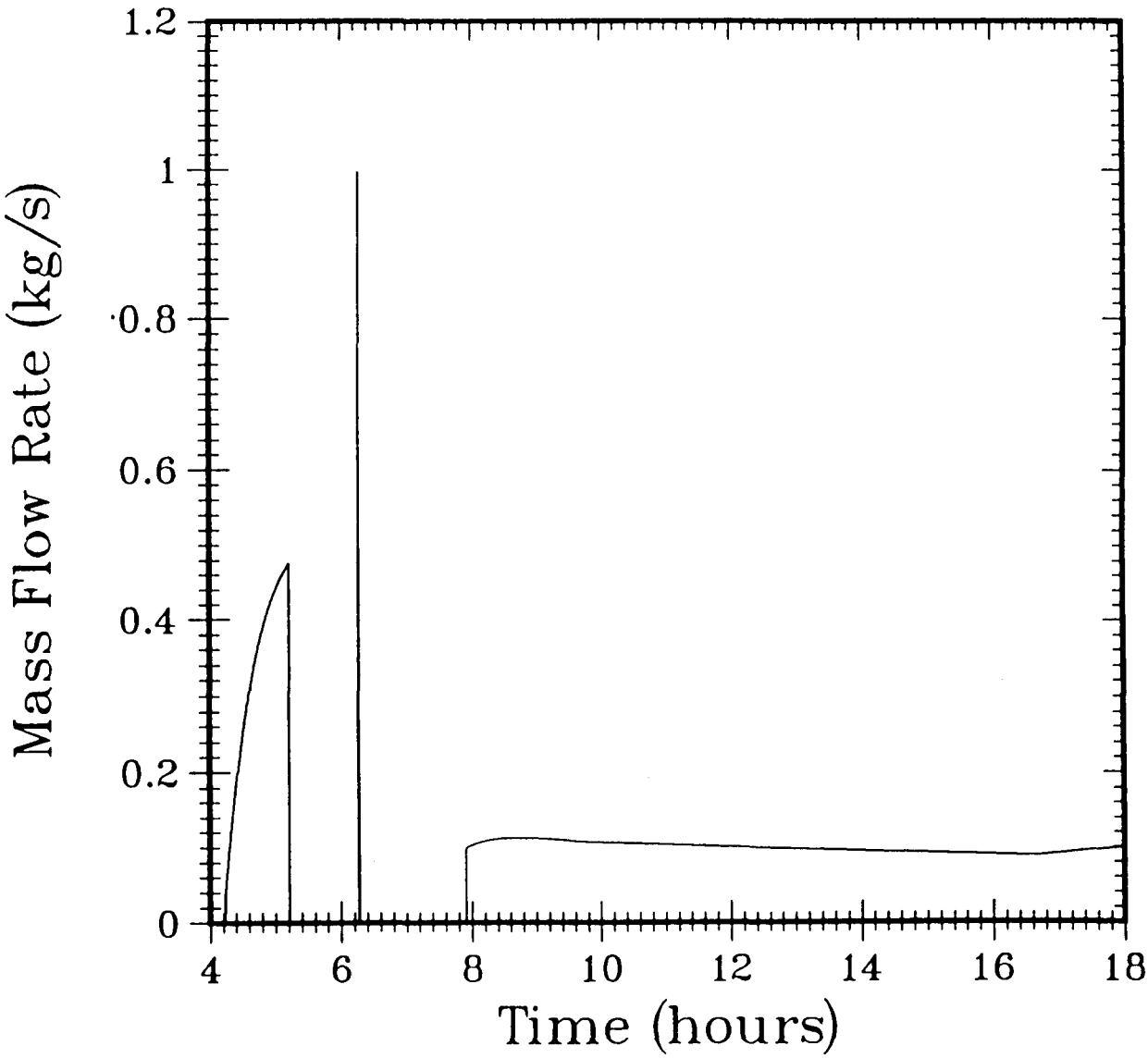

Figure 5. Carbon Dioxide Release Rate from Core-Concrete Interactions Predicted by MAAP

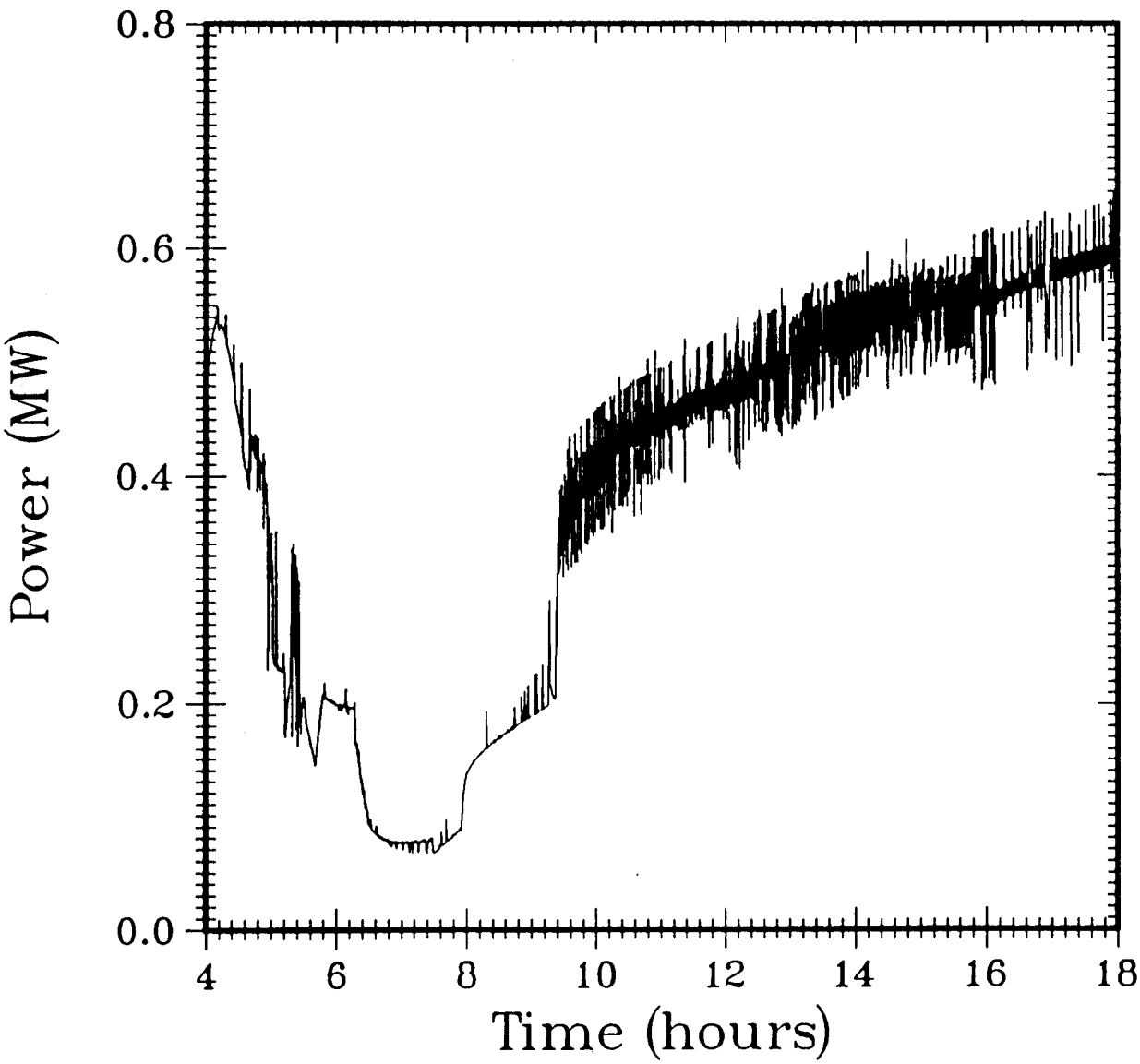

Figure 6. Heat Transfer Rate from the Corium to the Bulk Gases in the Reactor Cavity by Convection Predicted by MAAP

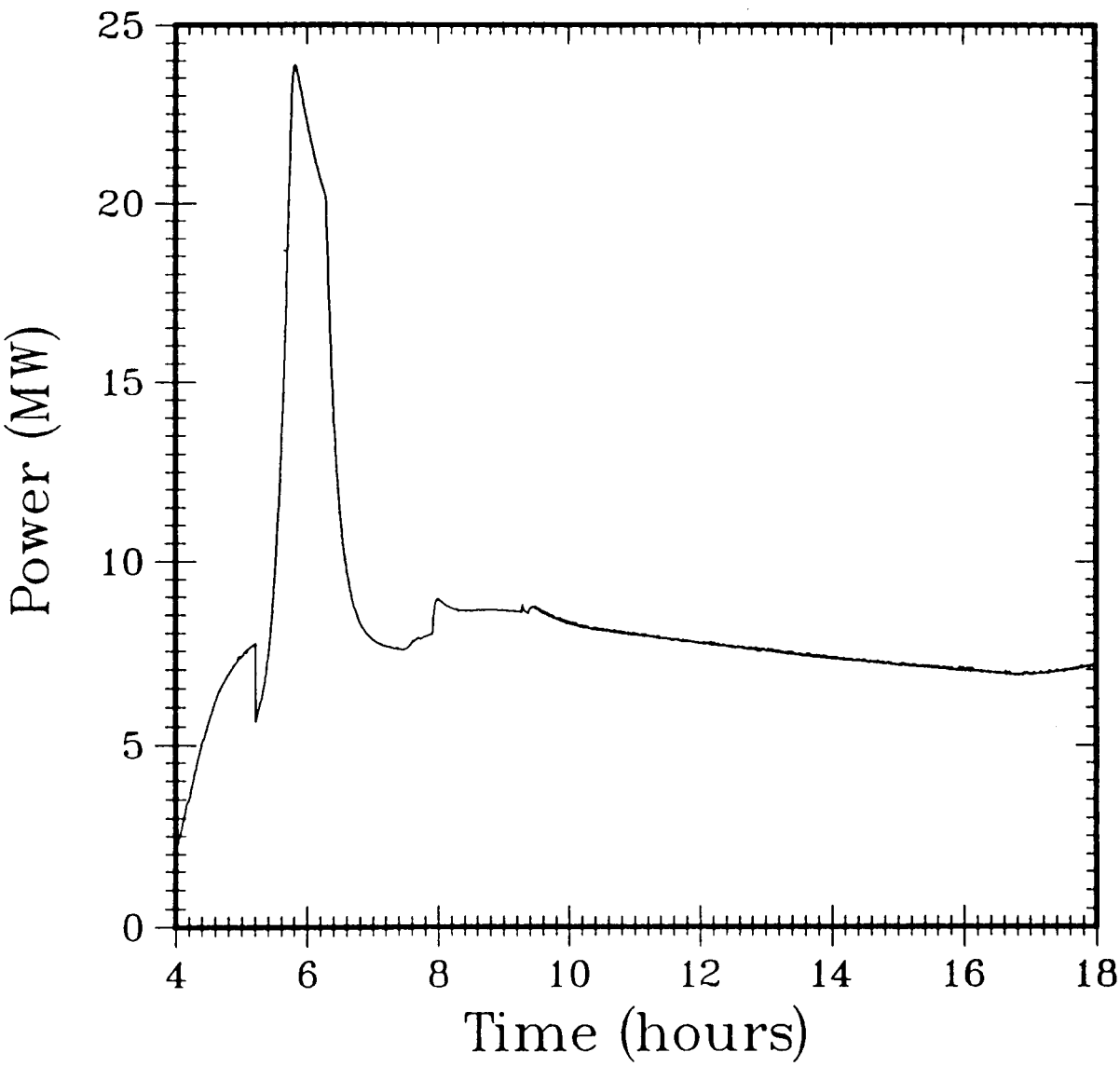

Figure 7. Heat Transfer Rate from the Corium to Walls in the Reactor Cavity by Radiation Predicted by MAAP

3. MODELING DIFFERENCES BETWEEN HECTR AND MAAP

Before presenting HECTR analyses of the second part of the standard problem, a review of the gas transport and continuous burning models used in HECTR and in MAAP would be useful. Since the discrete-burning model has been reviewed in the other report [4], this report will emphasize the modeling differences of the gas transport mechanism (especially the natural circulation flow between the reactor cavity and lower compartment) and the in-cavity oxidation process.

3.1 Natural Convection

Neither HECTR nor MAAP solves the complete Navier-Stokes equations for the flow between the lower compartment and reactor cavity. In HECTR, the momentum equation for predicting flow at the junction between compartments is governed by the pressure difference, gravity effect due to density differences, inertia effect, and frictional losses with respect to walls and area changes. (More description of the governing momentum equation can be found in Appendix A of Reference 2). The following assumptions were made when formulating and solving the momentum equation in HECTR: (1) flow at the junction is low speed, (2) molecular diffusion is neglected, (3) any turbulence effects are minimal. For modeling gas transport in a nuclear reactor containment, HECTR has been found to be reasonably accurate [7, 8, 9].

In MAAP, material transport is driven by forced convection due to pressure difference and by buoyancy effect. Two separate equations are written to model material transport between compartments. The first governing equation for the flow driven by the pressure differences is:

$$P_i = \sum_k \pm \frac{\partial P_i}{\partial W_k} W_k + P_{eq} \qquad \text{(Eqn. 2.1)}$$

where P_i is the pressure to be equalized to the final equilibrium pressure P_{eq}.

W_k is the mass flow rate at the junction driven by the pressure difference across the junction.

and plus and minus signs represent the flow exiting from and entering into compartment i.

The second equation is written for the natural circulation loop which balances the density difference with friction loss within the loop. The governing equation is:

$$\Delta P_j = \sum_k \pm \frac{C|w|wV}{2A^2} \qquad \text{(Eqn. 2.2)}$$

where ΔP_j is the loop buoyancy obtained by integrating $g\Delta z/V$ around the loop.

w is the mass flow rate of the circulation loop j driven by the density gradient along the flow path.

and V and A are the specific volume of the gas mixture and junction area, respectively.

Since the gas flow between the lower compartment and reactor cavity is likely to be low speed (Mach number to be less than 0.4), it is reasonable to assume pressure distribution within the containment is approximately uniform; that is neglecting the dynamic pressure distribution and only considering the static pressure distribution. For those cases in which the temperature difference between two adjacent compartments is small, the dominant term that governs the flow between the lower compartment and reactor cavity becomes the buoyancy term. In addition if our interest is restricted to the steady state and quasi-steady state problem, the governing momentum equation in HECTR for predicting flow at the junction can be simplified to be as Equation 2.2. Obviously, if the above conditions do not hold, the governing momentum equations for solving flow between compartments in HECTR and in MAAP are quite different.

Even though in this problem the governing momentum equations for predicting the natural recirculation flow in HECTR and in MAAP are quite similar, there are differences in how the lower compartment is being modeled. For studying the natural convective flow between the lower compartment and reactor cavity, we recommend that at least five control volumes are needed to represent the lower compartment. However in MAAP, only one control volume is used to model the lower compartment. With one control volume, only the bulk-averaged conditions within the lower compartment (such as pressure, temperature, and gas composition) will be calculated by the code. Any detailed information within the lower compartment will be averaged out. In some cases, a single control volume for the lower compartment is adequate if the conditions within the lower compartment are well mixed. However in other cases, multi-control volumes are required because a well-mixed environment in the lower compartment may not exist. For example during a severe accident, when core-concrete interactions are taking place in the reactor cavity, the plume of hot gases (steam, burnt and unburnt gases), which are coming up from the reactor cavity through the tunnel into the lower compartment, may follow the forced-convective flow

path driven by the fans, and escape into the upper compartment through the ice region, instead of instantaneously mixing with other cooler gases in the lower compartment. Since the natural circulation flow between the reactor cavity and the lower compartment is primarily driven by the density gradient along the flow path, using a single control volume to represent the lower compartment which averages out the density variation within the lower compartment, may not be sufficient and may have difficulty in predicting an accurate circulation flow between the lower compartment and the reactor cavity.

3.2 In-Cavity Oxidation Process

The ability to accurately predict the degree of in-cavity oxidation is a difficult task because a variety of phenomena that take place in the cavity at the same time can have substantial influence on the process. Three key phenomena that contribute substantial uncertainties associated with high-temperature combustion will be considered here: (1) autoignition, (2) flammability limits at high temperature, and (3) characteristics of the diffusion flame in the cavity.

Autoignition of a combustible mixture without any ignition source requires a high gas temperature [10]. The gas temperature has to be above a critical temperature, known as the autoignition temperature [11]. For hydrogen and carbon monoxide in air at normal atmospheric pressure, the lowest autoignition temperatures measured are 833 and 878 K, respectively [10]. Autoignition temperature, however, depends on many parameters such as pressure, catalysts, oxygen, fuel and diluent gas concentrations.

During a severe accident such as an S2HF and with a dry cavity, heat released from the molten core, which has slumped onto the floor of the reactor cavity after the vessel breach, and heat from molten metal-water and molten metal-carbon dioxide reactions may be sufficient to initiate an autoignition, depending on the initial and boundary conditions [12]. However, in other cases such as a wet cavity without any hot surface, the temperature of the combustible mixture in the cavity may not be sufficiently high to autoignite. In order to determine whether autoignition will occur in the cavity, the autoignition temperature of the combustible mixture composed of hydrogen, air, steam, carbon monoxide, and carbon dioxide needs to be established. At present, the flammability limits of a hydrogen:air:steam:carbon monoxide:carbon dioxide mixture at high temperatures have not been well established because of insufficient experimental data [10, 13].

Once the ignition occurs in the cavity, either by autoignition or by some accidental source such as a hot surface, it is very difficult to determine whether this flame will be stable as a continuous combustion process. Substantial amounts of steam may be released into the reactor cavity when the vessel breaches and the core slumps onto the floor of the reactor cavity. The existence of a large quantity of steam acts as a diluent such that the standing flame may be highly unstable or may even be extinguished. Hence complete in-cavity oxidation may not occur.

In determining the criteria for autoignition of hot vapor jets/plumes, the MAAP code assumes that ignition occurs whenever the calculated jet/plume temperature exceeds a critical value of 1033 K (1400°F). HECTR is capable of simulating autoignition of hot mixtures as a user option, but on the basis of bulk gas average compartment temperature rather than jet/plume temperature. Once the ignition begins, MAAP allows the reaction to be continuous as long as there are sufficient oxygen molecules for reaction; steam has no effect - neither to slow the reaction rate nor to preclude any in-cavity oxidation. However, in HECTR, there are conditions to be checked at every time step to determine whether the reaction will continue; for example, steam inerting may preclude any reaction. Through user input, HECTR can terminate the in-cavity oxidation process for the following reasons: (1) bulk gas temperature is too low, (2) concentration of the combustible gases in the jet/plume is too low, (3) concentration of the diluent in the jet/plume is too high, (4) oxygen concentration in the burning compartment is too low, (5) steam concentration in the burning compartment is too high.

When analyzing the in-cavity oxidation process, HECTR as well as MAAP, do not model the comprehensive structure and characteristics of the diffusion flame such as the size of the diffusion flame, the possibility of the liftoff and blowoff. Premature quenching of the flame will prevent a complete oxidation of hydrogen and carbon monoxide in the cavity. Because most accident analyses use a coarse noding system for containment and an instantaneous chemical reaction for diffusion flame, hydrogen and carbon monoxide will react with oxygen to form steam and carbon dioxide, respectively, as soon as they are released to the environment. In reality, the gas mixture released from core-concrete interactions will rise up as a plume. The oxidation of combustible gases will carry on in the outer mixing-layer of the plume as a diffusive type of flame, and its rate will be controlled by the relative rate of diffusion of oxygen into the flame. An insufficient supply of oxygen, or the addition of steam to the atmosphere, will elongate the flame [14]. A large steam mole fraction is very likely to exist during core-concrete interactions. Hence the flame will probably be elongated, may exceed the height of the cavity, and extend out into the tunnel,

Fig. 8. If there is not sufficient oxygen for reaction, the flame will probably be extinguished at the tunnel. This will result in an incomplete in-cavity oxidation of hydrogen and carbon monoxide. Other considerations such as the instability of the flame, may also prevent a complete in-cavity oxidation, and will not be discussed in detail here; a general review can be found in Reference 15.

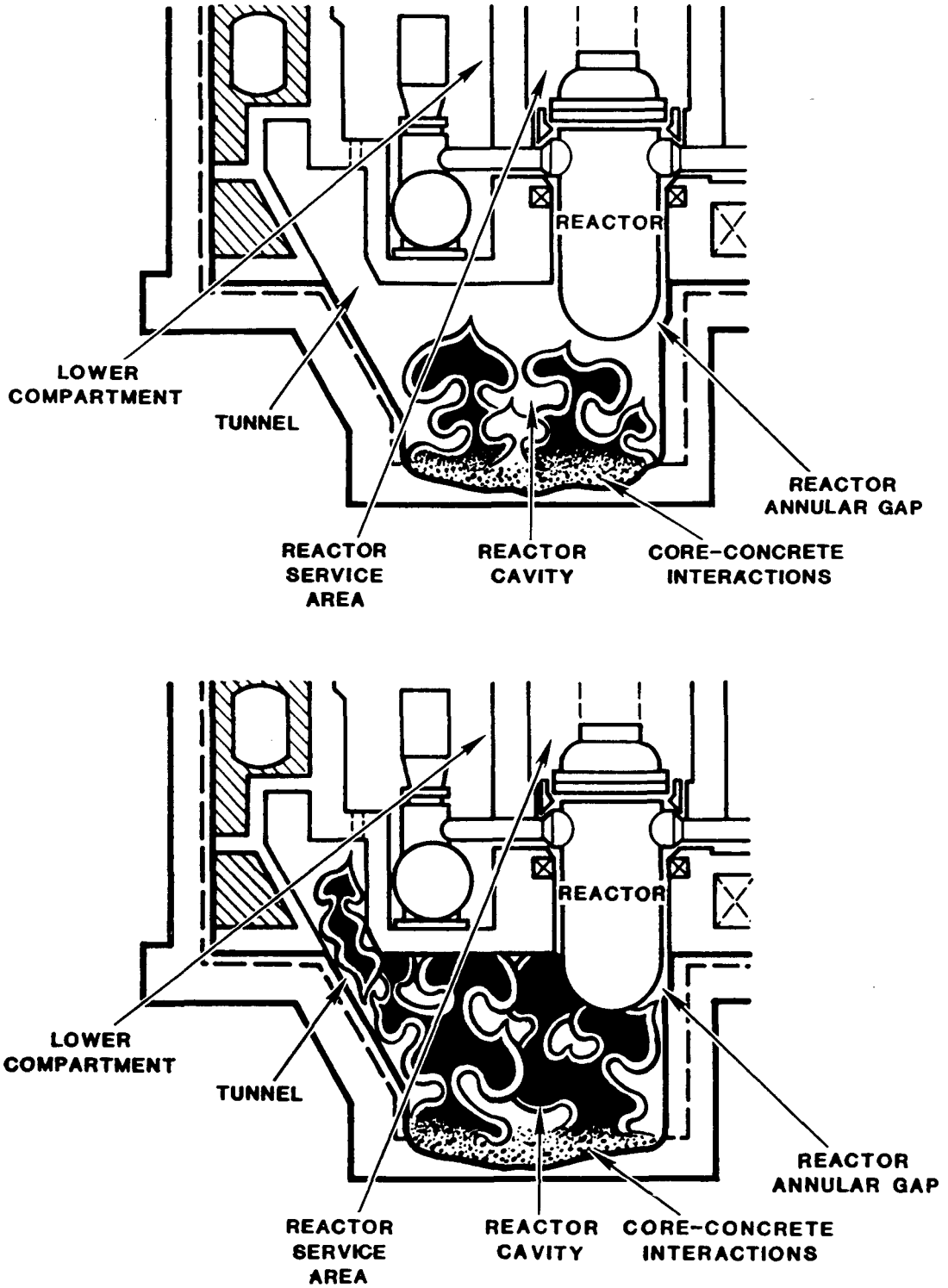

Figure 8. Schematic of In-Cavity Oxidation; Complete Oxidation (Top), Incomplete Oxidation (Bottom)

4. HECTR RESULTS OF THE STANDARD PROBLEM

In the following sections, HECTR analyses of the second part of the standard problem are presented and discussed in detail.

4.1 Modeling of the Reactor Containment

Three different noding systems were used to model the reactor containment (see Figure 9 and Appendix B). They are:

1. 12-compartment model with Sandia geometrical data.
2. 6-compartment model with Sandia geometrical data.
3. 6-compartment model with MAAP geometrical data.

Both 6-compartment models adopt the same noding system as in the MAAP code for the Sequoyah Ice-Condenser Containment [3, 6]. The differences between these two 6-compartment models are the geometrical data used in these calculations (Table 1). The MAAP geometrical data are those used in the MAAP analysis. The Sandia geometrical data were obtained either from the Final Safety Analysis Report of the Sequoyah Nuclear Power Plant [16] or from Reference 17. The major differences between these two data sets are the total free volume in the lower compartment, the total surface area, and the time delay for the air-return fans to be activated after the set-point is satisfied. Since substantial time and effort are needed to resolve these differences, the better and economic way to overcome this potential problem is to perform two calculations using different geometric data and determine the impact of the differences.

The 12-compartment model is extracted from the 40-compartment model used in Reference 18. Since in the second part of the standard problem, all the ice has melted, the effect of the recirculation flow in the ice bed region would be minimal. Therefore, using one control volume to represent the whole ice condenser is reasonable. However, in the lower compartment region, because our main objective is to accurately predict the natural circulation flow between the lower compartment and the reactor cavity, it is necessary to employ a finer noding system so that detailed information about the density and temperature distributions can be obtained.

In HECTR analyses of the second part of the standard problem, the problem starts at the time when core-concrete interactions begin (4.2 hours or 15044 seconds) and arbitrarily ends at 18 hours. At 4.2 hours, the air-return fans have been on for a long period of time and the containment spray system has failed because switching over to the recirculation mode is unsuccessful. Hence, the discrepancy with respect to the time delay for fan activation does not affect the outcome of this

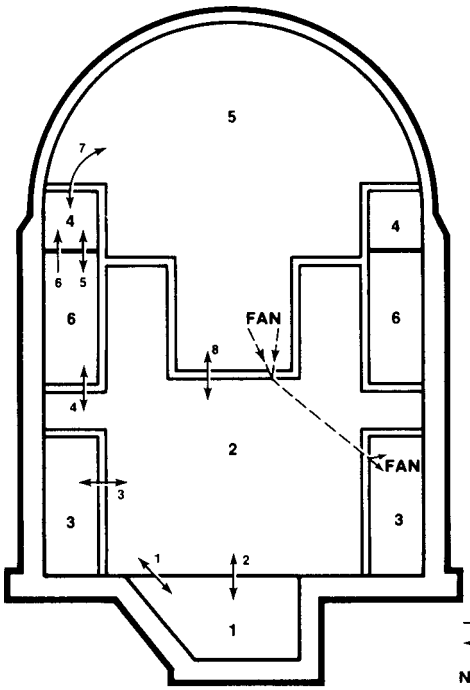

6-COMPARTMENT MODEL

COMPARTMENT DESCRIPTORS	ID NUMBER
UPPER COMPARTMENT	5
UPPER PLENUM	4
LOWER COMPARTMENT	2
DEAD-ENDED REGION	3
ICE COMPARTMENT	6
REACTOR CAVITY	1

KEY

1- COMPARTMENT NUMBER
1- FLOW JUNCTION NUMBER
→ ONE-WAY FLOW JUNCTION
↔ TWO-WAY FLOW JUNCTION

NOTE: IGNITERS PRESENT IN COMPARTMENTS 2, 3, 4, AND 5

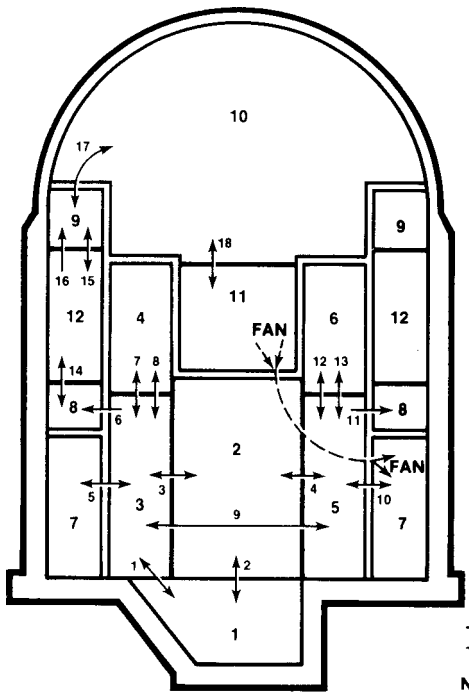

12-COMPARTMENT MODEL

COMPARTMENT DESCRIPTORS	ID NUMBER
UPPER COMPARTMENT	10, 11
UPPER PLENUM	9
LOWER PLENUM	8
LOWER COMPARTMENT	2, 3, 4, 5, 6
DEAD-ENDED REGION	7
ICE COMPARTMENT	12
REACTOR CAVITY	1

KEY

1- COMPARTMENT NUMBER
1- FLOW JUNCTION NUMBER
→ ONE-WAY FLOW JUNCTION
↔ TWO-WAY FLOW JUNCTION

NOTE: IGNITERS PRESENT IN COMPARTMENTS 2, 3, 5, 7, 9 AND 11

Figure 9. Containment Noding Systems used in HECTR Analyses of the Standard Problem (6-Compartment Model and 12-Compartment Model).

Table 1. Major Differences between HECTR and MAAP Input Data

	HECTR	MAAP
1. Reactor Cavity:		
Total Volume	396.0	419.09 m^3
2. Lower Compartment:		
Total Volume	6334 m^3	8184 m^3
Sump Area	59.2 m^2	502.6 m^2
Steel Area	5940 m^2	2780 m^2
Concrete Area	3569 m^2	1796 m^2
3. Annular Region:		
Sump Area	0	446.8 m^2
Steel Area	1834 m^2	0
Concrete Area	3257 m^2	1027 m^2
4. Upper Plenum:		
Steel Area	1000 m^2	0
5. Upper Compartment:		
Concrete Area	4085 m^2	3760 m^2
Steel Area	2000 m^2	1065 m^2
6. Ice Condenser:		
Wall Structure - Wt.	2.0×10^5 kg	-
- Area	2058 m^2	-
Baskets - Wt.	1.47×10^5 kg^2	-
- Area	9920 m^2	-
7. Air-Return Fans:		
Delay time	600 s	0.167 s
LC to Annular Region Vol. flow rate	1.17 m^3/s	0

standard problem. However, since the containment spray system is working in the injection mode before it fails to switch over to the recirculation mode, water will accumulate in various locations including the reactor refilling area. At the start of the second part of the problem, the HECTR input deck has been modified to reflect the accumulation of water in the sumps, which, in turn, decreases the gas-free volume of those compartments involved. In the original set-up of the compartment model, the compartment that models the reactor refilling area will be deleted because it is filled with water and becomes useless in our calculations. Therefore, only 12 compartments were used in the present calculations.

In the following discussion, the HECTR 6-compartment model using the MAAP geometrical data will be referred as the HECTR/MAAP 6-compartment model, while the HECTR 6-compartment and the HECTR 12-compartment model, respectively, will represent the 6-compartment and 12-compartment models using the Sandia geometrical data.

4.2 HECTR Default Calculations Using a 12-Compartment Model

The second part of the standard problem was performed using a modified version of HECTR 1.5. The added features in this version of HECTR are: (1) restart capability, (2) modification of the source input, (3) capability to read in external heat fluxes. These improvements were needed before any analysis of the second part of the standard problem could proceed. In HECTR version 1.5, the default ignition criterion for hydrogen combustion has been changed such that combustion will occur if the hydrogen mole fraction within a compartment is above 7 percent instead of 8% [2]

Since our objective is to study the impact of in-cavity oxidation on containment loadings and since HECTR does not model such a complex phenomenon in detail, we have performed parametric studies and bounding calculations. A 12-compartment model has been set up and bounding calculations have been performed such that (1) incomplete in-cavity oxidation will take place if there is insufficient oxygen (less than 5%) to support in-cavity oxidation or excess steam (more than 55%) to inert the environment, (2) complete in-cavity oxidation will occur if any oxygen exists in the reactor cavity regardless of the steam concentration, or (3) any in-cavity oxidation will not be allowed (Part I in Table 2). The criteria used in the first bounding calculation are based on the results of experiments to study the flammability of hydrogen:air:steam at a temperature less than 400 K [13, 19, 20]. Because the flammability limits expand and cover a larger range at temperatures greater than 400 K, a conservative approach uses the limits at a temperature of about 400K. On the other hand, excluding the effect of steam inerting would be an

Table 2. Criteria for In-Cavity Oxidation in the Reactor Cavity used in HECTR Analyses

Case Description	Mole Fraction			
	Completeness	Combustible Gases (H_2+CO)	O_2	Diluents (H_2O+CO_2)
Part I				
a. 12-Compartment Model	100%	> 0%	> 5%	< 55%
b. 12-Compartment Model	100%	> 0%	> 0%	< 100%
c. 12-Compartment	0%	-	-	-
Part II				
a. 12-Compartment Model	100%	> 0%	> 0%	< 100%
b. 6-Compartment Model	100%	> 0%	> 0%	< 100%
c. 6-Compartment	100%	> 0%	> 5%	< 55%

optimistic approach. The approach in (3) is similar to earlier severe accident analyses involving hydrogen combustion in which in-cavity oxidation of combustible gases from core-concrete interactions are totally neglected [17].

The results of the bounding calculations showed that in all cases combustible gases built up in the lower and upper compartments, which led to one or more global burns. These burns were all initiated in the lower compartment and eventually propagated into the upper compartment. Each of these global burns generated a substantial peak pressure above 285 kPa (41 psia).

In the first HECTR calculation (Case a of Part I in Table 2), the problem was set up such that in-cavity oxidation would take place as long as the oxygen concentration was above 5% and the steam plus CO_2 concentration was less than 55% in the cavity. When the debris bed began to dry up at 5.2 hours, most hydrogen generated from core-concrete interactions would completely oxidize in the reactor cavity. At 5.29 hours, a substantial amount of steam was built up in the cavity and it terminated the in-cavity oxidation, Fig. 10. Because of this steam inerting effect, HECTR estimated that less combustible gases would be reacted in the cavity and more combustible gases would build up in the lower and upper compartments. Three global burns were predicted, and their corresponding peak pressures were 285 kPa (41 psia) at 6.32 hours, 371 kPa (54 psia) at 6.98 hours, and 411 kPa (60 psia) at 9.12 hours, respectively, Fig. 11.

The second case (Case b of Part I in Table 2) was set up such that (a) continuous oxidation would take place in the reactor cavity as long as there was any oxygen, and (b) the steam inerting effect on in-cavity oxidation would be neglected. By neglecting steam inerting, more combustible gases would be reacted in the cavity. However, HECTR predicted that insufficient oxygen was transported into the cavity from the lower compartment to support complete in-cavity oxidation after 5.56 hours, Fig. 12. Continuous oxidation still occurred in the cavity after this time, but less complete. Combustible gases reacted with oxygen when it was available in the cavity. Since not all combustible gases reacted in the cavity, they accumulated in the lower and upper compartments. Ignition occurred at 7.36 hours and generated a peak pressure of 384 kPa or 56 psia, Fig. 13.

As in other severe accident analyses involving hydrogen combustion [17], the third case (Case c of Part I in Table 2) totally neglected the in-cavity oxidation of combustible gases from core-concrete interactions. Hence most of the combustible gases, hydrogen and carbon monoxide, would be convected up into

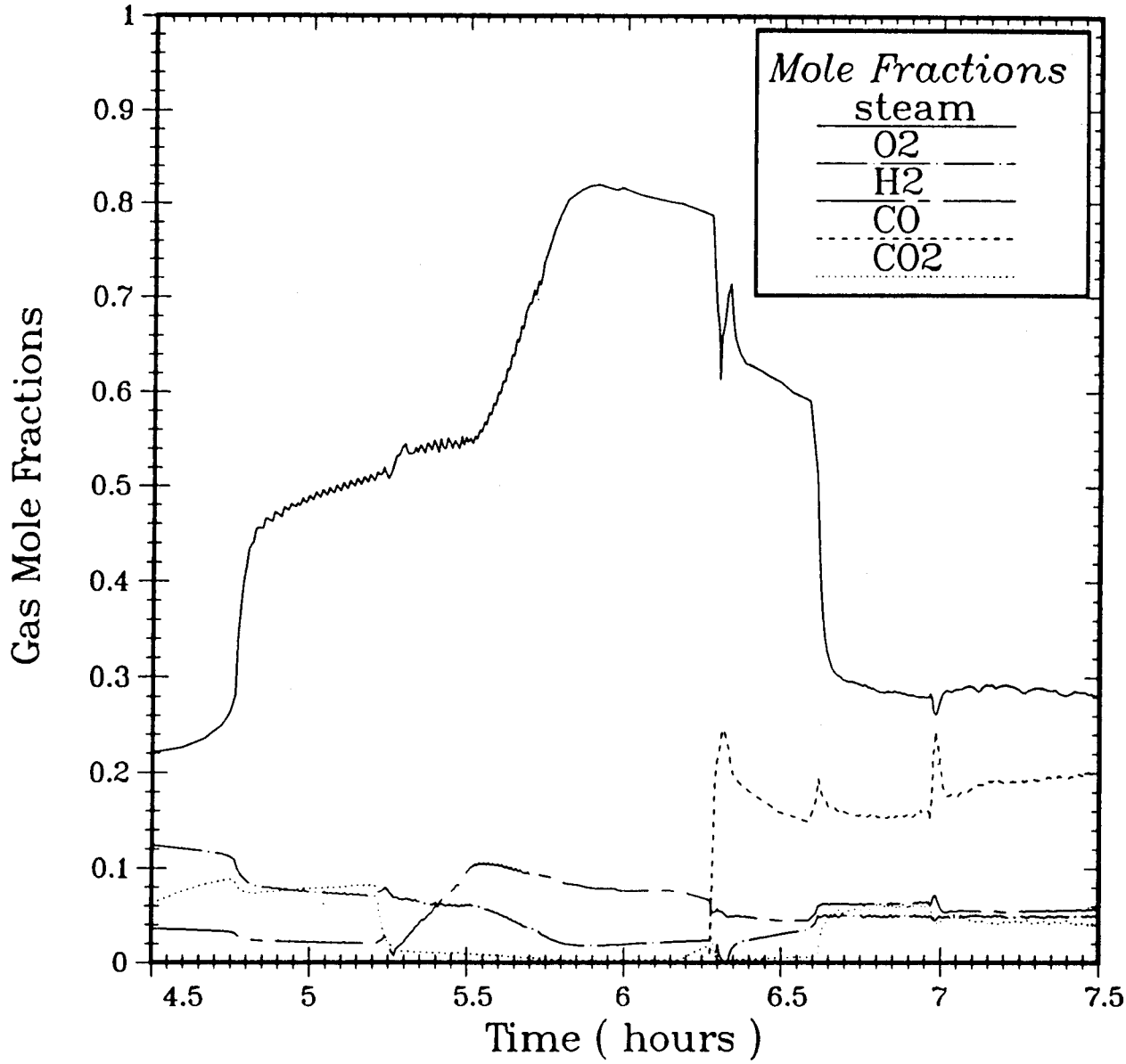

Figure 10. Gas Composition in the Reactor Cavity Predicted by HECTR (12-Compartment Model; Conditions for Continuous In-cavity Oxidation: $O_2 \geq 5\%$ and steam $\leq 55\%$).

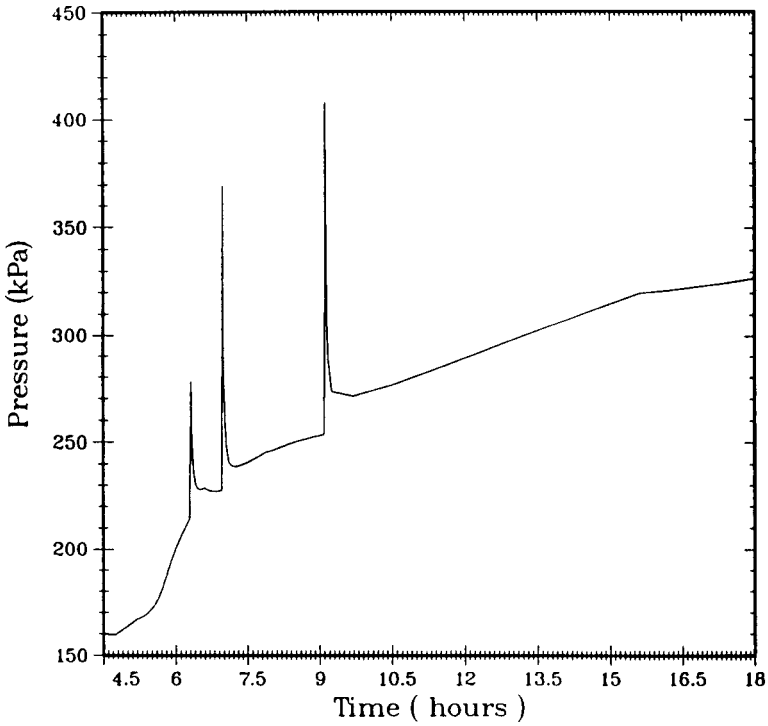

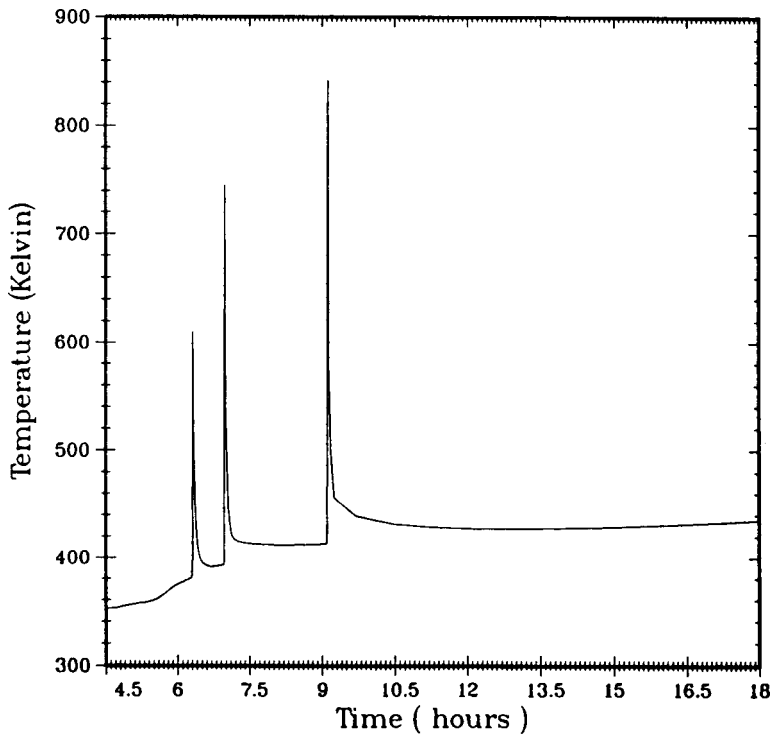

Figure 11. Pressure and Temperature Responses in the Upper Compartment Predicted by HECTR (12-Compartment Model; Conditions for Continuous In-cavity Oxidation: $O_2 \geq 5\%$ and steam $\leq 55\%$).

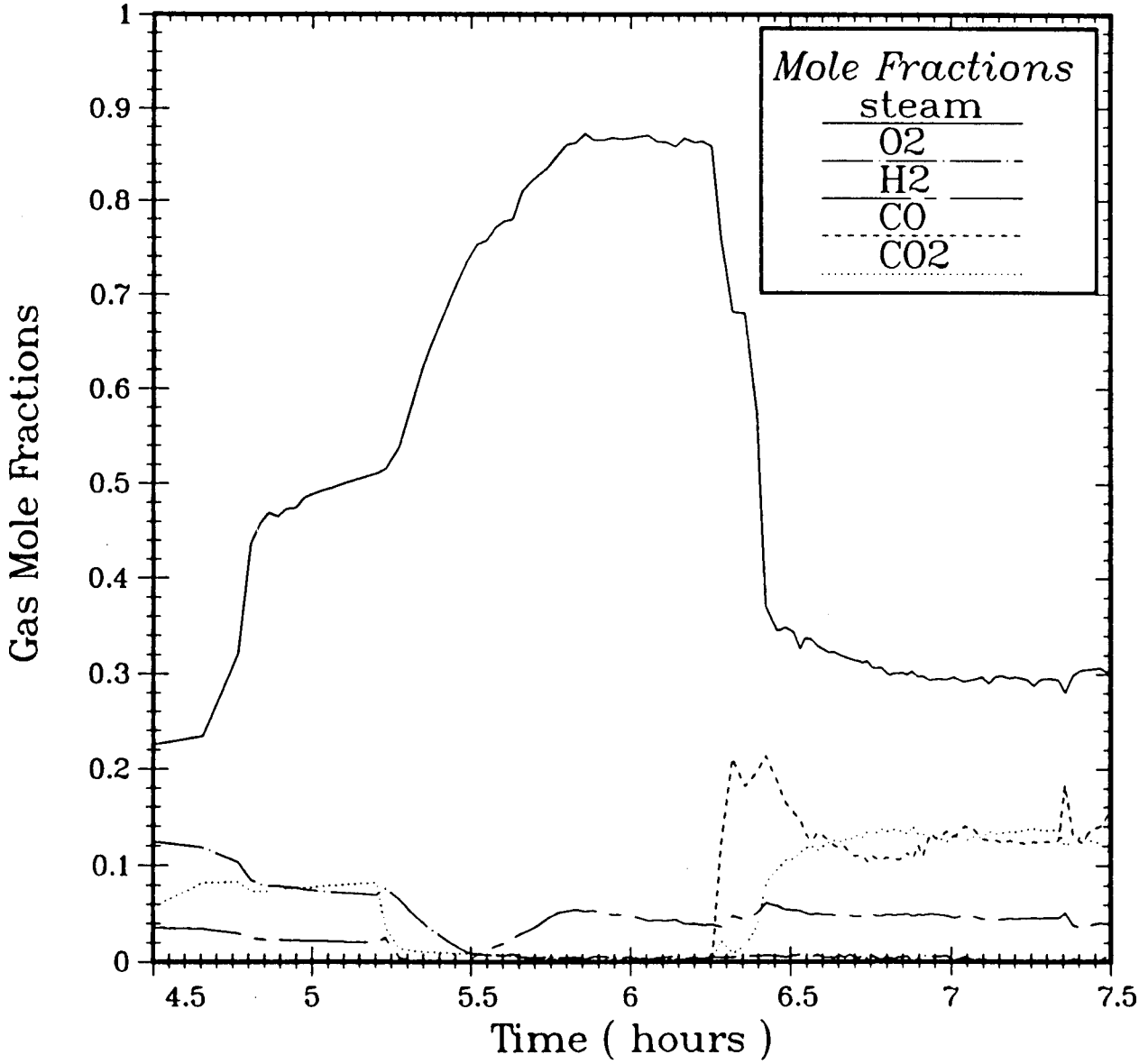

Figure 12. Gas Composition in the Reactor Cavity Predicted by HECTR (12-Compartment Model; Conditions for Continuous In-cavity Oxidation: $O_2 \geq 0\%$ and steam $\leq 100\%$).

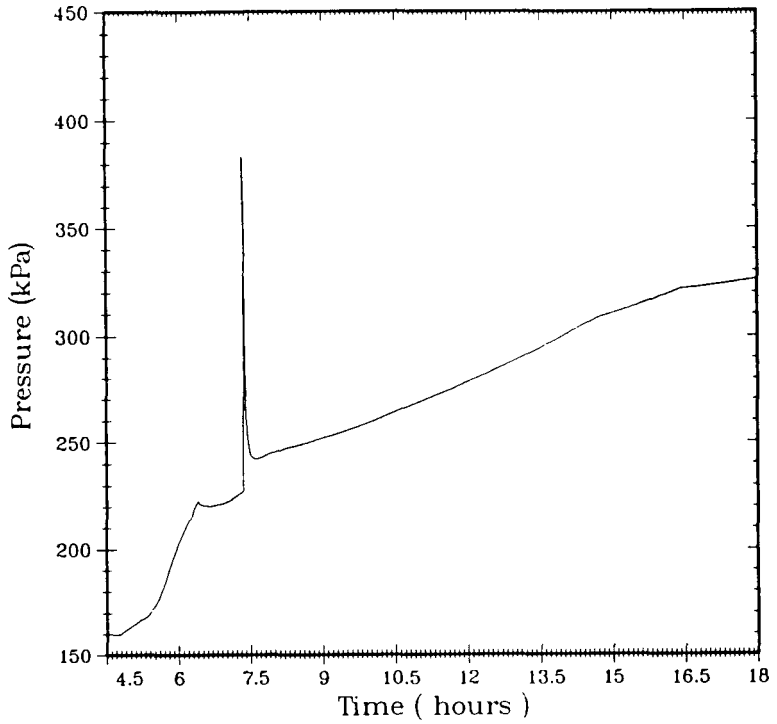

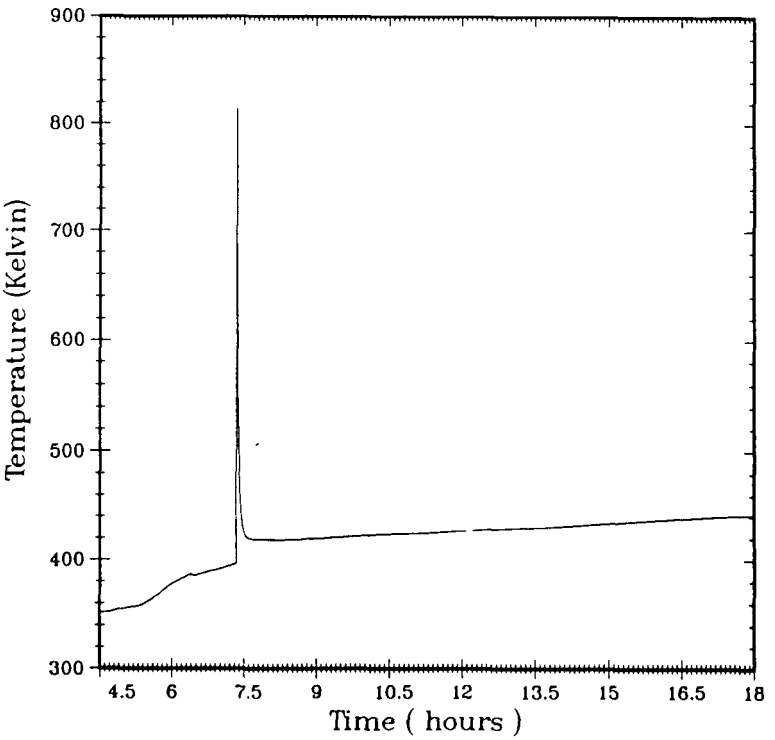

Figure 13. Pressure and Temperature Responses in the Upper Compartment Predicted by HECTR (12-Compartment Model; Conditions for Continuous In-cavity Oxidation: $O_2 \geq 0\%$ and steam $\leq 100\%$).

and accumulated in the lower and upper compartments, Fig. 14. Combustion occurred when the concentration of the mixture in these regions satisfied the ignition criterion. Four discrete burnings were predicted and the maximum peak pressure was 330 kPa or 48 psia, Fig. 15. The maximum peak pressure of the third case was relatively smaller than the first two cases, even though the ignition criteria in the upper and lower compartments were the same in all three cases. These differences in peak pressure between the three cases listed in Part 1 of Table 2 were predicted because if the combustible gases were reacted in the cavity, it raised the baseline initial pressure and temperature in the containment. Then when a discrete burn started in the lower compartment and completed in the upper compartment, even though the ratio of pressure increase to initial pressure approximately the same in these three cases, the total pressures were different. Thus totally neglecting in-cavity oxidation may not be as conservative as we thought in the past when studying containment loading due to hydrogen combustion.

What the bounding calculations have shown is that, even without any detailed modeling of the chemistry and diffusion-flame structure for the in-cavity process, for the given conditions, combustible gases were predicted to accumulate in the lower and upper compartments for all cases. This eventually led to ignition in the lower compartment and flame propagation to the upper compartment. HECTR results also imply that the effect of steam inerting could be very important under certain conditions (Case b); it was relatively minor for these calculations because the rate of the in-cavity oxidation was controlled by the rate at which oxygen was transported into the cavity. The only difference between these bounding calculations was that repetitive burns were predicted in the lower and upper compartments when steam inerting was considered instead of a single burn when steam inerting was not considered. More study of the steam inerting effect will be given in section 4.4.1.

4.3 HECTR Default Calculations Using a 6-Compartment Model

When setting up the MAAP code to perform containment analysis, an accident analyst cannot define and choose the number of compartments to model the containment. The total number of compartments used to model an ice-condenser containment is fixed at six, with only one control volume representing the lower compartment. This setup is probably sufficient for some cases when forced convection is a dominant transport mechanism (as shown in part I of the standard problem). However, if natural convection becomes important, a single control volume for the lower compartment may not be sufficient, especially to predict

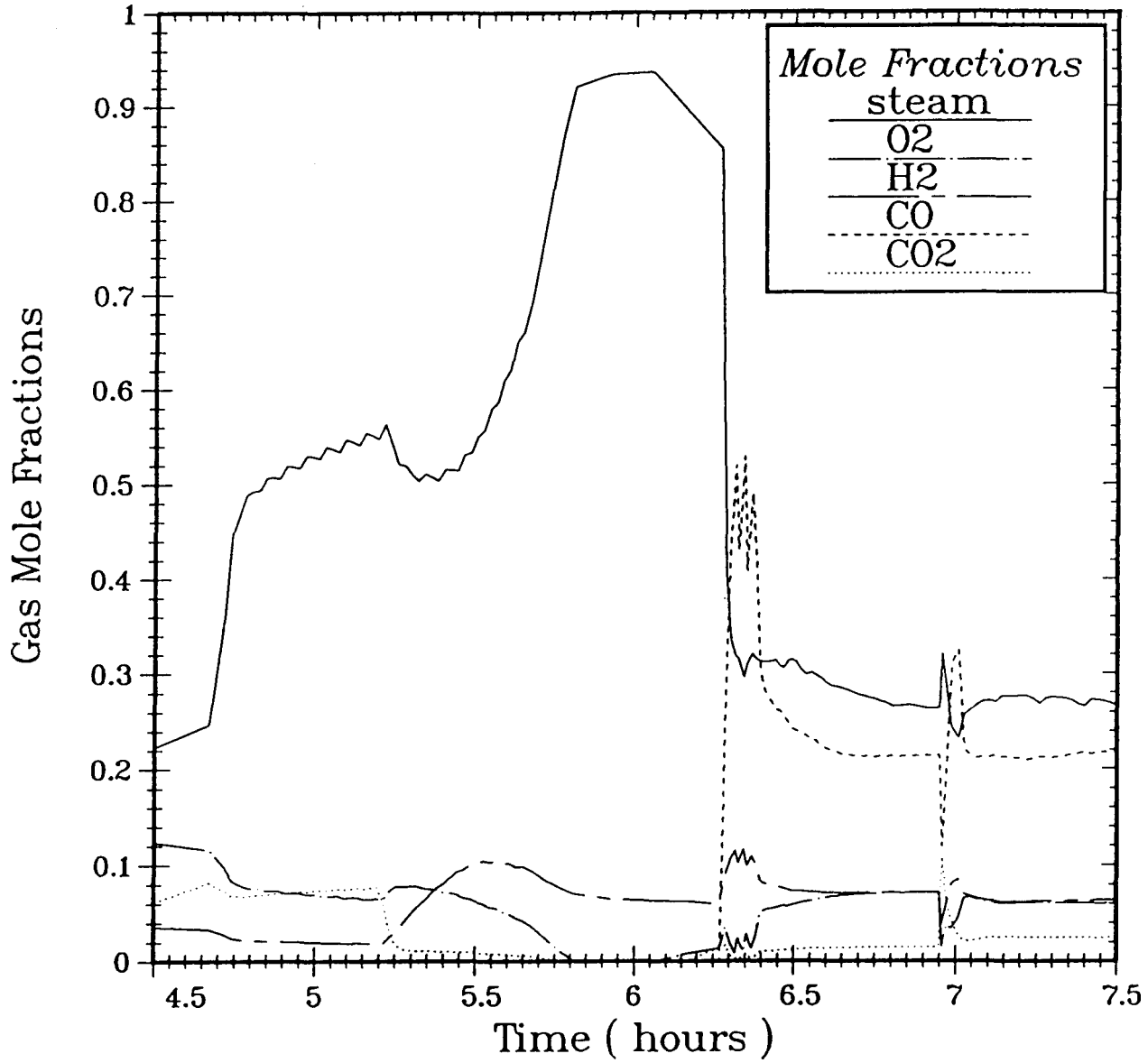

Figure 14. Gas Composition in the Reactor Cavity Predicted by HECTR (12-Compartment Model; In-Cavity Oxidation is Totally Neglected).

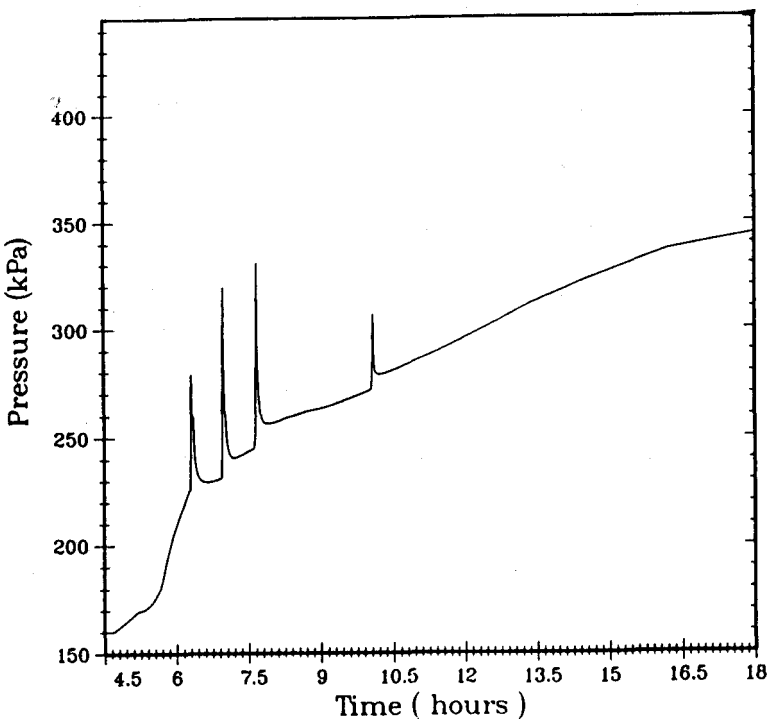

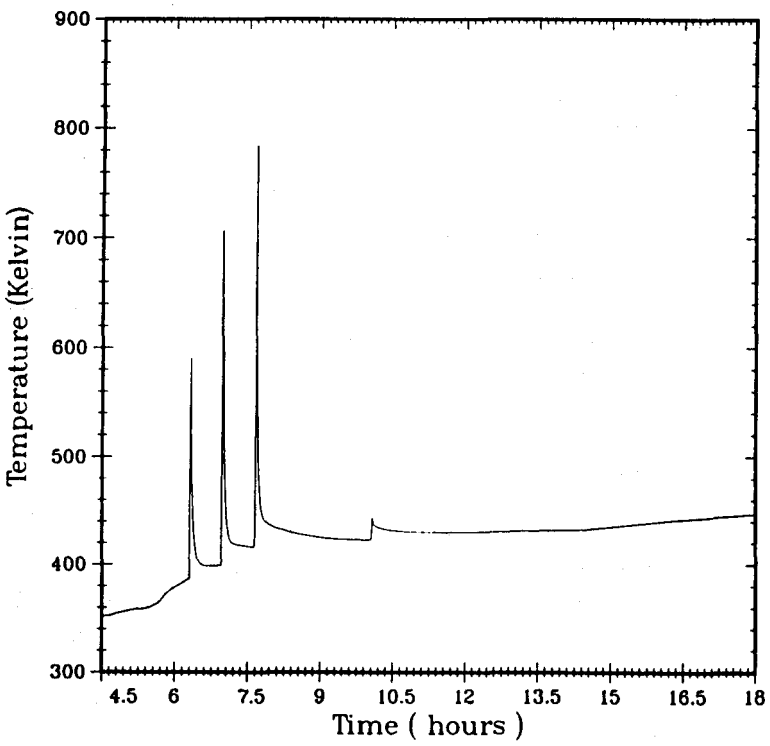

Figure 15. Pressure and Temperature Responses in the Upper Compartment Predicted by HECTR (12-Compartment Model; In-Cavity Oxidation is Totally Neglected).

natural recirculation flow between the lower compartment and the reactor cavity.

As discussed in section 3.2, the rate of the in-cavity oxidation can be controlled by the rate of oxygen being transported into the reactor cavity region. Buoyancy-driven flow is the dominant gas transport mechanism between the reactor cavity and the lower compartment. During the period of core-concrete interactions and in-cavity oxidation, a hot mixture of combustion products and steam rises up through the tunnel into the lower compartment. To complete the natural circulation loop, cooler air is entrained down into the cavity through the reactor annular gap. For computer codes performing containment analyses using the lumped-volume technique, the choice of noding system becomes very important in determining the natural circulation flow rate.

The recirculation flow between the reactor cavity and the lower compartment is primarily driven by the density gradient along the flow path. The hot gas mixture (steam, hydrogen, carbon monoxide, and carbon dioxide) will escape through the tunnel into the lower compartment. Cold air will be entrained into the cavity from the reactor service area through the annular gap between the reactor vessel and the shielding concrete. Since the air-return fans are operating in the S2HF accident sequence, the hot plume will rise up along the forced-convection flow path through the ice region into the upper compartment. This minimizes the mixing in the lower compartment. Hence it is important to model the lower compartment correctly. In MAAP [3], a single control volume is used to represent the lower compartment. Setting up the noding system in this way introduces an artificial instantaneous mixing mechanism within the lower compartment. Since the natural circulation flow rate depends on the density gradient along the flow path, the resulting inaccurate density distribution leads to an inaccurate prediction of the flow rate.

Using a 12-compartment model, which has five control volumes representing the lower compartment, Fig. 16a, HECTR predicted that when in-cavity oxidation was taking place, the temperature and density distributions in the lower compartment were not uniform, as shown in Figs. 17 and 18. The region near the exit of the tunnel (control volume 3) was the hottest, while the other region in the lower compartment (control volumes 5 and 6) was relatively cool. Thus, along the natural-circulation flow path, the density gradient in this case was smaller than the case with uniform density distribution in the lower compartment.

In the 6-compartment model, Fig. 16b, a single control volume was used to represent the lower compartment. This implied

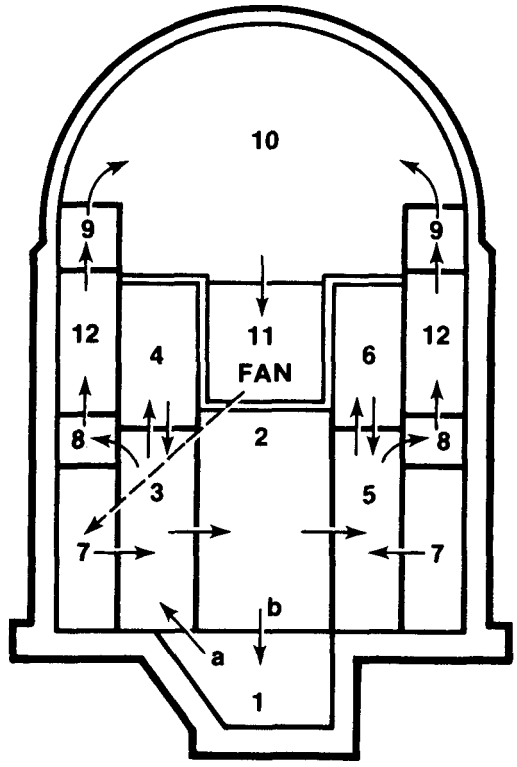

12-COMPARTMENT MODEL

COMPARTMENT DESCRIPTORS	ID NUMBER
UPPER COMPARTMENT	10, 11
UPPER PLENUM	9
LOWER PLENUM	8
LOWER COMPARTMENT	2, 3, 4, 5, 6
DEAD-ENDED REGION	7
ICE COMPARTMENT	12
REACTOR CAVITY	1

JUNCTION DESCRIPTORS	ID NUMBER
TUNNEL	a
REACTOR ANNULAR GAP	b

6-COMPARTMENT MODEL

COMPARTMENT DESCRIPTORS	ID NUMBER
UPPER COMPARTMENT	5
UPPER PLENUM	4
LOWER COMPARTMENT	2
DEAD-ENDED REGION	3
ICE COMPARTMENT	6
REACTOR CAVITY	1

JUNCTION DESCRIPTORS	ID NUMBER
TUNNEL	a
REACTOR ANNULAR GAP	b

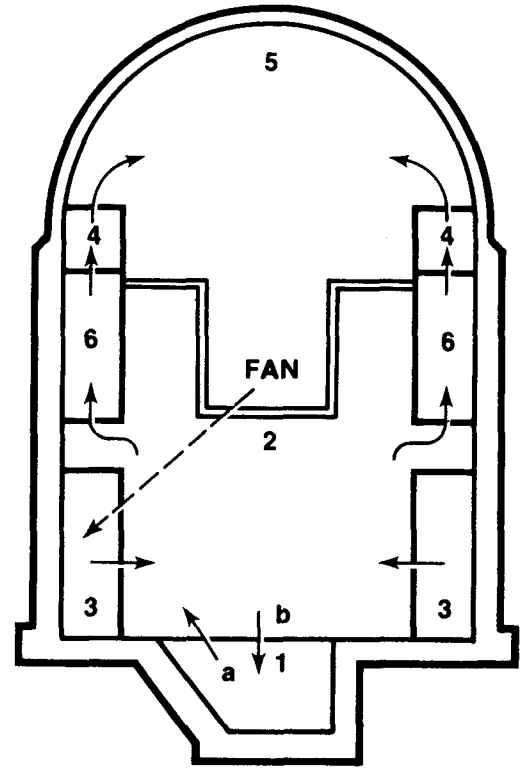

Figure 16. Containment Noding System Used in HECTR Analyses and Flow Directions at the Junctions During the Period of In-Cavity Oxidation Predicted by HECTR (12-Compartment Model vs 6-Compartment Model).

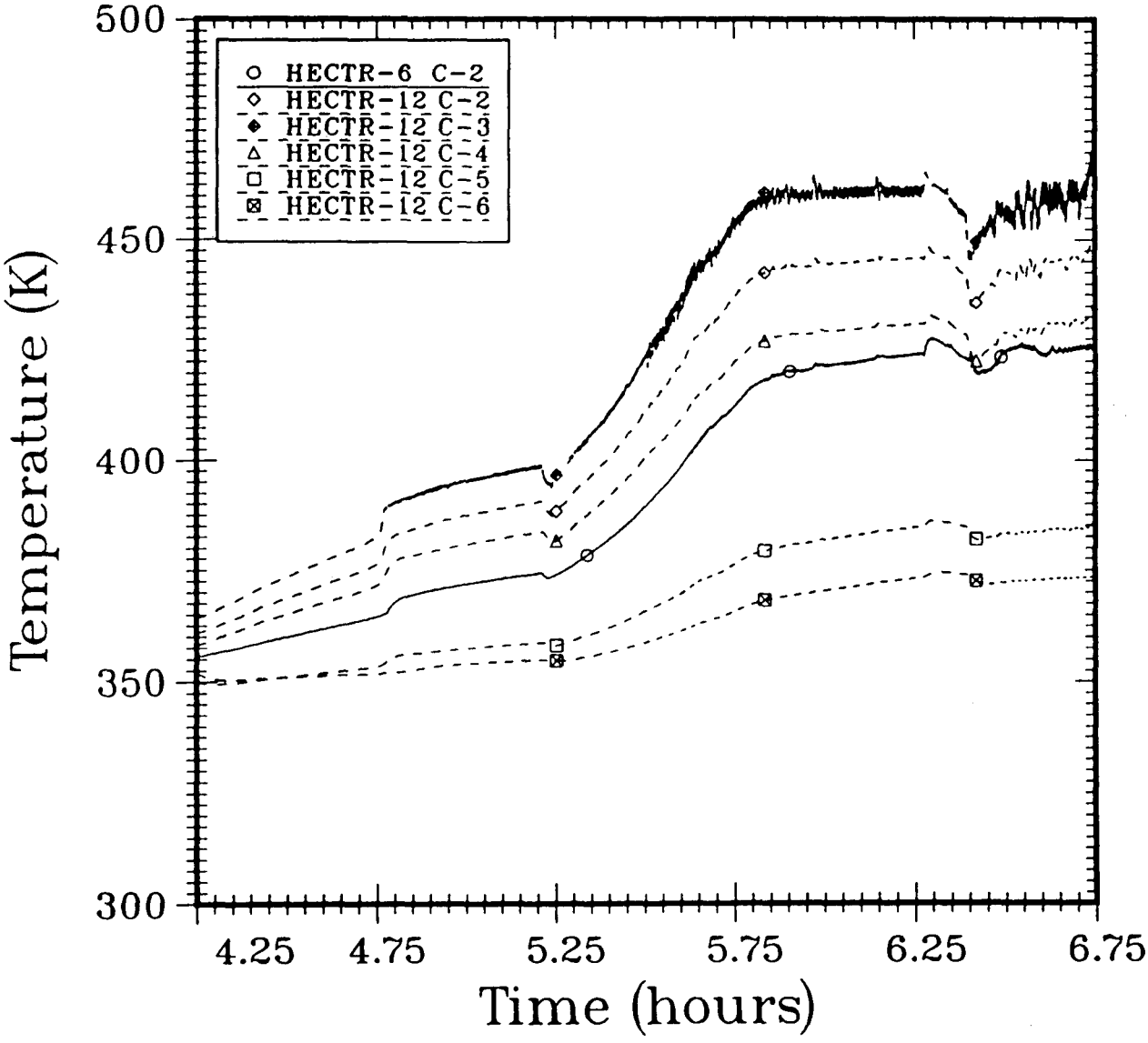

Figure 17. Comparison of Temperature Distribution in the Lower Compartment Between the 12-Compartment and 6-Compartment Models Predicted by HECTR.

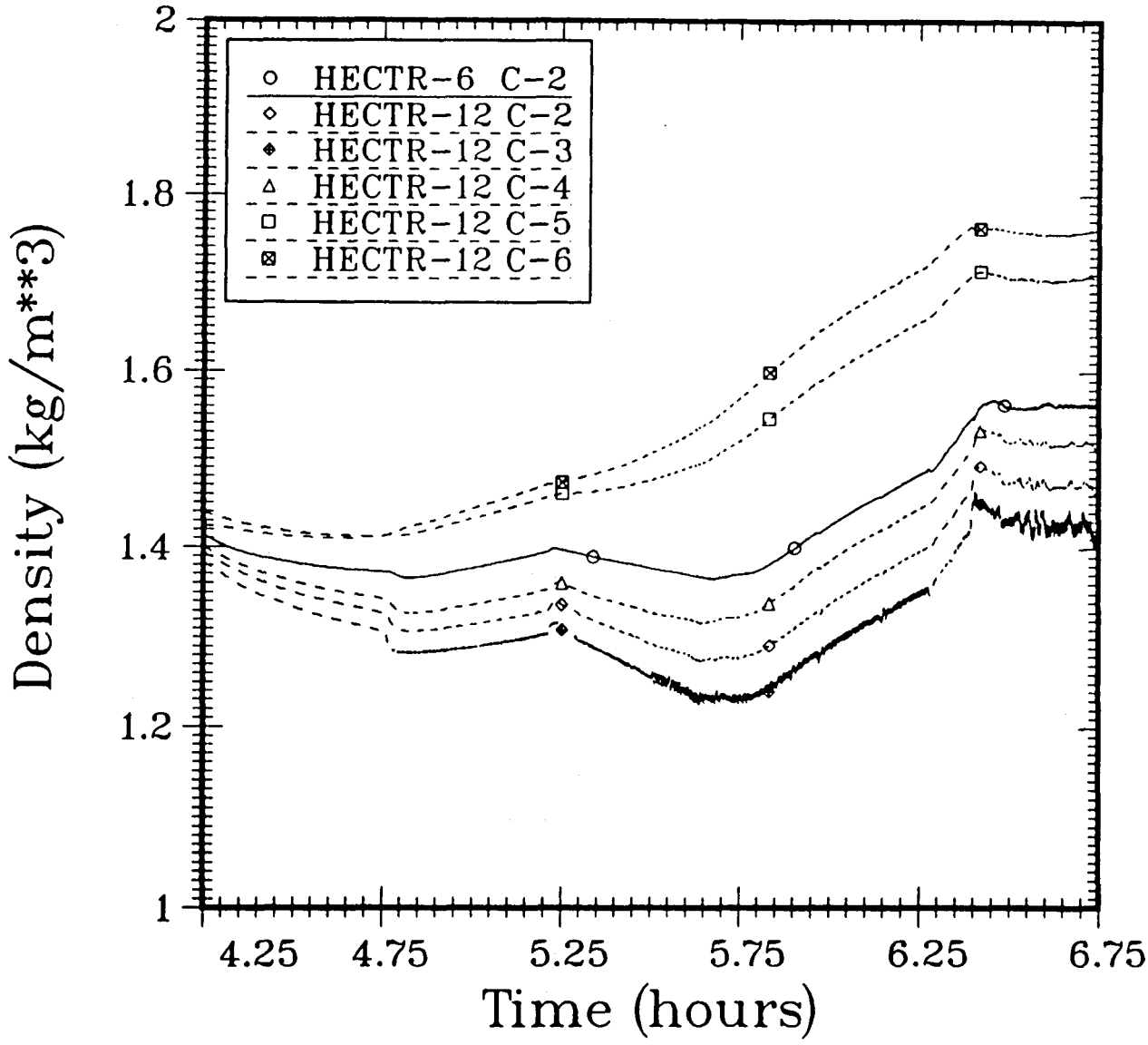

Figure 18. Comparison of Density Distribution in the Lower Compartment Between the 12-Compartment and 6-Compartment Models Predicted by HECTR.

uniform temperature and density distributions within the lower compartment, and it produced a higher density gradient along the flow path. As a result, a higher natural circulation flow rate was predicted, Fig. 19. A larger flow rate between the lower compartment and the reactor cavity provided sufficient oxygen to support complete in-cavity oxidation. Since most of the combustible gases were reacted in the cavity, Fig. 20, no accumulation of the combustible gases in the lower and upper compartments was calculated at the early stage of the transient (i.e., 3 hours after the vessel breach.) Later, only after most of the oxygen in the containment had been depleted, combustible gases started to accumulate. Without any discrete burning in the lower and upper compartment, the pressure gradually increased to 332 kPa (48 psia) at the end of the problem, about 18 hours, Figs. 21 and 22.

In summary, HECTR analyses using 6- and 12-compartment models show the importance of using proper compartment nodalization. Use of too few compartments yields inaccurate gas transport information; however, too many compartments can lead to a long code execution time and higher cost. To determine the natural circulation loop between the lower compartment and the reactor cavity, a single control volume representing the lower compartment is not sufficient. In our analyses, it predicted a different result from a multi-control volume model. By using a single control volume to represent the lower compartment as in MAAP, a substantial natural convective flow between the cavity and lower compartment was calculated. This natural convective current provided sufficient oxygen into the cavity to sustain complete in-cavity oxidation. Hence no accumulation and subsequent combustion of hydrogen and carbon monoxide in the upper and lower compartments were calculated, and there was no early threat to containment integrity. However, when five control volumes were used to represent the lower compartment, HECTR predicted that the condition in the lower compartment was not well mixed and the natural convective current into the cavity was lower than the prediction of the model using a single control volume representing the lower compartment. As a result, there was not sufficient oxygen in the cavity to sustain a complete in-cavity oxidation. This led to a buildup of combustible gases in the upper and lower compartment. At 7.4 hours into the transient, a severe burn was initiated in the lower compartment and propagated into the upper compartment. This global burn generated a peak pressure of 384 kPa (56 psia) that the model using a single control volume representing the lower compartment and other analysis [6] did not predict. This pressure compares to the failure pressure for an ice-condenser containment at about 448 kPa (65 psia).

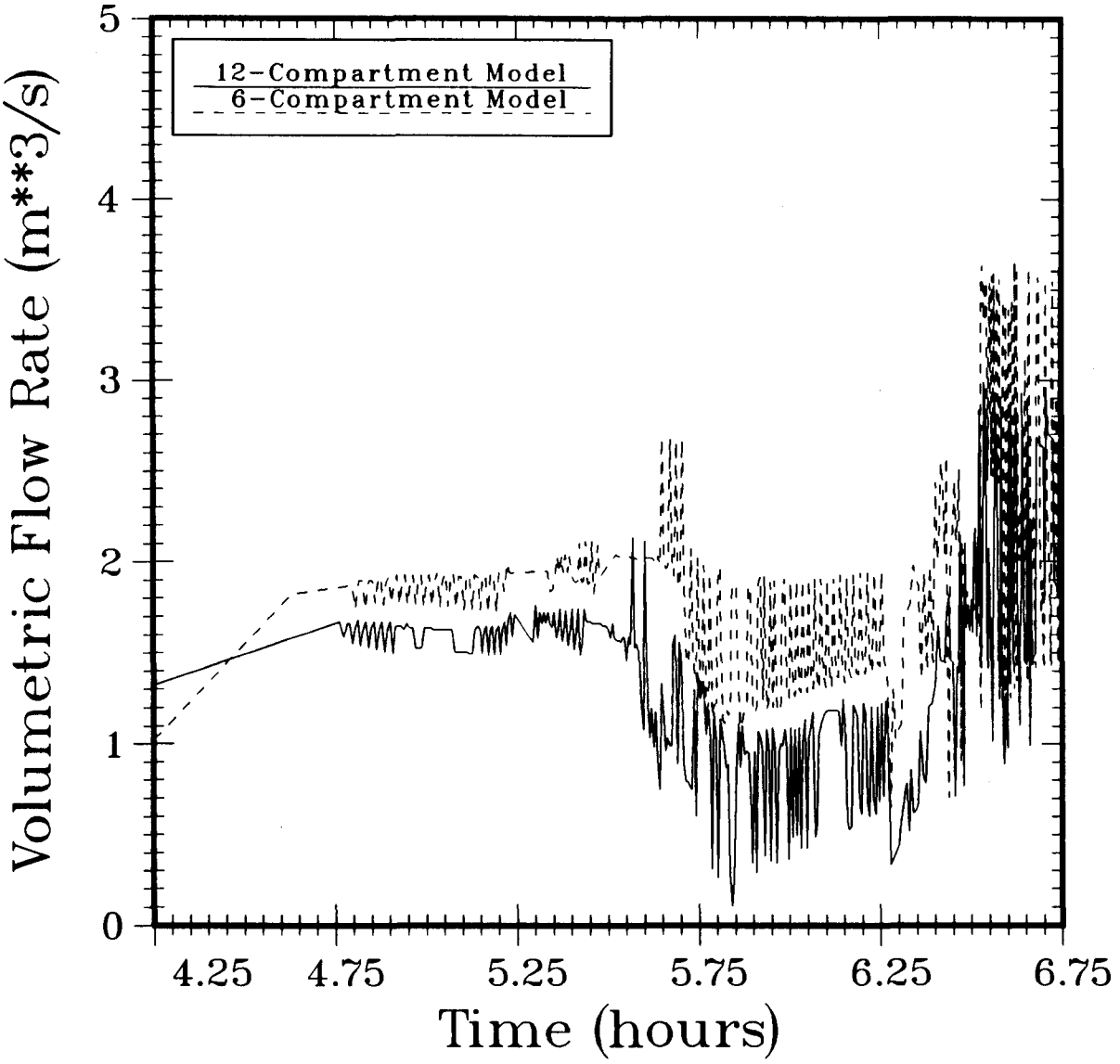

Figure 19. Comparison of Gas Flow Rates through the Junction at the Reactor Annular Gap Predicted by the HECTR 12-Compartment Model and 6-Compartment Model (Flow Direction is from the Lower Compartment to Reactor Cavity).

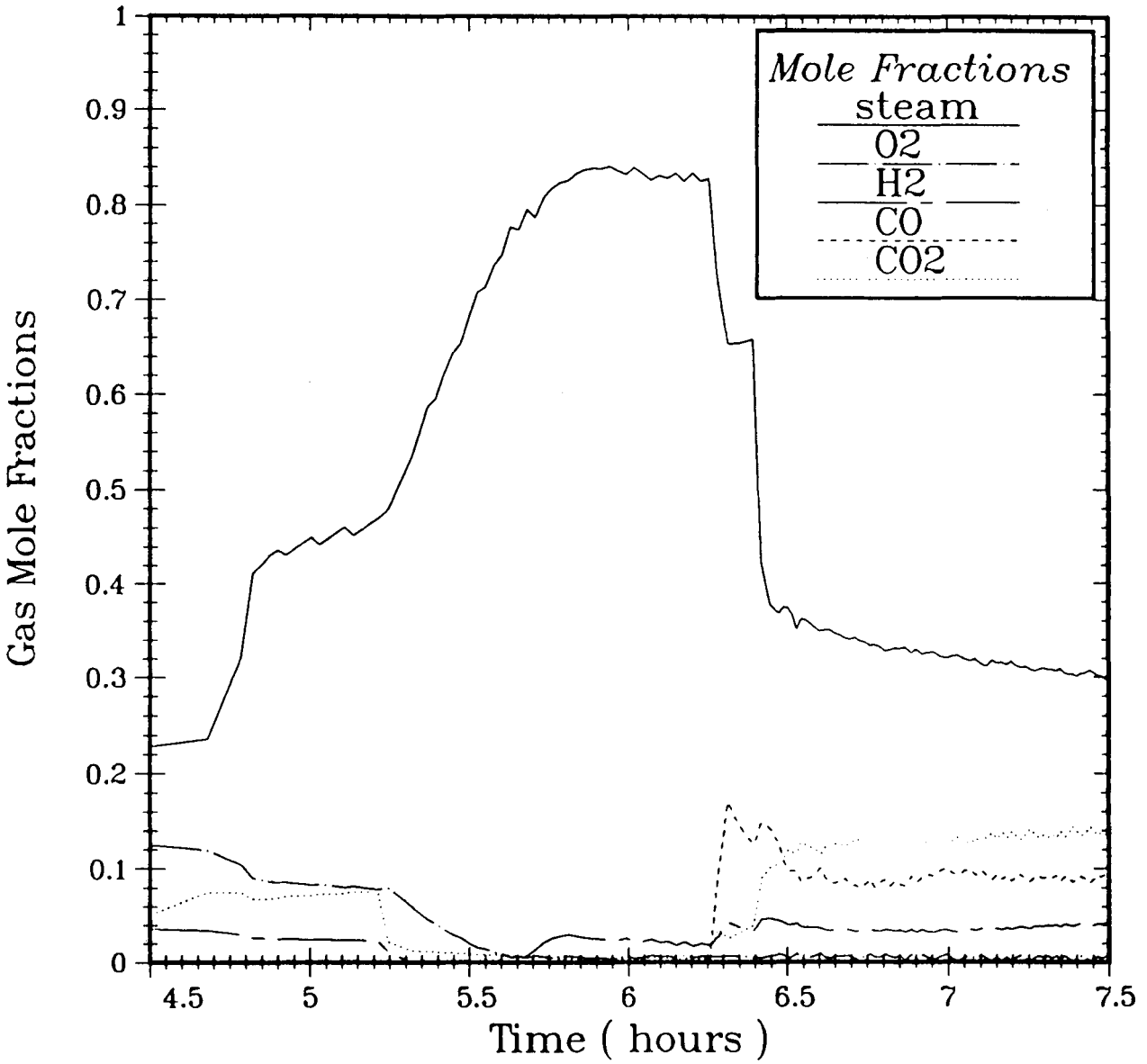

Figure 20. Gas Composition in the Reactor Cavity Predicted by HECTR (6-Compartment Model; Conditions for Continuous In-cavity Oxidation: $O_2 \geq 0\%$ and steam $\leq 100\%$).

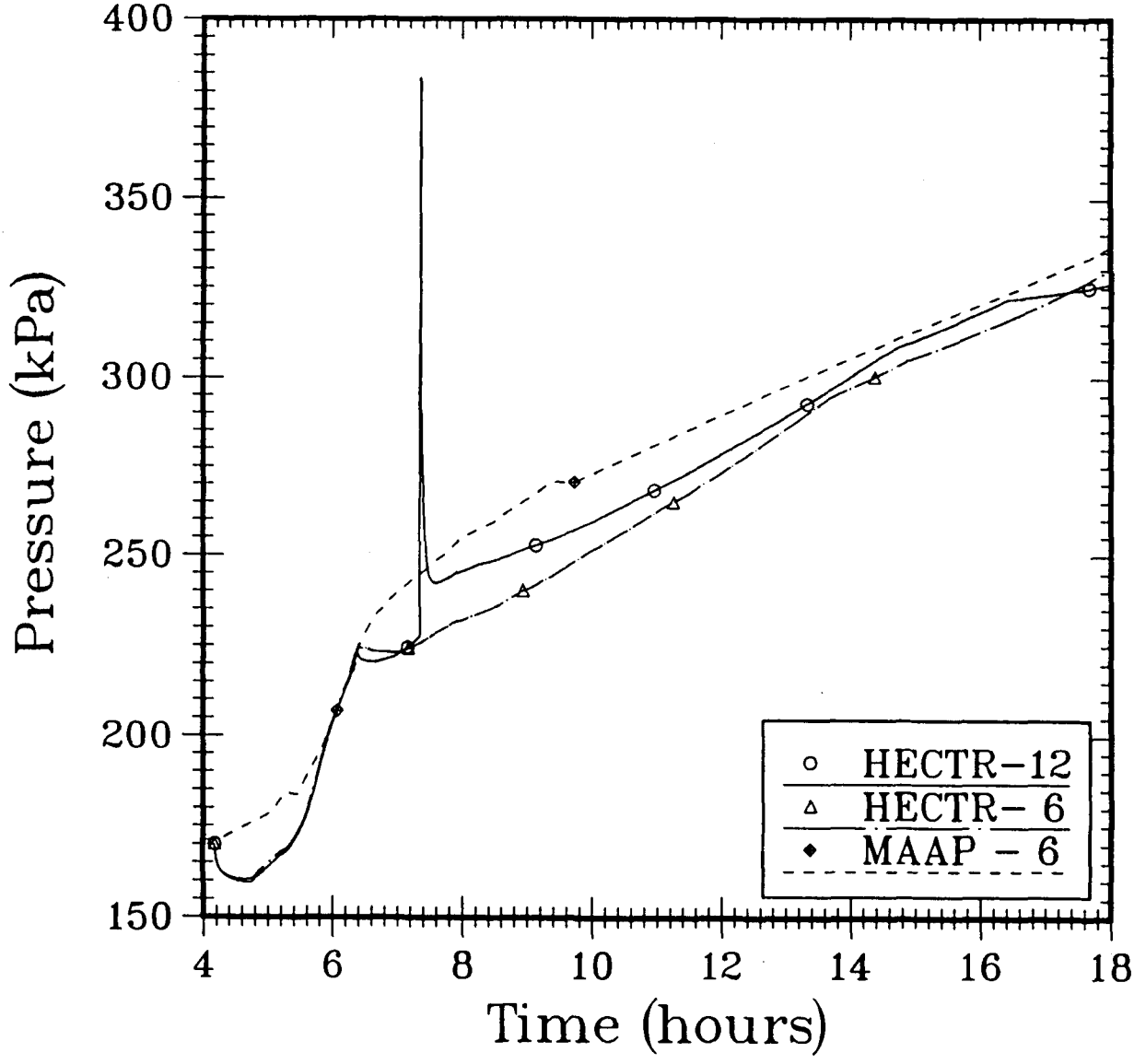

Figure 21. Comparison of Pressure Responses in the Upper Compartment between HECTR and MAAP Predictions (12-Compartment Model vs 6-Compartment Model; Conditions for Continuous In-cavity Oxidation: $O_2 \geq 0\%$ and steam $\leq 100\%$).

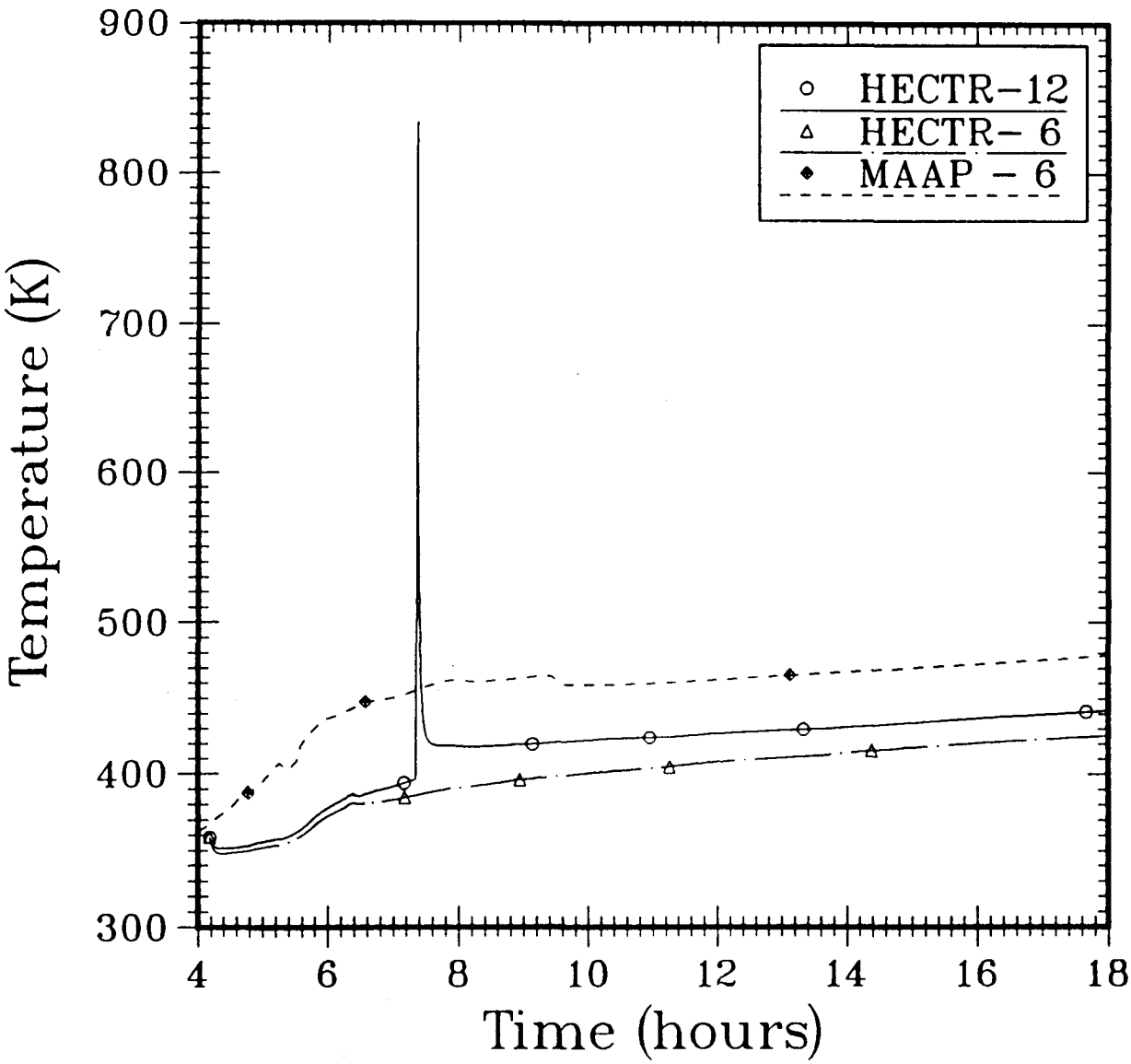

Figure 22. Comparison of Temperature Responses in the Upper Compartment between HECTR and MAAP Predictions (12-Compartment Model vs 6-Compartment Model; Conditions for Continuous In-cavity Oxidation: $O_2 \geq 0\%$ and steam $\leq 100\%$).

4.4 Sensitivity Studies

4.4.1 Steam Inerting Effect

HECTR results of the 12-compartment model imply that the steam inerting effect could be very important under certain conditions. However, this effect was not substantial when comparing containment loadings predicted by the 12-compartment model, because oxygen-transport into the reactor cavity was the dominant factor controlling the degree of in-cavity oxidation in these cases. In order to show the importance of the steam inerting effect, HECTR analysis of the problem was repeated using the 6-compartment model and considering the steam inerting effect (Case c of Part II in Table 2). Section 4.3 has shown that using the 6-compartment model and neglecting the steam inerting effect, a complete in-cavity oxidation would occur. No accumulation and subsequent combustion of hydrogen and carbon monoxide was predicted in the upper and lower compartments. However, if considering the steam inerting effect based on the results of experiments performed at a temperature of 400 K [13], in-cavity oxidation would be terminated by the excess amount of steam existing in the reactor cavity, Fig. 23. Accumulation and subsequent combustion of hydrogen and carbon monoxide would take place in the upper and lower compartments, Figs. 24 and 25. Hence the difference would be substantial; the calculated peak pressure would be much higher for the case including the steam inerting effect, 411 vs. 330 kPa. In summary, the effect of steam inerting on in-cavity oxidation cannot be neglected.

4.4.2 Matching Solution

A HECTR calculation was performed using the HECTR/MAAP 6-compartment model in an attempt to match the MAAP prediction. The results are shown in Figures 26 and 27. Overall, the qualitative behavior of the containment response predicted by HECTR is quite similar to MAAP results. No accumulation of the combustible gases in the lower and upper compartments was predicted at the early part of the transient. The pressure response calculated by HECTR is slightly higher than MAAP prediction. The temperature response in the containment calculated by HECTR is also similar to MAAP prediction except in the reactor cavity. HECTR calculated a higher bulk gas temperature in the reactor cavity than MAAP; 2100 K vs. 1540 K, Fig. 27b. My only explanation is that the difference in the formulation of the problem between the two codes may cause this difference in the temperature prediction.

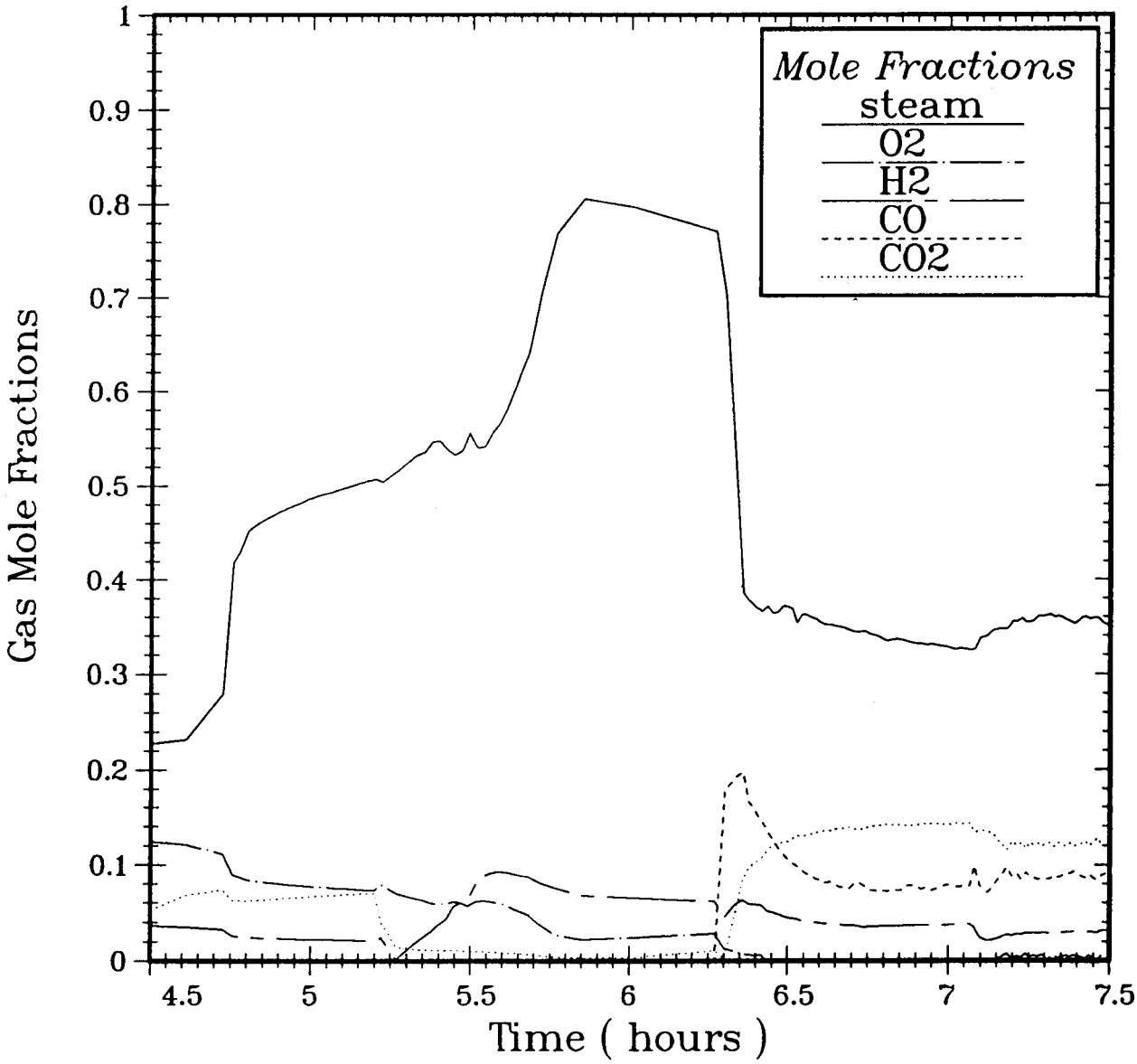

Figure 23. Gas Composition in the Reactor Cavity Predicted by HECTR (6-Compartment Model; Conditions for Continuous In-cavity Oxidation: $O_2 \geq 0\%$ and steam $\leq 55\%$).

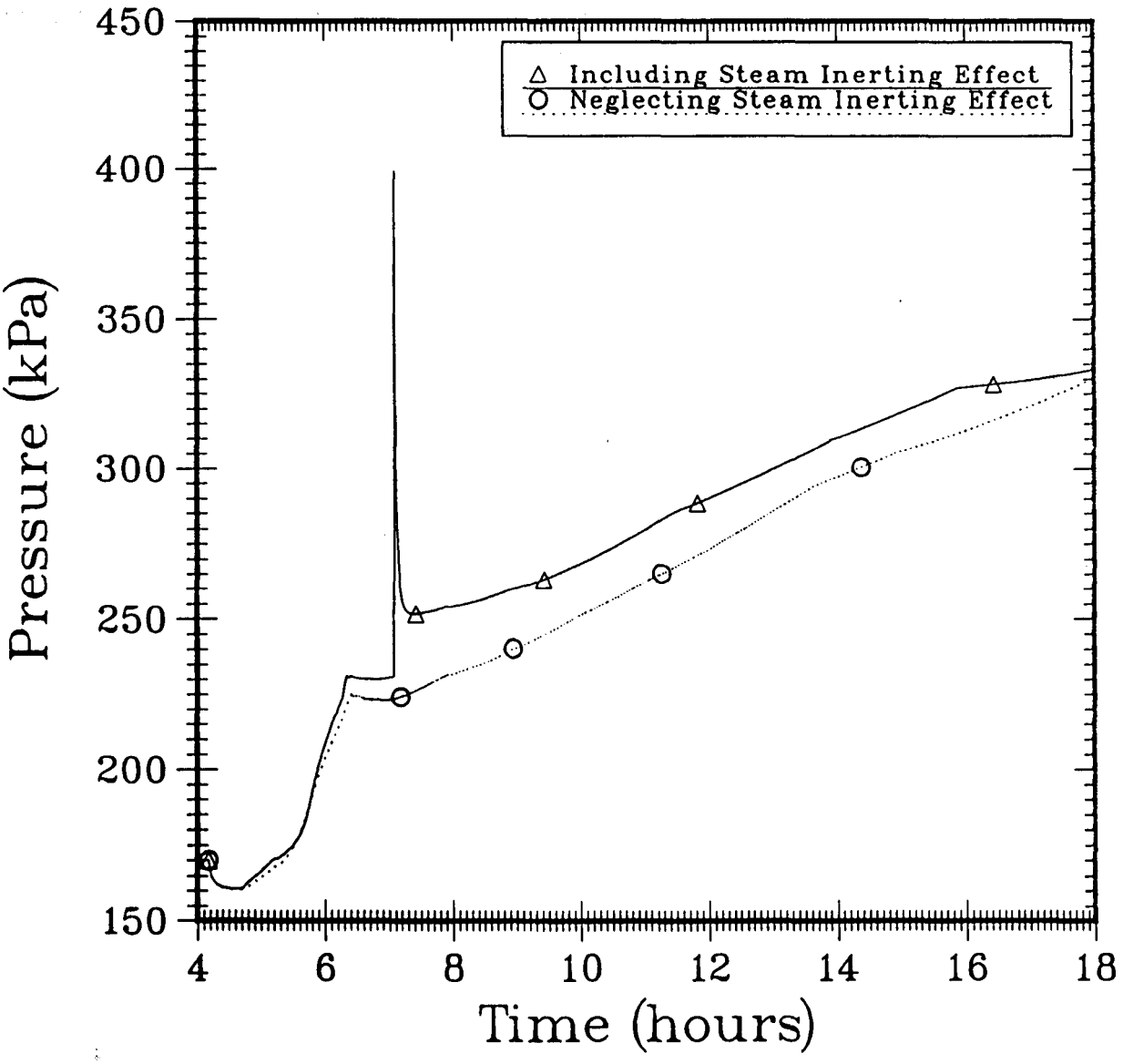

Figure 24. Comparison of Pressure Responses in the Upper Compartment Predicted by HECTR (6-Compartment Model; Conditions for Continuous In-cavity Oxidation: $O_2 \geq 0\%$ and steam $\leq 55\%$).

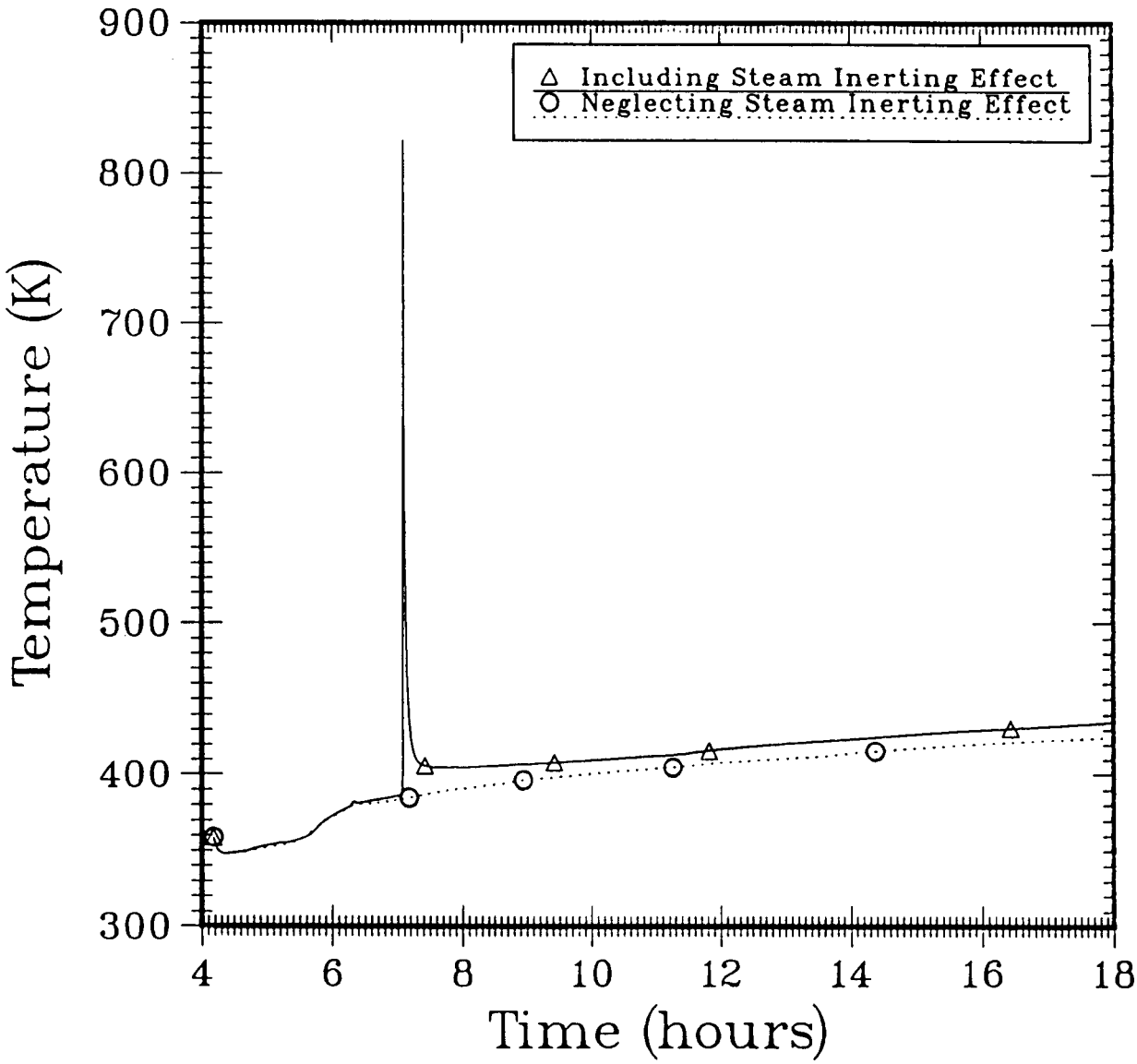

Figure 25. Comparison of Temperature Responses in the Upper Compartment Predicted by HECTR (6-Compartment Model; Conditions for Continuous In-cavity Oxidation: $O_2 \geq 0\%$ and steam $\leq 55\%$).

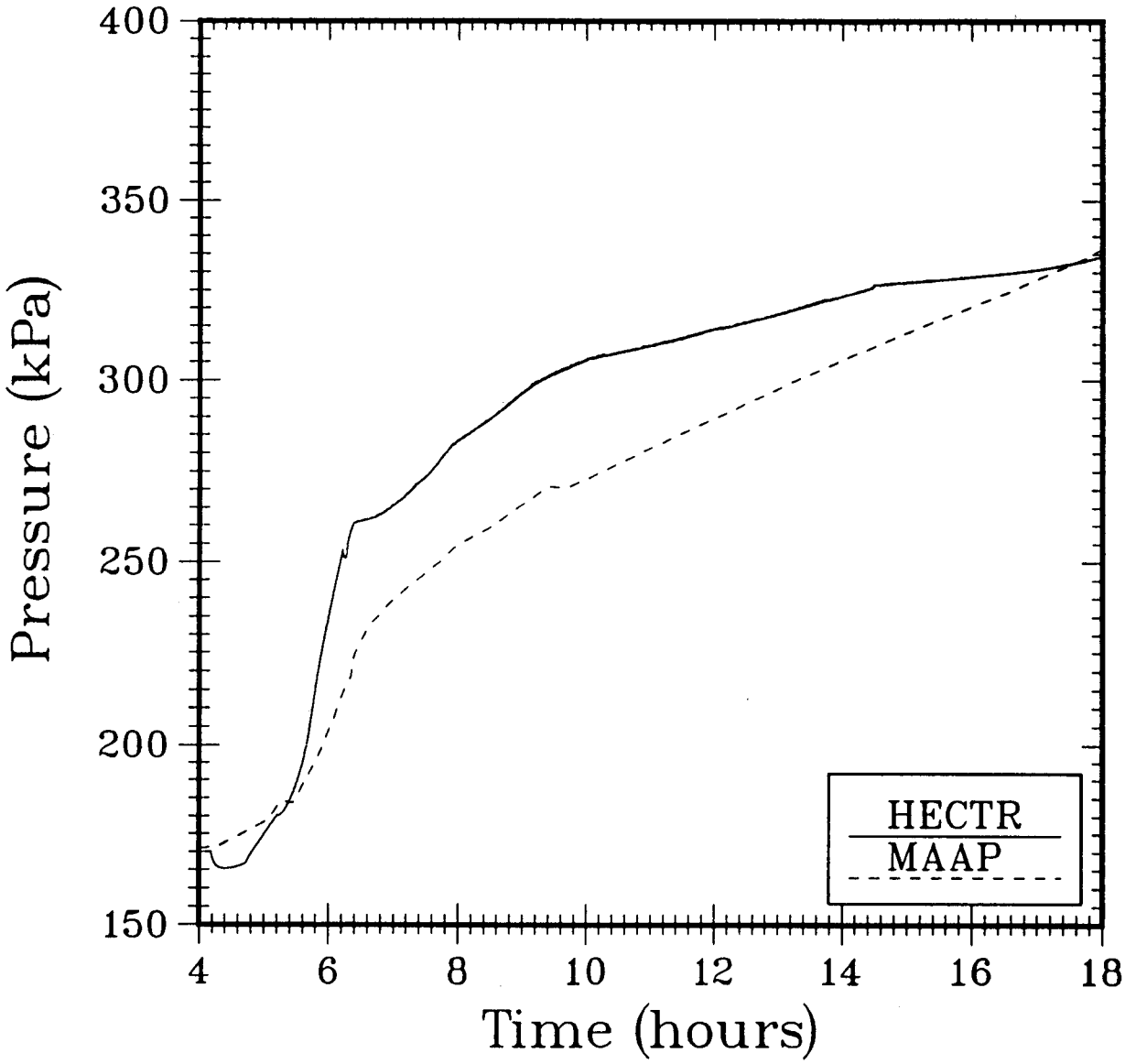

Figure 26. Pressure Response in the Lower Compartment Predicted by HECTR (HECTR/MAAP 6-Compartment Model; Conditions for Continuous In-cavity Oxidation: $O_2 \geq 0\%$ and steam $\leq 100\%$).

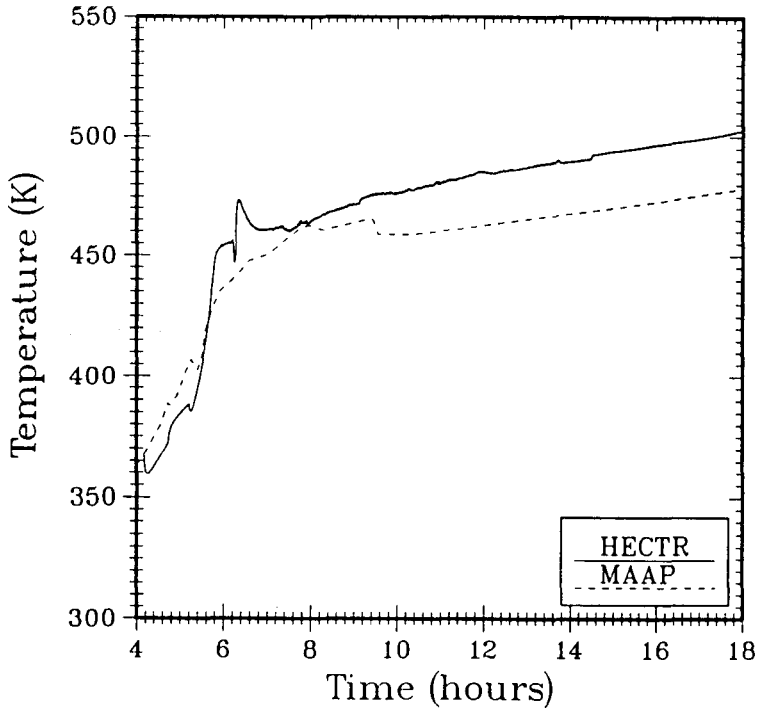

a. Lower Compartment

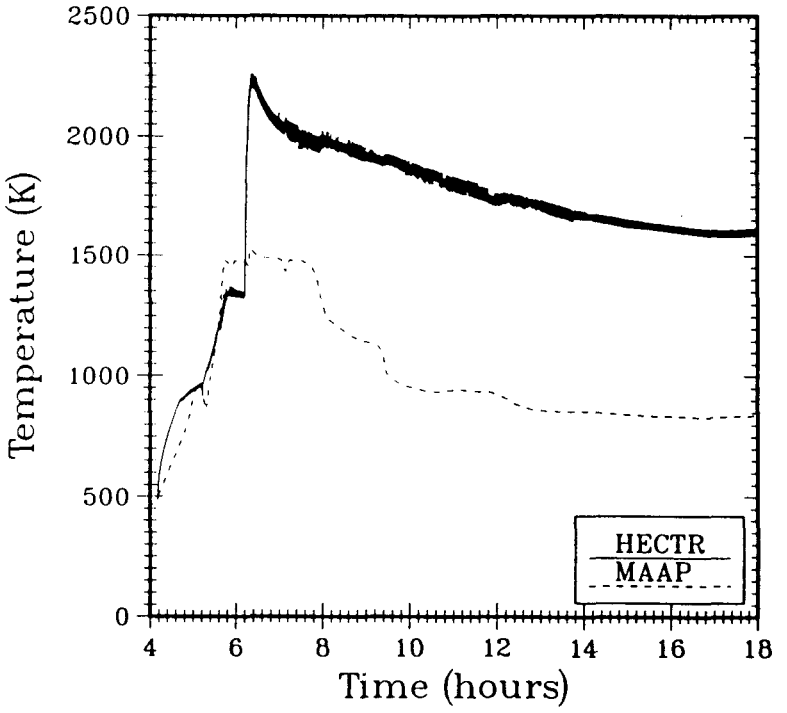

b. Reactor Cavity

Figure 27. Temperature Responses in the Lower Compartment (a) and Reactor Cavity (b) Predicted by HECTR (HECTR/MAAP 6-Compartment Model; Conditions for Continuous In-cavity Oxidation: $O_2 \geq 0\%$ and steam $\leq 100\%$).

4.4.3 Loss Coefficient

HECTR analyses of the second part of the standard problem show that the 12-compartment model, which uses five control volumes to model the lower compartment, is more appropriate to use to predict the natural circulation flow between the lower compartment and the reactor cavity. The results of the 12-compartment model showed that the temperature distribution within the lower compartment was highly non-uniform and this resulted in a lower natural circulation flow rate than the prediction based on the assumption of a well-mixed lower-compartment (as in the 6-compartment model with one control volume for the lower compartment). The impact of this difference is that an incomplete in-cavity oxidation would occur and it would lead to an accumulation and subsequent combustion of hydrogen and carbon monoxide. In the next set of sensitivity studies, I concentrated on the 12-compartment model and performed HECTR calculations to study the effect of the following factors: (1) to increase the natural circulation flow rate by decreasing the loss coefficient at the junctions by factor of ten, (2) to enhance more mixing in the lower compartment by turning the air-return fans off.

The loss coefficient at the junction, which is a user input, is to model form loss with respect to area changes and frictional loss due to walls. The loss coefficients at each junction used in the completed HECTR calculations were determined by the formula given in reference 7. In the following HECTR calculation, the loss coefficients at those flow junctions along the natural circulation loop between the lower compartment and reactor cavity were decreased by a factor of ten. This would promote more natural circulation between the lower compartment and reactor cavity. However, this might also generate some numerical instability and unrealistic results as stated in reference 7.

Decreasing the loss coefficient by a factor of ten promoted more natural circulation into the reactor cavity, Fig. 28. This enhanced more oxygen-transport into the cavity and increased the degree of in-cavity oxidation. No accumulation of the combustible gases in the lower and upper compartments was predicted at the early stage of the second part of the standard problem. There was some buildup of the combustible gases at the later time of the problem. At that time, most of the oxygen in the reactor containment had been depleted by the in-cavity oxidation process and there would not be sufficient oxygen to support any more combustion. No burn was predicted, Fig. 29.

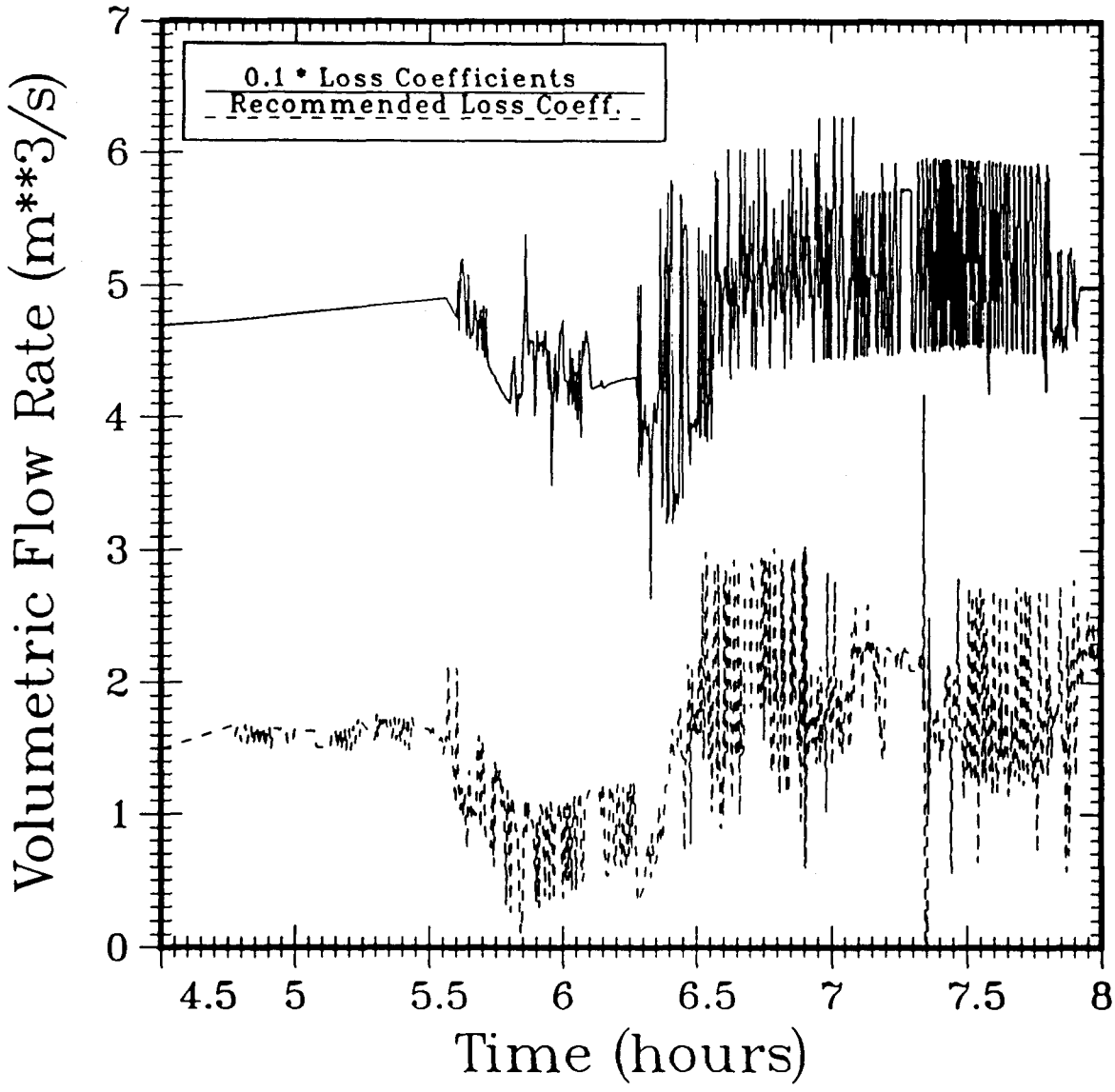

Figure 28. Comparison of Gas Flow Rate through the Junction at the Reactor Annular Gap Predicted by the HECTR Using the 12-Compartment Model But With Two Different Sets of Loss Coefficients (Flow Direction is from the Lower Compartment to Reactor Cavity).

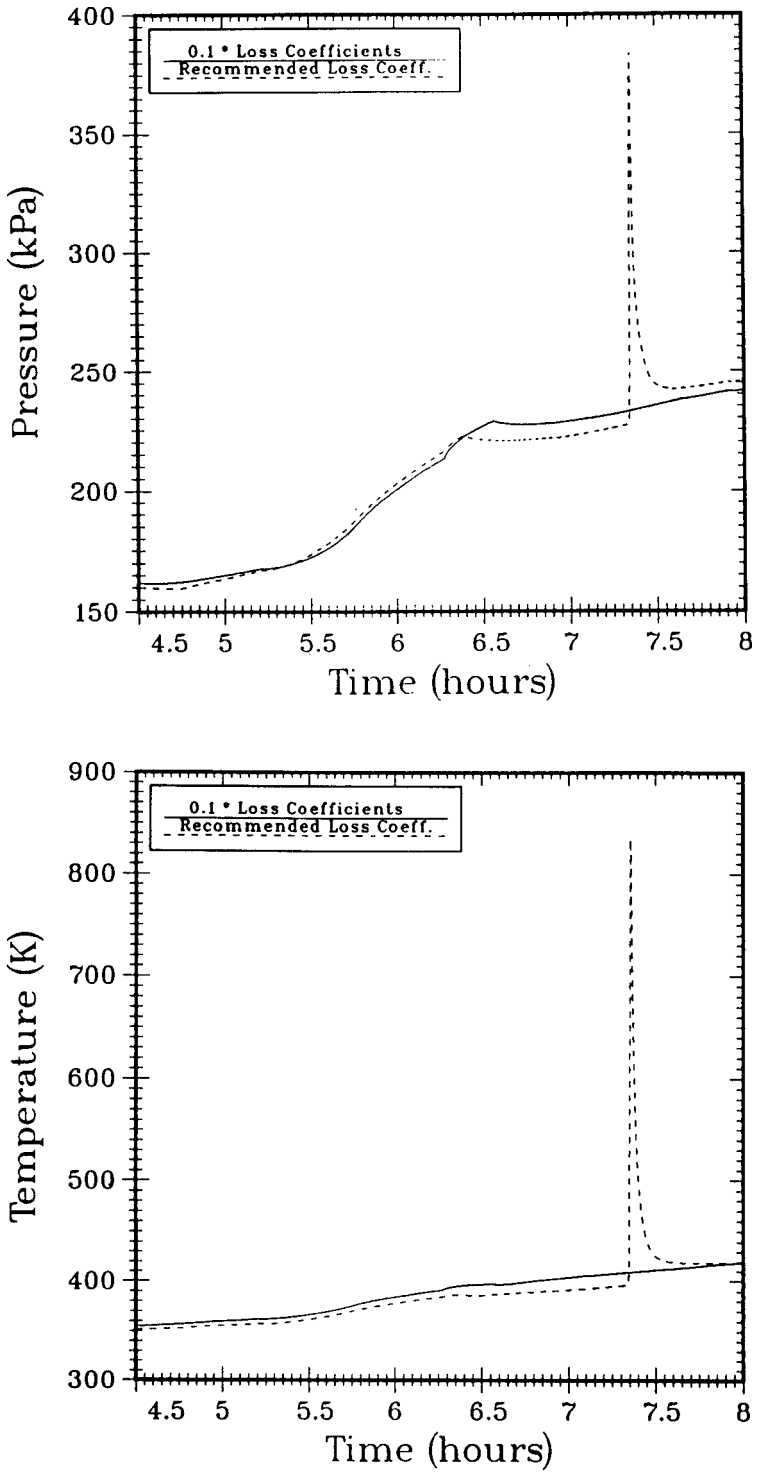

Figure 29. Pressure and Temperature Responses in the Upper Compartment Predicted by HECTR (12-Compartment Model with Much Smaller Loss Coefficients; Conditions for Continuous In-cavity Oxidation: $O_2 \geq 0\%$ and steam $\leq 100\%$).

4.4.4 Air-Return Fans

All the HECTR calculations reported so far have the air-return fans operating at 100% capacity. The fans circulate air between the upper and lower compartments. The forced convective flow path is as follows: lower compartment, lower plenum, ice condenser, upper plenum, upper compartment, annular region, and back to lower compartment. When core-concrete interactions are taking place in the reactor cavity, the plume of hot gases, which are convecting out of the reactor cavity into the lower compartment, will be drawn mostly into the upper compartment through the ice condenser by the fans. HECTR predictions show that the hot plume is unlikely to mix well with other gases in the lower compartment. Thus the next sensitivity study will be on the effect of the air-return fans on the mixing process in the lower compartment.

If the air-return fans are turned off during the accident, HECTR predicts that more mixing would take place in the lower compartment. Still the temperature and gas composition distributions within the lower compartments were far from being uniform, Fig. 30. The positive result of this action - by switching off the fans, is that less combustible gases were predicted to exist in the the upper compartment. Most of the combustible gases remained in the lower compartment. Hence ignition occurred at an earlier time and involved a lesser amount of combustible gases. Only one global burn, which started in the lower compartment and propagated into the upper compartment, and 13 local burns in the upper plenum were predicted. After the completion of the global burn, the lower compartment became steam-inerted. Thereafter, only local minor burns appeared in the upper plenum. Eventually, the containment would run out of oxygen to support any more combustion. The peak calculated pressure was 266.2 kPa (38.61 psi) at 9.30 hour, Fig. 31.

The above sensitivity study shows that the forced convective current induced by the air-return fans would transport more combustible gases into the upper compartment and enhance less mixing in the lower compartment. Therefore, the burn in the fans-on case is more severe than the fans-off case. Other sensitivity studies show that it is important to model the lower compartment correctly; improper noding system or inaccurate loss coefficient at the flow junctions can give a completely different and possibly inaccurate prediction.

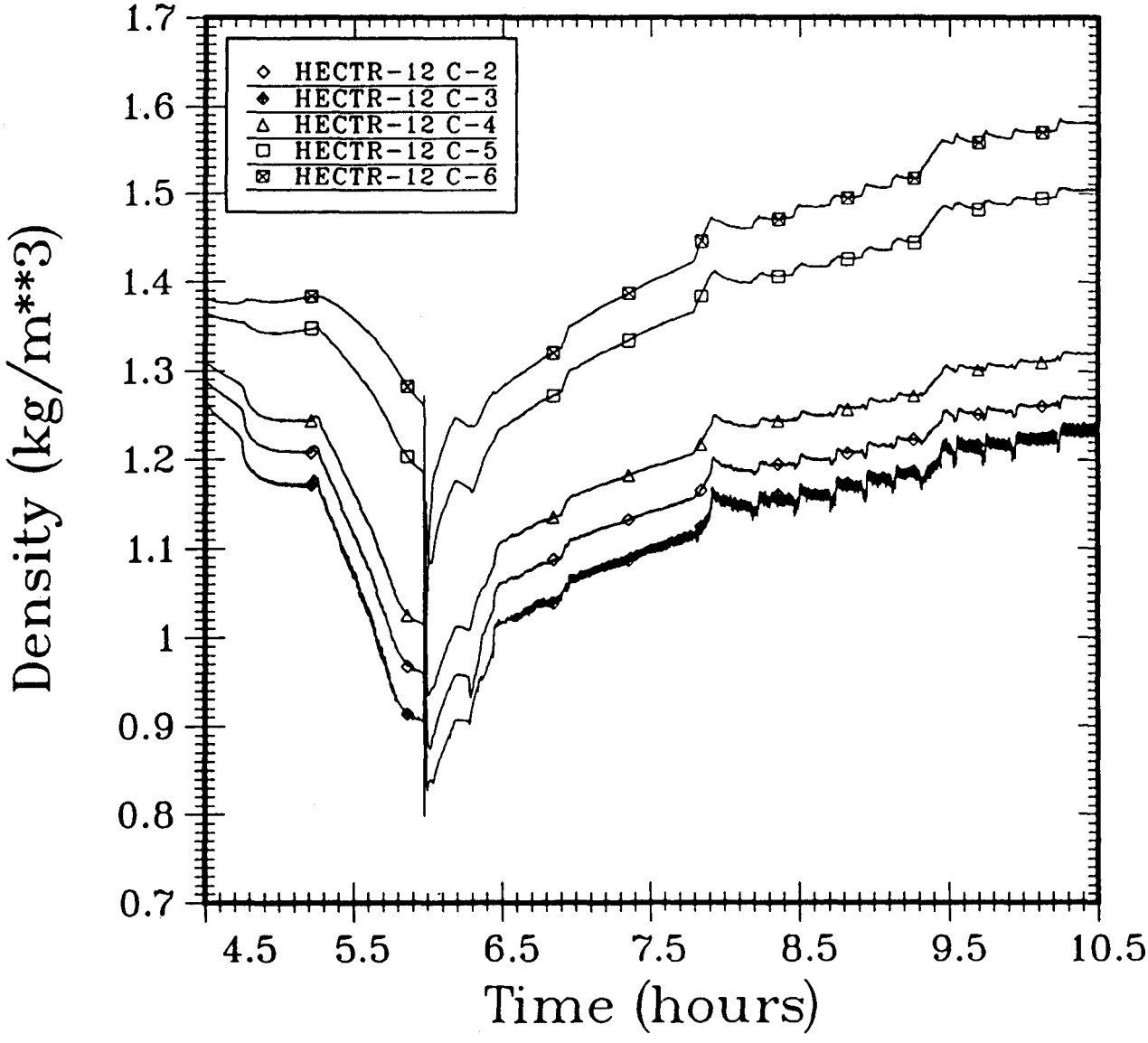

Figure 30. Density Distributions in the Lower Compartment Predicted by HECTR (12-Compartment Model with Fans-Off; Conditions for Continuous In-cavity Oxidation: $O_2 \geq 0\%$ and steam $\leq 100\%$).

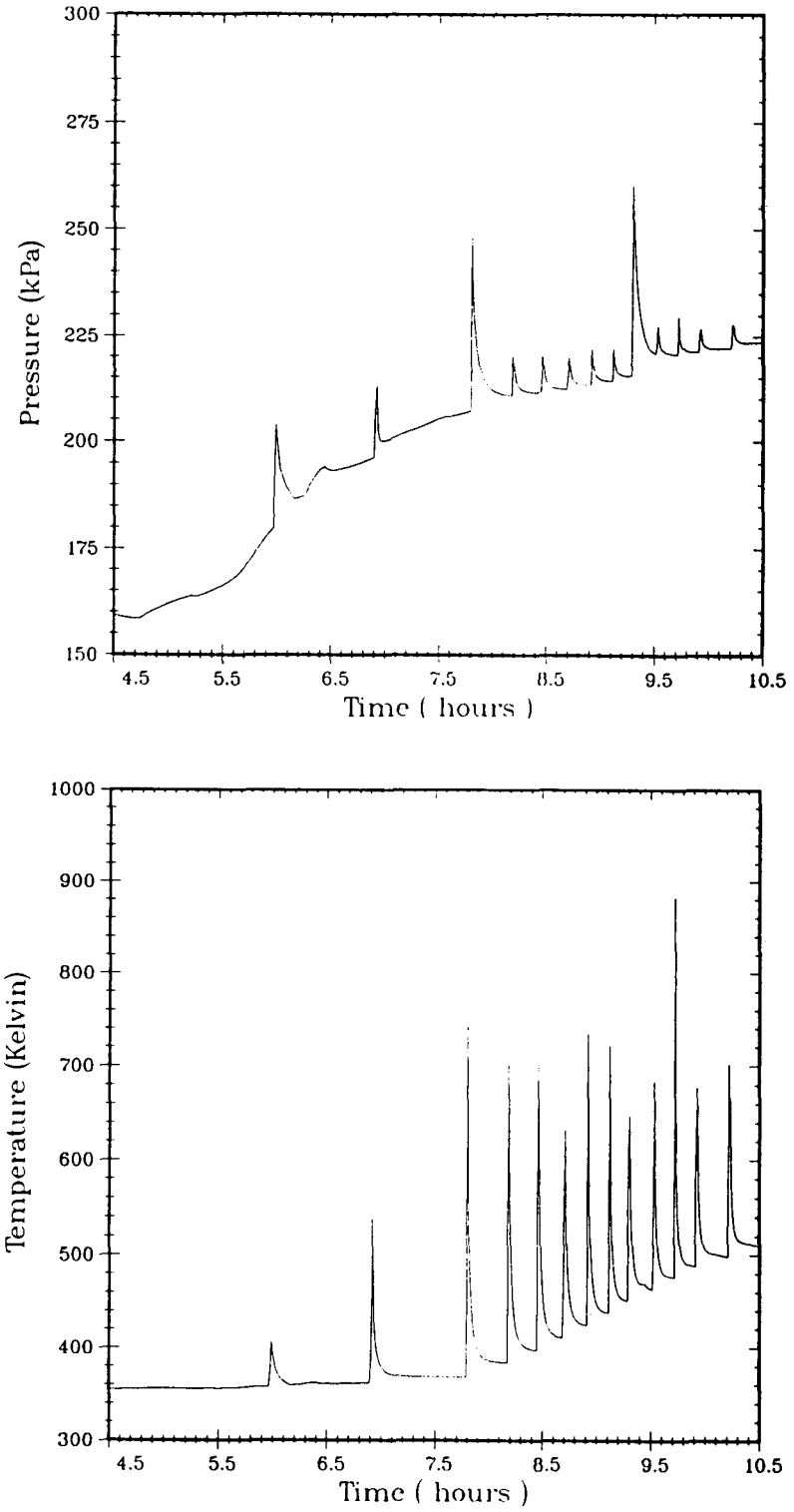

Figure 31. Pressure and Temperature Responses in the Upper Plenum Predicted by HECTR (12-Compartment Model with Fans-Off; Conditions for Continuous In-cavity Oxidation: $O_2 \geq 0\%$ and steam $\leq 100\%$).

4.4.5 Forced Convection From Gas Generation

The last set of sensitivity studies were performed to investigate whether the forced convective flow induced by the gases generated from core-concrete interactions has any influence on the flow between the lower compartment and reactor cavity. The following studies will concentrate on HECTR predictions of the volumetric flow rates at the tunnel and at the annular gap during the early part of core-concrete interactions (between 4.2 and 5.1 hours). In this study, I first calculated the gas release rates predicted by MAAP (mainly steam and carbon dioxide) in terms of kg-moles per second. Then I performed several HECTR calculations assuming the gas released to the atmosphere to be either pure nitrogen or hydrogen instead of a mixture of steam and carbon dioxide but with an equivalent release rate in term of kg-moles per second. The released gases had the same temperature as the bulk-averaged temperature in the reactor cavity, which had already been changed to be equal to the temperature in the lower compartment as predicted by MAAP. This arrangement would minimize any temperature or density difference between the lower compartment and reactor cavity, and allow us to isolate and study each phenomenon governing the flow effectively.

Four HECTR calculations using the 6-compartment model were performed. Each calculation had a different sources or different source conditions: (1) the gas released was nitrogen and no heat was added directly to the atmosphere in the cavity, (2) there was no gas released but an equivalent amount of heat as predicted by MAAP (see Fig. 6) was added directly to the atmosphere in the cavity, (3) the gas released was nitrogen and an equivalent amount of heat was added directly to the atmosphere in the cavity, (4) the gas released was hydrogen and no heat was added directly to the atmosphere in the cavity. The equivalent amount of heat added to the atmosphere in the cavity was the total amount of thermal energy carried by the released gases (mainly steam and carbon dioxide) from core-concrete interactions as predicted by MAAP. Other direct or indirect heat transfer between the corium and the bulk gases in the cavity had been neglected. Nitrogen was chosen in this analysis because its density was similar to air. Thus we could minimize the buoyancy effect. On the contrary, hydrogen was also chosen to maximize the buoyancy effect.

The results of these calculations show that the convective flow between the lower compartment and rector cavity was primarily buoyancy-driven. The added heat, which simulated the thermal energy carried by the source, substantially heated up

the atmosphere in the cavity and increased the density difference between the lower compartment and cavity, which in turn induced the flow, Figs. 32 and 33. Without any heating in the cavity, the flow rate was calculated to be relatively small or negligible. When the nitrogen source was replaced by hydrogen, a much lighter gas, a substantial density difference between the lower compartment and cavity occurred; that also induced natural convective flow between the lower compartment and cavity. Hence during core-concrete interactions, natural convection is shown to be the most dominant gas transport mechanism between the lower compartment and reactor cavity.

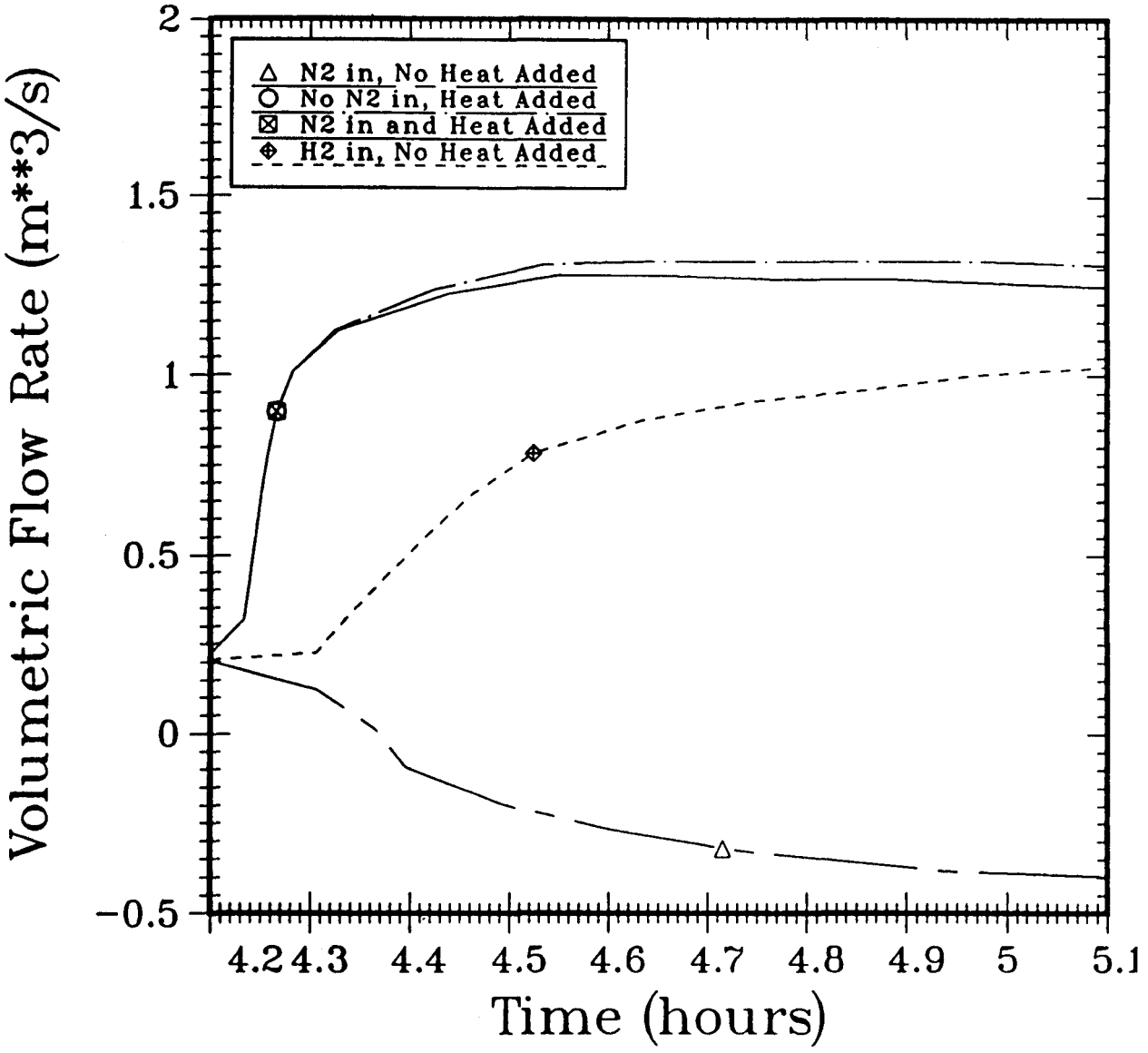

Figure 32. Comparison of Volumetric Flow Rate at the Annular Gap With Respect to Different Sources and Conditions

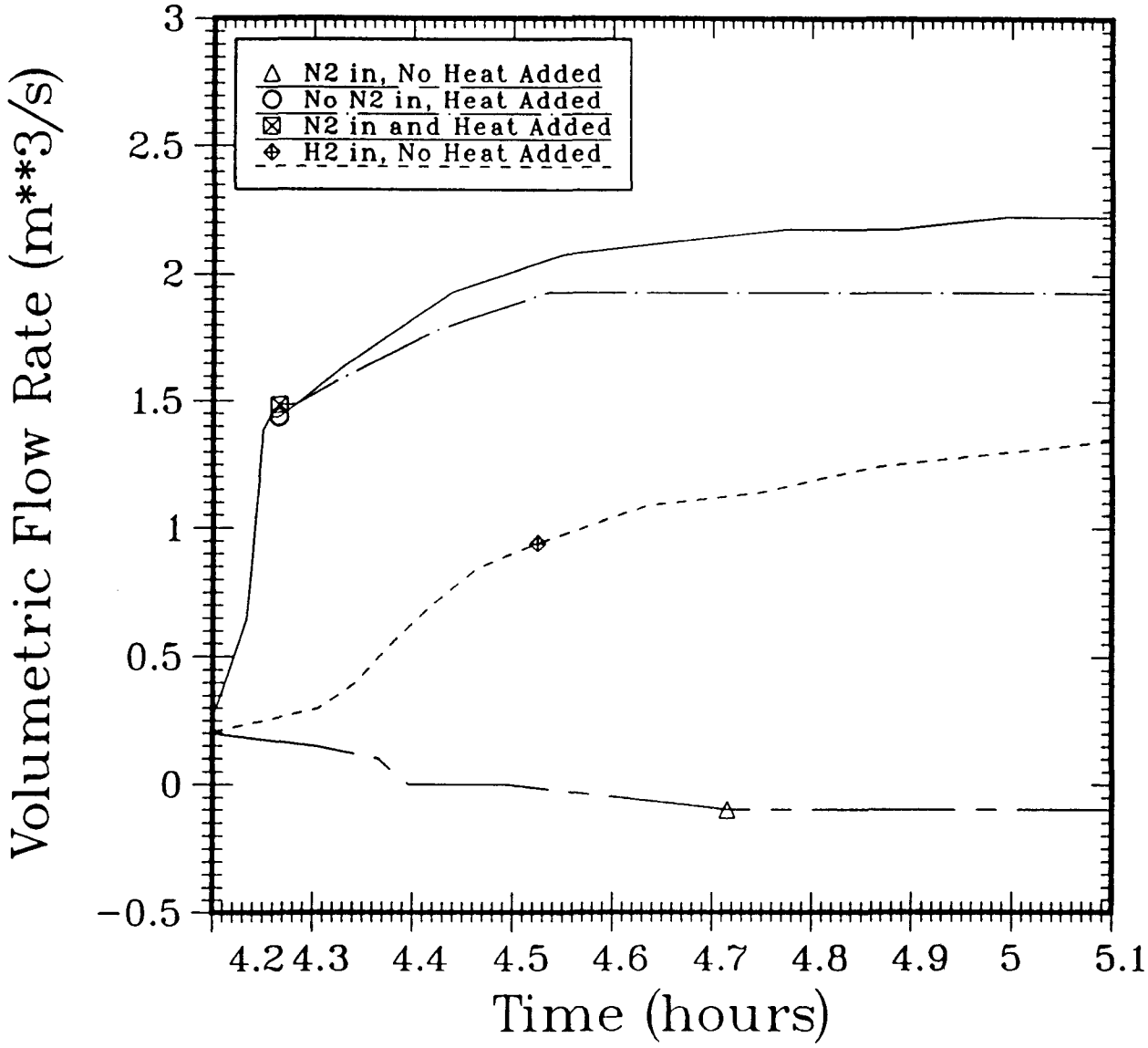

Figure 33. Comparison of Volumetric Flow Rate at the Tunnel With Respect to Different Sources and Conditions

5. CONCLUSIONS

Since HECTR is using the sources and initial conditions generated by the MAAP code, the completed HECTR results do not represent our best estimate of the pressure-temperature response of an ice-condenser containment during an S2HF accident. These HECTR analyses are intended to develop an understanding of the differences in the combustion models between two computer codes.

HECTR analyses of the containment responses of an ice-condenser plant for an S2HF drain-closed-accident sequence have shown that assuming a complete in-cavity oxidation may be overly optimistic because a variety of phenomena may occur. These phenomena will reduce the degree of in-cavity oxidation that takes place. Bounding calculations were performed to consider the effect of uncertainty in modeling some of these phenomena (e.g., steam inerting).

The effect of steam inerting could be very important under certain conditions, even though HECTR results of two bounding calculations did not directly show it for this particular accident sequence. For example, if there is sufficient oxygen being transported into the reactor cavity to support complete oxidation of the combustible gases, the effect of steam inerting would become important. For the case ignoring the steam inerting effect, a complete in-cavity oxidation would be predicted and no accumulation and subsequent combustion of hydrogen and carbon monoxide would occur in the upper and lower compartments. However, for the case including the steam inerting effect, an incomplete in-cavity oxidation and a global burn could occur. This would lead to a much higher peak pressure than the case excluding the effect, 411 vs 220 kPa. Thus the steam inerting effect could be substantial.

It is very important to model the lower compartment correctly. HECTR overpredicted the natural convective flow between the cavity and lower compartment and predicted a complete in-cavity oxidation when a single control volume was used to represent the lower compartment. However, when using five control volumes to represent the lower compartment, HECTR results showed that the lower compartment was not well mixed and the natural convective current into the cavity was lower than the prediction when one control volume represented the lower compartment. An incomplete in-cavity oxidation was predicted. This led to an accumulation and subsequent combustion of combustible gases in the upper and lower compartment at 7.4 hours. This global burn generated a peak pressure of 384 kPa (56 psia) that the single-volume model did not predict.

6. REFERENCES

1. A. Camp, M. Wester, and S. Dingman, HECTR Version 1.0 User's Manual, Sandia National Laboratories, Albuquerque, N.M., NUREG/CR-3913, SAND84-1522, February 1985.

2. S. Dingman, A. Camp, C.C. Wong, D. King, and R. Gasser, HECTR Version 1.5 User's Manual, Sandia National Laboratories, Albuquerque, N.M., NUREG/CR-4507, SAND86-0101, April 1986.

3. MAAP, Modular Accident Analysis Program, User's Manual - Volume II, IDCOR Technical Report 16.2-3, August 1983.

4. C. Channy Wong, A Standard Problem for HECTR-MAAP Comparison: Incomplete Burning, Sandia National Laboratories, Albuquerque, N.M., NUREG/CR-4993, SAND87-1858, July 1988.

5. Letter from Marty Plys, Fauske & Associates, Inc., to C. Channy Wong, Sandia National Laboratories, Albuquerque, dated October 8, 1985.

6. Sequoyah Nuclear Plant - Integrated Containment Analysis, IDCOR Task 23.1 Final Report, December 1984.

7. S.R. Ivanauskas, M.L. Corradini, Sensitivity Study on the Momentum Equation in the HECTR Computer Model, UWRSR No. 47, University of Wisconsin, Madison, WI, July 1986.

8. M. J. Wester and A. L. Camp, An Evaluation of HECTR Predictions of Hydrogen Transport, Sandia National Laboratories, Albuquerque, N.M., NUREG/CR-3463, SAND83-1814, September 1983.

9. M. J. Wester, D. J. Rzepecki, and A. L. Camp, "Evaluation of HECTR Predictions of Hydrogen Transport," Proceedings of the International Meeting on Light Water Reactor Severe Accident Evaluation, Cambridge, MA, P. 16.8-1 to 16.8-8, August 1983.

10. G.G. DeSoete, The Flammability of Hydrogen-Oxygen-Nitrogen Mixtures at High Temperature, La Rivista dei Combustibili, Vol. XXIX, No. 5-6, P. 166-172, May-June 1975.

11. M. Sheldon, Understanding Auto-ignition Temperature, Fire Engineers Journal, Vol. 43, No. 133, P. 27 - 32, June 1984.

12. D.A. Powers, Sustained Molten Steel/Concrete Interactions Tests, Sandia National Laboratories, Albuquerque, N.M., NUREG/CR-0166, SAND77-1423, June 1978.

13. B. Marshall, Hydrogen:Air:Steam Flammability Limits and Combustion Characteristics in the FITS Vessel, Sandia National Laboratories, Albuquerque, N.M., NUREG/CR-3468, SAND84-0383, December 1986.

14. J.E. Shepherd, Hydrogen-Steam Jet-Flame Facility and Experiments, Sandia National Laboratories, Albuquerque, N.M., NUREG/CR-3638, SAND84-0060, February 1985.

15. B. Lewis and G. Von Elbe, Combustion, Flames and Explosions of Gases, P. 259, 2nd Edition, Academic Press, New York (1961).

16. Sequoyah Nuclear Plant, Units 1 and 2. License Application, Final Safety Analysis Report, Volume 5, Tennessee Valley Authority, DOCKET-50327-77, April 1981.

17. A. Camp, V. Behr, and F. Haskin, MARCH-HECTR Analysis of Selected Accidents in an Ice-Condenser Containment, Sandia National Laboratories, Albuquerque, N.M., NUREG/CR-3912, SAND83-0501, December 1984.

18. S. Dingman, and A. Camp, "Pressure-Temperature Response in an Ice-Condenser Containment for Selected Accidents", Proceedings of the 13th Water Reactor Safety Research Information Meeting, Gaithersburg, Maryland, NUREG/CP-0072, Vol. 1, P. 223-243, October 22-25, 1985.

19. M.G. Zabetakis, Research on the Combustion and Explosion Hazards of Hydrogen-Water Vapor-Air Mixtures, Bureau of Mines, Division of Explosives Technology, Pittsburgh, PA., NTIS, USAEC Report AECU-3327, September 1957.

20. H. Tamm, R.K. Kumar, W.C. Harrison, "A Review of Recent Experiments at WNRE on Hydrogen Combustion," in Proceedings of the Second International Conference on the Impact of Hydrogen Water Reactor Safety, NUREG/CP-0038, EPRI RP1932-35, SAND82-2456, P. 633-650, October 1982.

APPENDIX A

GAS RELEASE RATES PREDICTED BY THE CORCON PROGRAM

In section 2, we have raised questions about MAAP predictions of the timing and release rate of gases generated from core-concrete interactions for the S2HF accident in a PWR ice-condenser containment. In order to assess MAAP predictions of gases released from core-concrete interactions, David R. Bradley of Sandia National Laboratories had used the CORCON code [A.1], a computer code developed at Sandia National Laboratories for predicting the nature of a high-temperature core debris attack on concrete, to calculate the gas release rates produced from core-concrete interactions under similar accident conditions as specified in MAAP. Figure A.1 compares the gas release rates in terms of volumetric flow rate per second predicted by the CORCON and MAAP codes. There are substantial differences in the timing and rate of gases released from core-concrete interactions that are predicted by the codes. To resolve these differences, one needs to review these two codes (CORCON and MAAP) in detail. Since it is beyond my task to compare the modeling differences between these two codes with respect to core-concrete interactions, my interest will concentrate on the impact of these differences on the containment loadings, that is, to study the containment response with respect to different source release rates. In the following HECTR calculation, I will use the gas release rates predicted by CORCON and the direct and indirect energy transfer rate between the corium and the reactor cavity predicted by MAAP, and perform a HECTR analysis to study the containment response.

The results of the HECTR analysis of the new problem are shown in Figs. A.2 to A.5. Fig. A.2 plots the mole fraction of gases existing in the reactor cavity during core-concrete interactions. At 5.6 hours, there was not sufficient oxygen in the cavity to support a complete in-cavity oxidation. Hydrogen started to build up in the containment. The accumulation of hydrogen led to a global deflagration at 6.18 hours and several local burns in the lower compartment. The burnings occurred at an earlier time than the HECTR analyses which used the gas release rates predicted by MAAP. The calculated pressure and temperature responses in the lower and upper compartments are presented in Figs. A.3 and A.4, respectively. The peak combustion pressure is lower than the other HECTR analysis using the gas release rates predicted by MAAP, 313 kPa (45.4 psig) vs 384 kPa (55.7 psig). The bulk gas temperature in the cavity predicted by HECTR is shown in Fig. A.5. The temperature was high enough to autoignite.

REFERENCES

A.1 R.K. Cole, D.P. Kelly, M.A. Ellis, CORCON-Mod2: A Computer Program for Analysis of Molten-Core Concrete Interactions, Sandia National Laboratories, Albuquerque, N.M., NUREG/CR-3912, SAND84-1246, August 1984.

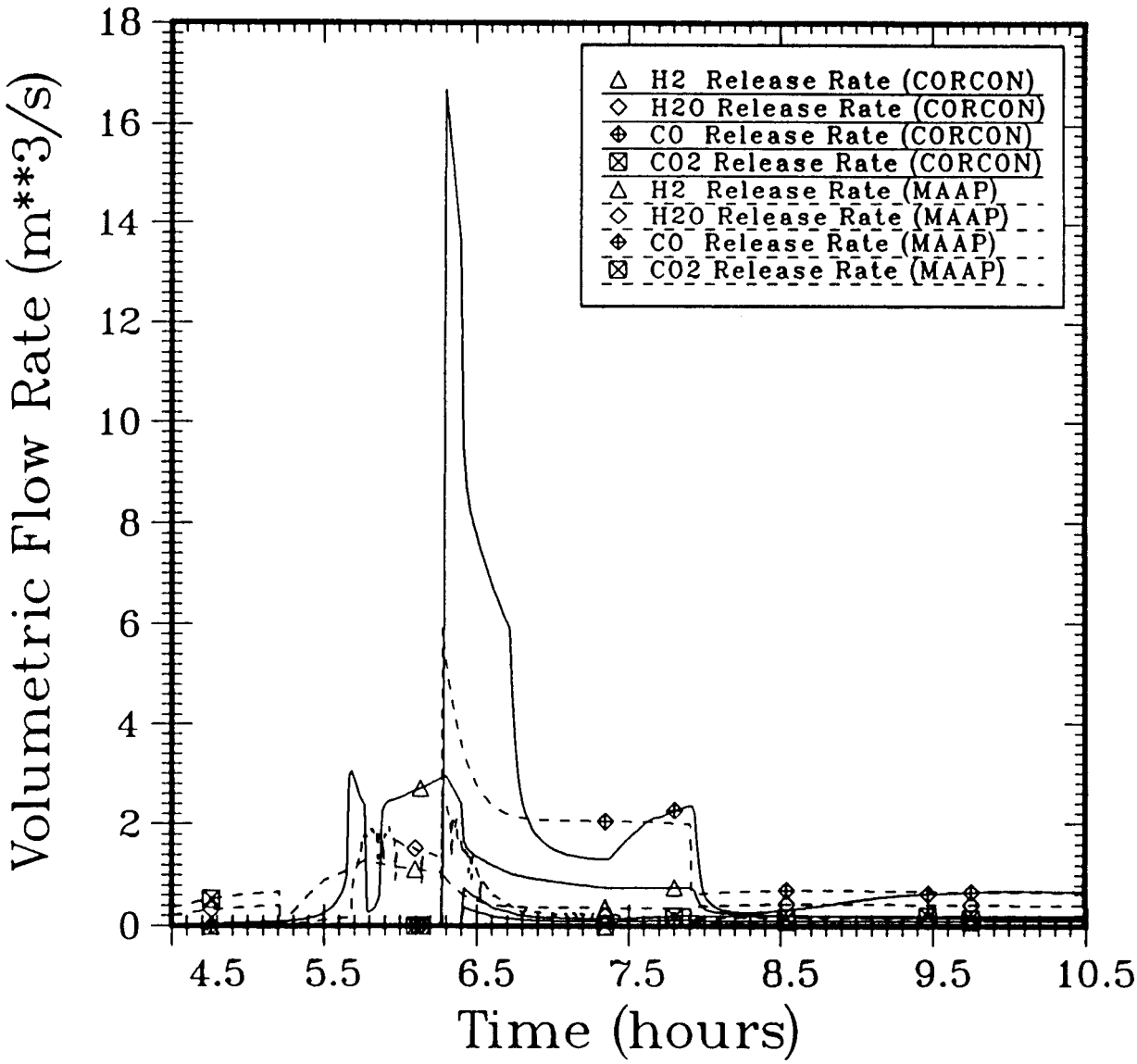

Figure A.1a. Comparison of Gas Release Rates from Core-Concrete Interactions Predicted by CORCON and MAAP.

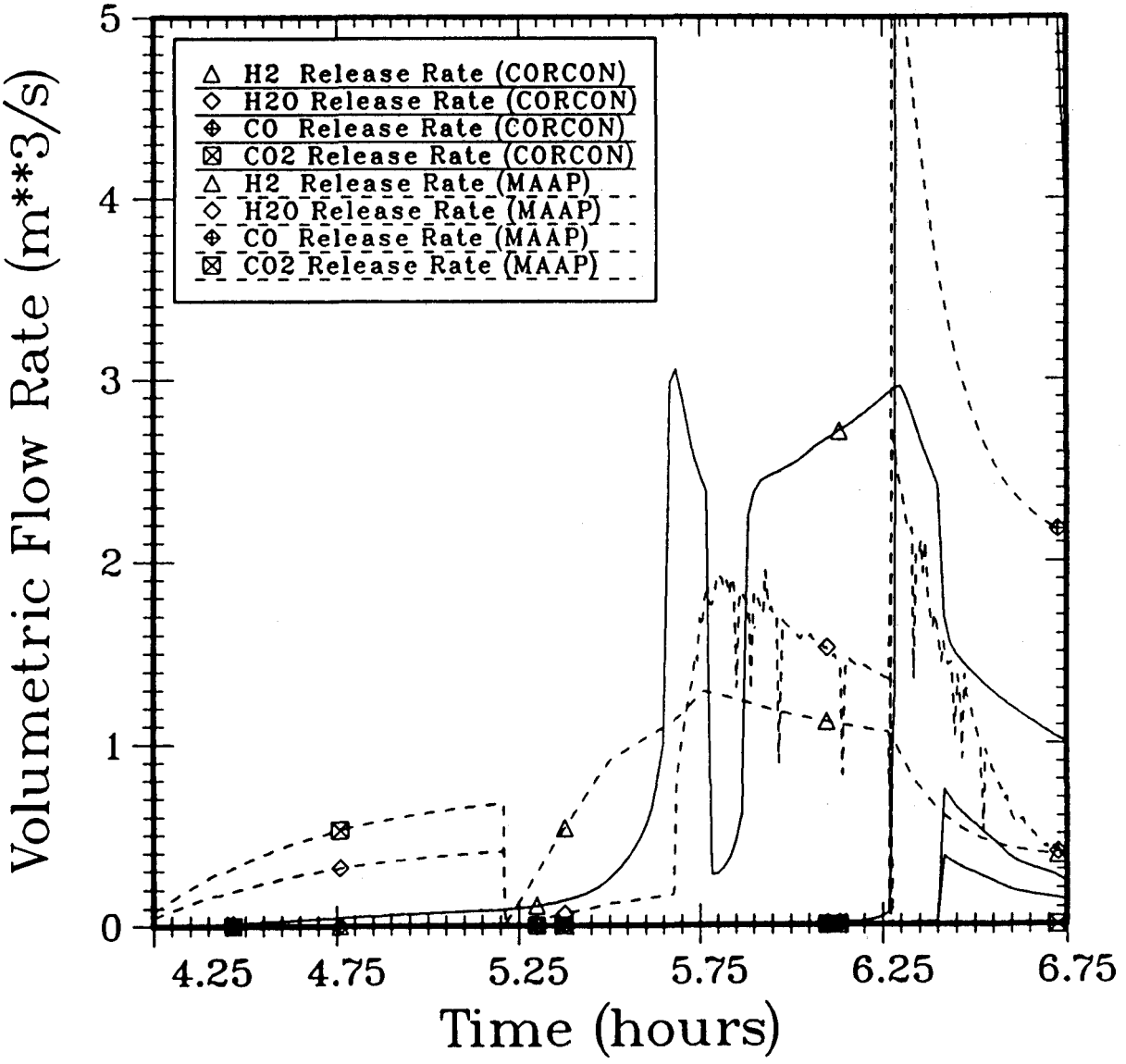

Figure A.1b. Comparison of Gas Release Rates from Core-Concrete Interactions Predicted by CORCON and MAAP.

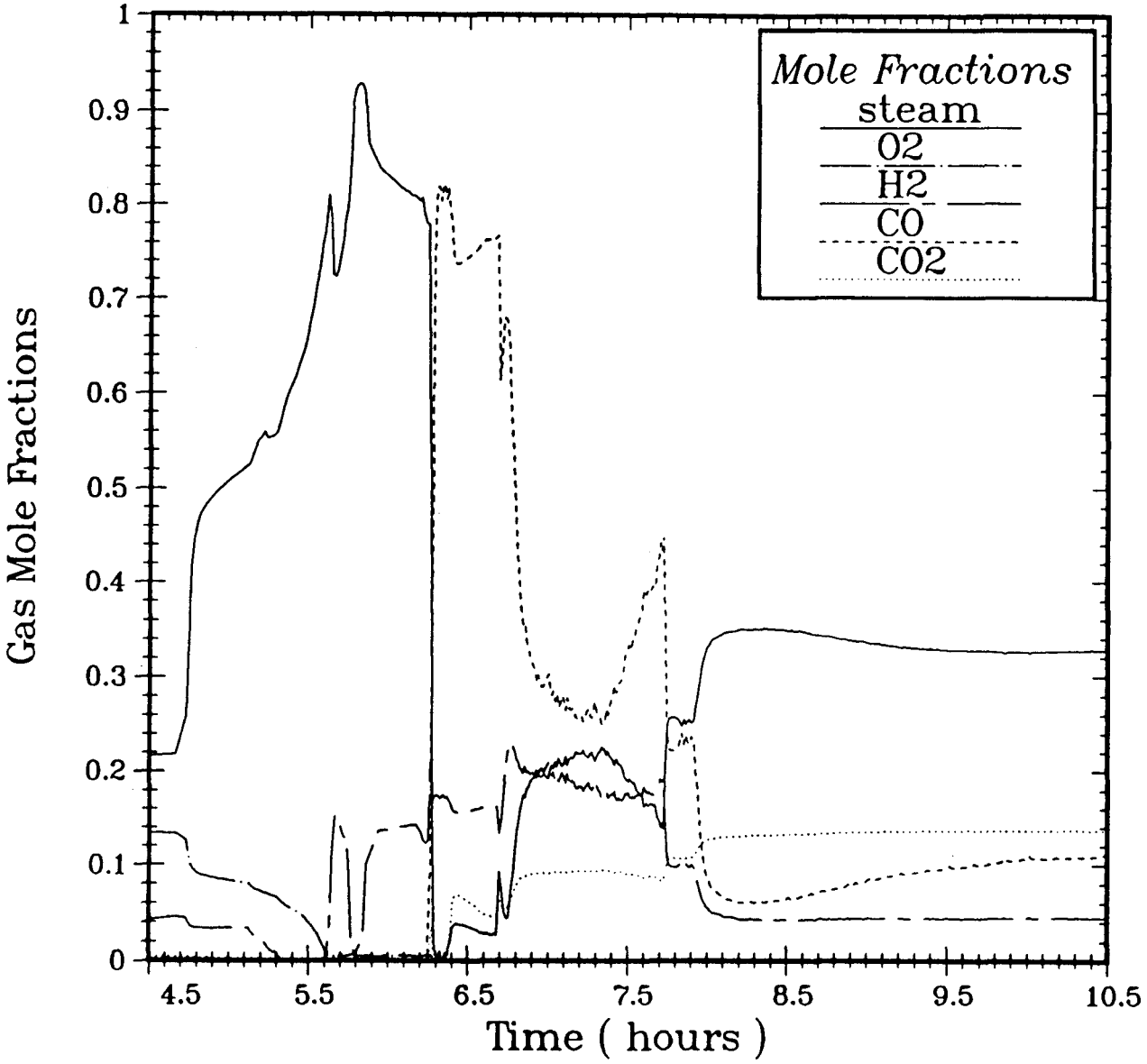

Figure A.2. Mole Fraction of Gases in the Reactor Cavity During Core-Concrete Interactions and In-Cavity Oxidation Predicted by HECTR.

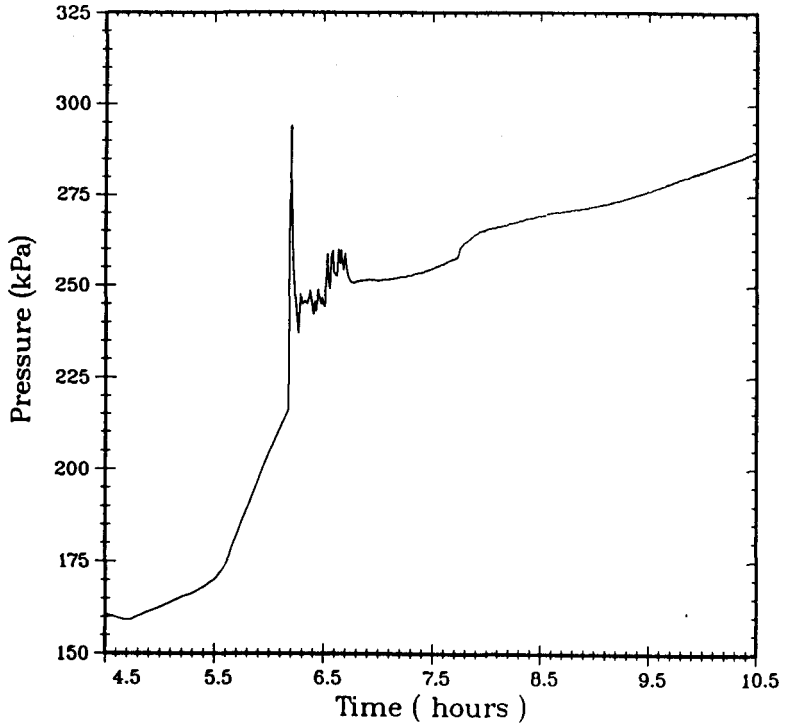

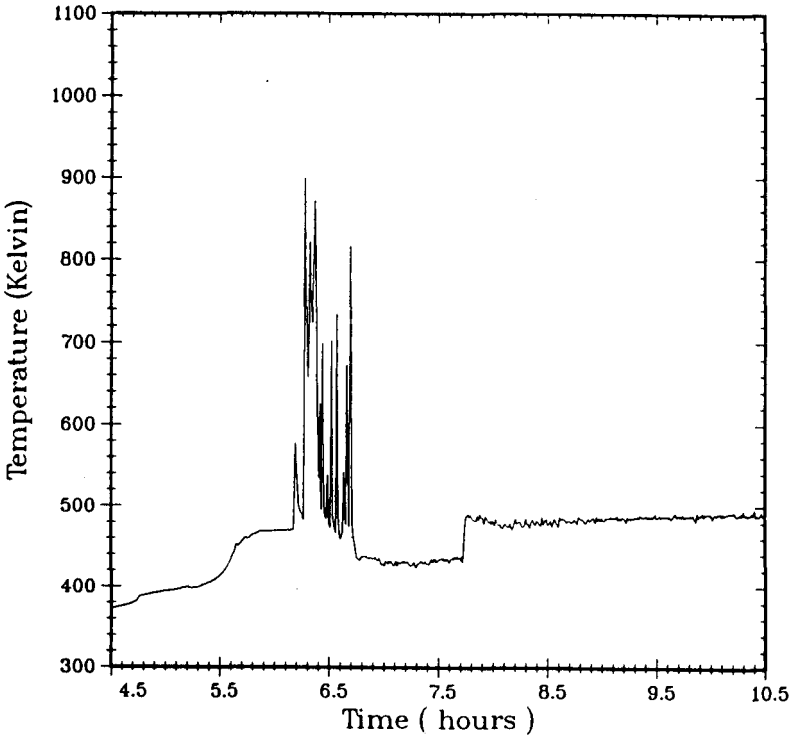

Figure A.3. Pressure and Temperature Responses in the Lower Compartment Predicted by HECTR (12-Compartment Model with CORCON Sources; Conditions for Continuous In-cavity Oxidation: $O_2 \geq 0\%$ and steam $\leq 100\%$).

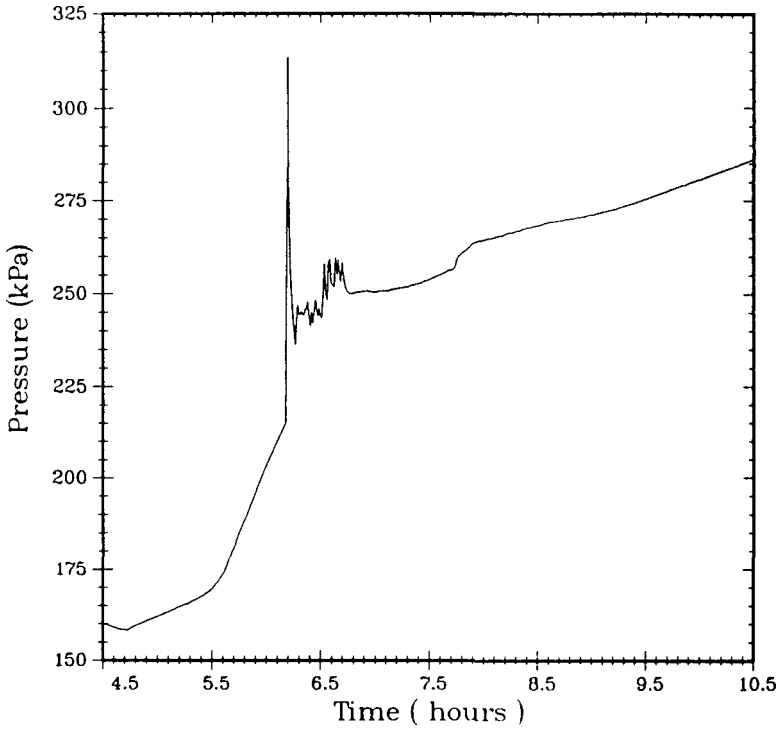

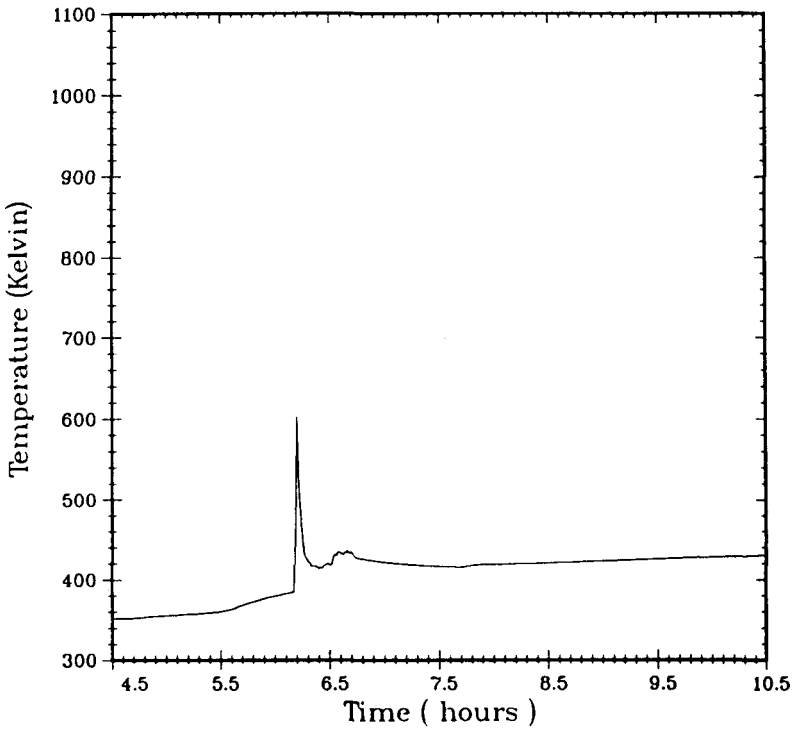

Figure A.4. Pressure and Temperature Responses in the Upper Compartment Predicted by HECTR (12-Compartment Model with CORCON Sources; Conditions for Continuous In-cavity Oxidation: $O_2 \geq 0\%$ and steam $\leq 100\%$).

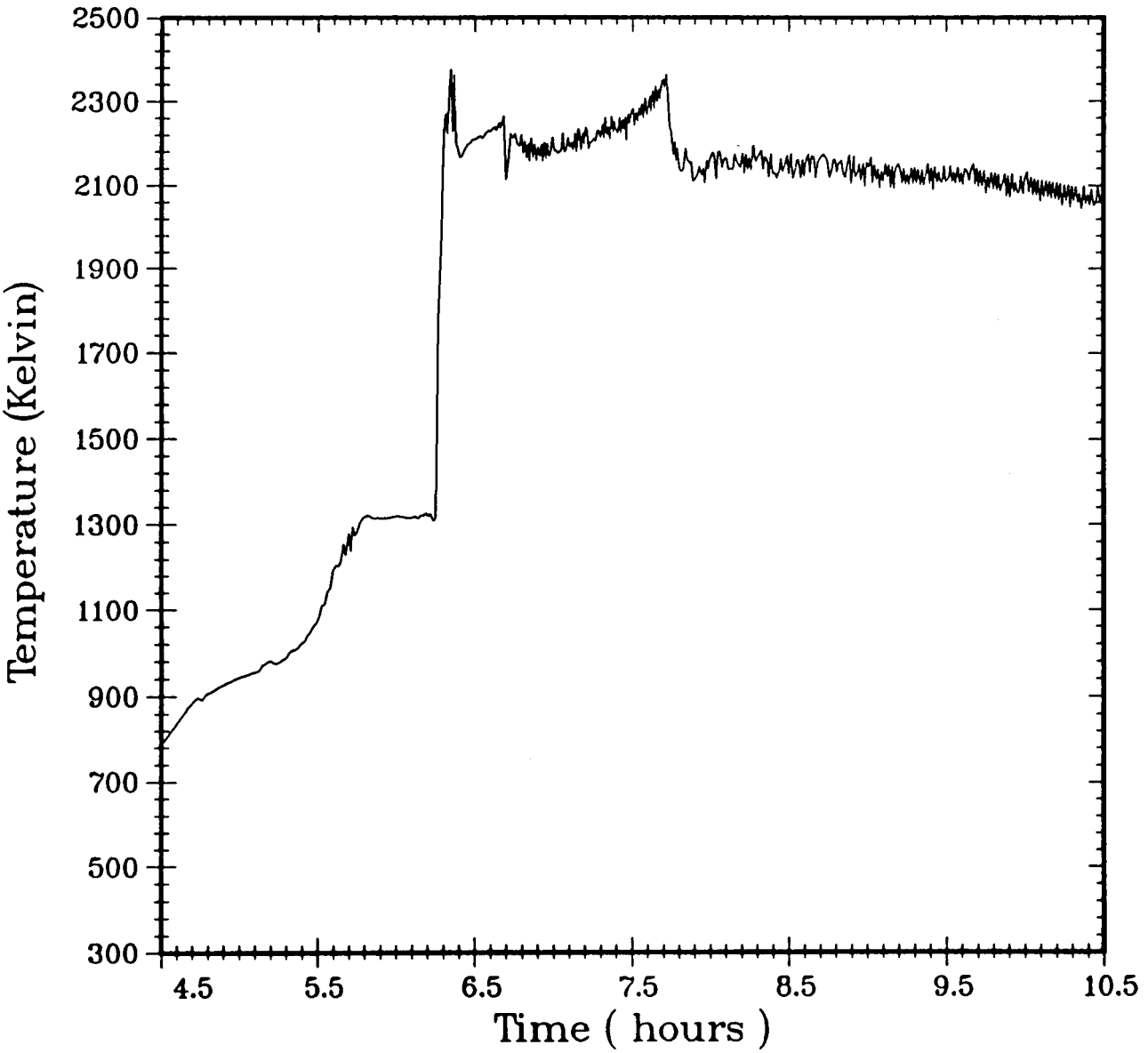

Figure A.5. Temperature Response in the Reactor Cavity Predicted by HECTR (12-Compartment Model with CORCON Sources; Conditions for Continuous In-cavity Oxidation: $O_2 \geq 0\%$).

APPENDIX B

HECTR INPUT FOR THE STANDARD PROBLEM

This appendix contains all of the HECTR input information used in the second part of the standard problem. They are listed in the following order: (1) HECTR 12-compartment model, (2) HECTR 6-compartment model, and (3) HECTR/MAAP 6-compartment model.

(1) HECTR 12-Compartment Model

```
!$$$$$$$$$$$$$$$$$$$$$$$$$$$$$$$$$$$$$$$$$$$$$$$$$$$$$$$$$$$$$$$$$$$$$$$
!       ICE CONDENSER INPUT DECK
!$$$$$$$$$$$$$$$$$$$$$$$$$$$$$$$$$$$$$$$$$$$$$$$$$$$$$$$$$$$$$$$$$$$$$$$
ICE CONDENSER CONTAINMENT$

THIS IS THE INPUT DECK FOR ICE CONDENSER STANDARD PROBLEM.
DATA ARE REDUCED FROM THE 41 COMPARTMENT MODEL AND MARCH-HECTR REPORT.
15 VOLUMES, 1-D ICE BED ARE TREATED IN THIS CASE.
REFUELING CANAL HAS BEEN DELETED BECAUSE IT IS FULL OF WATER
LOWER BOUND FAILURE PRESSURE (36 PSIG / 350000 Pa)
PART II: EX-VESSEL HYDROGEN PRODUCTION FROM CORE-CONCRETE INTERACTION
ICE-CONDENSER BECOMES COMPARTMENT 12

12 ! NUMBER OF COMPARTMENTS INCLUDING THE NEW ICE COMPARTMENT
!
! FOR EACH COMPARTMENT: THE VOLUME, ELEVATION, FLAME PROPAGATION
! LENGTH, NUMBER OF SURFACES, AND INTEGERS SPECIFYING WHICH SUMP
! TO DUMP EXCESS WATER (FROM SUPERSATURATION) INTO AND WHICH SUMP
! THE SPRAYS FALL INTO.
!
! WHERE SIMILAR NUMBERED COMPARTMENTS OCCUR ,E.G. C2 - C5,
! THEY ARE SPECIFIED BY COUNTING CLOCKWISE FROM THE REFUELING
! CANAL.
!
C1 - REACTOR CAVITY
382.89      0.      10.     2     1     1
C2 - REACTOR SPACE
439.        16.15   3.9     2     1     1
C3 - LOWER COMPARTMENT 1 (CONNECT TO CAVITY & PRESSURIZER)
938.30      12.33   7.71    3     2     2
C4 - PRESSURIZER DOGHOUSE
135.        26.95   13.6    2     2     2
```

```
C5 - LOWER COMPARTMENT 2 (STEAM GENERATORS)
2196.63     12.33    7.71     3      2      2
C6 - SG DOGHOUSE
1450.0      26.95    13.58    2      2      2
C7 - ANNULUS
2658.96     10.56    13.30    2      2      2
C8 - LOWER PLENUM
681.06      18.75    3.5      3      3      3
C9 - UPPER PLENUM
1330.       37.60    9.0      1      3      3
C10 - UPPER COMPARTMENT - DOME
12764.78    44.20    17.53    3      4      4
C11 - LOWER DOME
4590.95     27.71    13.89    2      4      4
C12 - ICE CONDENSER
3654.50     27.69    14.53    2      2      2
!
! FOR EACH SUMP, SUMP NUMBER, MAXIMUM VOLUME, SUMP NUMBER THAT
! THIS SUMP OVERFLOWS TO
!
1 396.  2  ! SUMP IN REACTOR CAVITY
2 1450. 1  ! LOWER COMPARTMENT SUMP
3 16.50 2  ! LOWER PLENUM SUMP (2 INCH DEPTH)
4 1300. 0  ! REFUELING CANAL SUMP (2 INCH DEPTH - NO SPRAYS)
$
!
! FOR EACH SURFACE: TYPE OF SURFACE, MASS OF SURFACE, AREA OF
! SURFACE, CHARACTERISTIC LENGTH, SPECIFIC HEAT, EMISSIVITY,
! INTEGER INDICATING WHICH SUMP THE CONDENSATE GOES INTO.  FOR
! SLABS (STYPE = 1), THE NUMBER OF LAYERS IN THE SURFACE, AND FOR
! EACH, THE THICKNESS, THERMAL DIFFUSIVITY, AND THERMAL
! CONDUCTIVITY.  FINALLY, THE NODING INFORMATION AND BOUNDARY
! CONDITIONS ARE SPECIFIED (0'S INDICATE THE CODE WILL DETERMINE
! THE VALUES INTERNALLY). NOTE THAT SOME OF THE NUMBERS SET TO 1.
! ARE NOT USED FOR THAT SURFACE TYPE.
!
! REACTOR CAVITY - C1 - SURFACES 1 - 2
!
SUMP 1
3  1.311E4   59.20    5.18  1.0   0.94   1
!
RC CONCRETE
1  1.   234.86   5.18  854.15  0.9    1
1
1.524   7.18E-7  1.453
0  0.   0.       0.
!
! REACTOR SPACE - C2 - SURFACES 3 - 4
!
```

```
RS STEEL
1  1.    207.93    1.83  1.     0.9     1
1
0.069    1.28E-5   47.25
0  0.    0.        0.
!
RS CONCRETE
1  1.    247.36    9.14  1.     0.9     1
1
1.       5.8E-7    1.454
0  0.    0.        0.
!
! LOWER COMPARTMENT- C3 - SURFACES 5 - 7
!
LC1 STEEL
1  1.    611.      2.     1.     0.9     2
1
0.069    1.28E-5   47.25
0  0.    0.        0.
!
LC1 CONCRETE
1  1.    726.87    2.     1.     0.9     2
1
0.1      5.8E-7    1.454
0  0.    0.        0.
!
LC1 SUMP
3  3.517E5  105.9     11.    1.     0.94    2
!
! PRESSURIZER - C4 - SURFACES 8 - 9
!
PR STEEL
1  1.    63.94     1.     1.     0.9     2
1
0.069    1.28E-5   47.25
0  0.    0.        0.
!
PR CONCRETE
1  1.    76.07     1.     1.     0.9     2
1
0.1      5.8E-7    1.454
0  0.    0.        0.
!
! LOWER COMPARTMENT- C5 - SURFACES 10 - 12
!
LC2 STEEL
1  1.    1430.37   2.     1.     0.9     2
1
0.069    1.28E-5   47.25
0  0.    0.        0.
```

```
!
LC2 CONCRETE
1  1.    1701.     2.     1.     0.9     2
1
0.1      5.8E-7    1.454
0  0.    0.        0.
!
LC2 SUMP
3  8.234E5  247.      10.67 1.     0.94    2
!
! STEAM GENERATOR ENCLOSURES (INSIDE) - C6 - SURFACES 13 - 14
!
SG STEEL
1  1.    686.77    1.     1.     0.9     2
1
.069     1.28E-5   47.25
0  0.    0.        0.
!
SG CONCRETE
1  1.    817.03    1.     1.     0.9     2
1
0.1      5.8E-7    1.454
0  0.    0.        0.
!
! ANNULUS AROUND LOWER COMPARTMENT - C7 - SURFACES 15 - 16
!
A STEEL
1  1.    1834.     4.     1.     0.9     2
1
0.031    1.28E-5   47.25
0  0.     0.     0.
!
A CONCRETE
1  1.    3257.     4.     1.     0.9     2
1
0.448    5.8E-7    1.454
0  0.    0.        0.
!
! LOWER PLENUM COMPARTMENTS - C8 - SURFACES - 17 - 19
!
LP SUMP
3  3.940E3  310.0    4.     1.     0.94    3
!
LP WALL
1  1.    280.      3.     1.     0.9     3
1
0.013    1.28E-5   47.25
0  0.    0.        0.
!
```

```
LP IC SUPPORT
1  1.    2660.     0.2    1.     0.9     3
1
0.0081   1.28E-5   47.25
0  0.    0.        0.
!
! UPPER PLENUM COMPARTMENTS - C9 - SURFACES 20
!
UP STEEL
1  1.    1000.     5.     1.     0.9     3
1
0.013    1.28E-5   47.25
0  0.    0.        0.
!
! UPPER COMPARTMENTS - C10 - SURFACES 21 - 23
!
UC DOME
1  1.    1762.     8.     1.     0.9     4
1
0.0127   1.28E-5   47.25
0  0.    5.        300.
!
UC CONCRETE
1  1.    648.73    5.     1.     0.9     4
1
0.91     5.8E-7    1.454
0  0.    0.        0.
!
UC STEEL
1  1.    2000.     1.     1.     0.9     4
1
0.013    1.28E-5   47.25
0  0.    0.        0.
!
! LOWER DOME REGION - C11 - SURFACE 24
!
LDR CONCRETE
1  1.    1822.14   14.    1.     0.9     4
1
0.91     5.8E-7    1.454
0  0.    0.        0.
!
! REFUELING CANAL SPACE - C11 - SURFACES 25
!
RC SUMP
3  1.261E6  67.75     6.     1.     0.94    4
!
! ICE COMPARTMENT - C12 - SURFACES 26 - 27
IC WALL+STRUCTURE
2  2.000E5   2058.00   14.53   485.7   0.9    2
```

```
!
IC BASKET
2  1.470E5   9920.00   14.53   460.5   0.9   2
!
$ NO CONTAINMENT LEAKS
!
! FLOW JUNCTION DATA: COMPARTMENT ID'S, TYPE OF CONNECTION, FLOW
! AREA, LOSS COEFFICIENT, L/A RATIO, RELATIVE POSITION OF
! COMPARTMENTS, AND JUNCTION ELEVATION. COMPARTMENT ID OF 0 INDICATES
! THE ICE CONDENSER.  JUNCTIONS WITHIN THE ICE CONDENSER ARE SET UP
! INTERNALLY.  ADDITIONAL INFORMATION IS PROVIDED FOR JUNCTION TYPES
! 3 AND 4.
!
1   3   1   4.95     3.     1.72    1   2.98
1   2   1   1.031    10.    11.82   1   0.668
2   3   1   7.45     4.     0.94    0   19.47
2   5   1   15.04    4.     0.47    0   19.47
3   7   1   8.80     4.2    0.68    0   10.60
3   8   3   29.64    1.     0.20    1   19.00
0.  0.  142.07  0.96
3   4   1   4.30     1.0    3.42    1   20.00
3   4   1   4.30     1.0    3.42    1   20.32
3   5   1   93.50    5.     0.17    0   12.30
5   7   1   18.89    4.2    0.32    0   10.60
5   8   3   69.16    1.     0.087   1   19.00
0.  0.  142.07  0.96
5   6   1   31.72    1.1    0.46    1   20.00
5   6   1   31.71    1.1    0.46    1   20.32
8  12   1   91.88    1.     0.038   1   20.42
12  9   1   1.86     10.    2.30    1   35.05
12  9   3   91.30    1.     0.047   1   35.05
0.  263.4   37910.  1.55
9   10  1   186.00   1.     0.035   1   40.16
10  11  1   363.12   1.     0.045  -1   34.65
11  5   4   0.204    1.5   10.00    1    7.86
2  750.
10  7   1   0.0022   10.   2277.0  -1   10.60
$
!
! ICE CONDENSER INPUT
!
$ ICE CONDENSER IS REPRESENTED AS COMPARTMENT 12
!
$ NO SUPPRESSION POOL
!
! FAN DATA
! TEMP. AND PRESS. SETPOINTS, DELAY TIME, AND TIME TO TURN OFF. HIGH
! VALUE FOR TEMP. SETPOINT INDICATES THAT VALUE WON'T BE USED.
10000.  121590.  600.  1.E10
```

```
! COMPARTMENT ID'S, FLOW RATE (- INDICATES USE OF HEAD CURVE),
! SHUTOFF
! HEAD (PA), EFFICIENCY, RELATIVE POSITION OF COMPARTMENTS.
11   7   -35.54 1327.3575  1.   -1
10   7   0.9439 1327.3575  1.   -1
6    7   0.1775 1327.3575  1.   -1
4    7   0.7079 1327.3575  1.   -1
2    7   0.2832 1327.3575  1.   -1
! SHUTOFF
! HEAD (PA), EFFICIENCY, RELATIVE POSITION OF COMPARTMENTS.
$ END OF FANS TABLE
$ END OF FANS INPUT
$ NO FAN COOLERS
!
! RADIATIVE BEAM LENGTHS - UPPER RIGHT HALF OF MATRIX IS INPUT.
! ICE SURFACES ARE NOT INCLUDED HERE. (THEY ARE DONE INTERNALLY)
!
! BEAM LENGTHS
!
   4.848000      4.848000      25*0.0
   4.848000      25*0.0
   3.471194      3.471194      23*0.0
   3.471194      23*0.0
   3.216579      3.216579      3.216579      20*0.0
   3.216579      3.216579      20*0.0
   3.216579      20*0.0
   3.471181      3.471181      18*0.0
   3.471181      18*0.0
   3.218120      3.218120      3.218120      15*0.0
   3.218120      3.218120      15*0.0
   3.218120      15*0.0
   3.471206      3.471206      13*0.0
   3.471206      13*0.0
   1.882381      1.882381      11*0.0
   1.882381      11*0.0
   0.7587692     0.7587692     0.7587692      8*0.0
   0.7587692     0.7587692     8*0.0
   0.7587692     8*0.0
   4.788000      7*0.0
   10.41850      10.41850      10.41850       4*0.0
   10.41850      10.41850      4*0.
   10.41850      4*0.0
   9.484990      9.484990      2*0.0
   9.484990      2*0.0
   1.098400      1.098400
   1.098400
 !
```

```
 ! VIEW FACTORS
 !
  0.2013000       0.7987000       25*0.0
  0.7987000       25*0.0
  0.4566979       0.5433021       23*0.0
  0.5433021       23*0.0
  0.4231976       0.5034528       7.3349632E-02   20*0.0
  0.5034528       7.3349632E-02   20*0.0
  7.3349714E-02   20*0.0
  0.4566817       0.5433183       18*0.0
  0.5433183       18*0.0
  0.4233906       0.5034972       7.3112182E-02   15*0.0
  0.5034972       7.3112175E-02   15*0.0
  7.3112249E-02   15*0.0
  0.4566897       0.5433103       13*0.0
  0.5433103       13*0.0
  0.3602436       0.6397564       11*0.0
  0.6397564       11*0.0
  9.5384613E-02   8.6153843E-02   0.8184615       8*0.0
  8.6153850E-02   0.8184615       8*0.0
  0.8184615       8*0.0
  1.000000        7*0.0
  0.3994804       0.1470800       0.4534397       4*0.0
  0.1470800       0.4534397       4*0.0
  0.4534397       4*0.0
  0.9641514       3.5848647E-02   2*0.0
  3.5848618E-02   2*0.0
  0.1718000       0.8282000
  0.8282000
!
! SPRAY INPUT
! NUMBER OF COMPARTMENTS WITH SPRAYS, AND ID OF THOSE
! COMPARTMENTS. SPRAY TEMP DURING INJECTION PHASE, FLOW RATE
! (M**3/S), NUMBER OF DROP SIZES, FREQUENCY AND DIAMETER
! (MICRONS) FOR EACH DROP SIZE.
1
10  313.56  0.593  2
0.95  309.
0.05  810.
! SPRAY CARRYOVER
10  11  1.
11  12  0.13
$
! COMPARTMENT ID AND SPRAY FALL HEIGHT FOR THAT COMPARTMENT.
10  14.72
11  13.88
12  12.87
$
```

```
! TEMPERATURE AND PRESSURE SETPOINTS, DELAY TIME FOR SPRAYS,
! TIME THAT SPRAYS REMAIN OPERATIVE AFTER INITIATION.
! HIGH TEMPERATURE INDICATES THAT NUMBER WON'T BE USED.
10000.  121590.  30.  1.E10
! INJECTION TIME, RATED SPRAY FLOW RATE (KG/S), HEAT EXCHANGER
! RATED EFFECTIVENESS (W/K), SECONDARY SIDE INLET TEMP, RATED
! SECONDARY SIDE FLOW RATE (KG/S), SUMP THAT WATER IS DRAWN FROM.
! (FROM MARCH-HECTR REPORT) 2000.   587.   3.74E6   301.5   7.55E2   2
$ NO SPRAY RECIRCULATION (S2HF ACCIDENT SCENARIO)
$
! ************************************************************
! ENTER INITIAL CONDITIONS AND ACCIDENT SCENARIO INFORMATION
! ************************************************************
! SIMULATION TIME (END TIME = 20 HRS. OR 72000 SEC)
25000.
!
! COMPARTMENT INITIAL CONDITIONS: TEMP; PARTIAL PRESSURES OF
! STEAM, NITROGEN, OXYGEN, HYDROGEN, CARBON MONOXIDE,
! CARBON DIOXIDE ; CONVECTIVE VELOCITY.
!
! C1 - CAVITY
482.33  38479.  101756.  22710.  6582.  0.  711.  0.3
! C2 - REACTOR SPACE
367.02  37990.  101968.  22757.  6590.  0.  712.  0.3
! C3 - LOWER COMP 1 (PRESSURIZER)
367.02  37990.  101968.  22757.  6590.  0.  712.  0.3
! C4 - PRESSURIZER SPACE
367.02  37990.  101968.  22757.  6590.  0.  712.  0.3
! C5 - LOWER COMP 2 (STEAM GENERATOR)
367.02  37990.  101968.  22757.  6590.  0.  712.  0.3
! C6 - STEAM GEN DOGHOUSES
367.02  37990.  101968.  22757.  6590.  0.  712.  0.3
! C7 - ANNULUS
355.19  37768.  101960.  22754.  6589.  0.  712.  0.3
! C8 - LOWER PLENUM
367.02  37990.  101968.  22757.  6590.  0.  712.  0.3
! C9 - UPPER PLENUM
367.91  38151.  101878.  22735.  6584.  0.  711.  0.3
! C10 - UPPER COMPARTMENT
358.57  38783.  101363.  22622.  6550.  0.  707.  0.3
! C11 - LOWER DOME REGION
358.57  38783.  101363.  22622.  6550.  0.  707.  0.3
! C12 - ICE CONDENSER COMPARTMENT
367.66  38105.  101912.  22744.  6586.  0.  712.  0.3
!
! SOURCE TERM
!
$ STEAM SOURCE FROM EXTERNAL TABLE
$ NO NITROGEN SOURCES
```

```
$ NO OXYGEN SOURCES
$ HYDROGEN SOURCE FROM EXTERNAL TABLE
$ CO SOURCE FROM EXTERNAL TABLE
$ CO2 SOURCE FROM EXTERNAL TABLE
$ NO SUMP WATER REMOVAL
$ NO ENERGY SOURCES
!
! CONTINUOUS BURNING
!
1
1.0E-2  1000.0  0.005  1.00  2000.0  1.0
$ END OF CONTINUOUS BURNING INPUT
!
! INITIAL SURFACE TEMPERATURES
!
! C1  RC
347.91
570.17
! C2  RS
354.73
347.69
! C3  LC1
354.73
347.42
339.04
! C4  PR
354.73
347.69
! C5  LC2
354.73
347.42
339.04
! C6  SG
354.73
347.69
! C7  AN
345.00
342.92
! C8  LP
328.52
347.69
354.73
! C9  UP
354.73
! C10 UC
347.44
320.78
349.16
```

```
! C11
306.89
315.53
! C12
357.00
357.00
!
! NAMELIST INPUT
!
SPRAYS = OFF
FANS = ON
TIMZER=15043.62
PCHMAX=1000.
DTMPMX=50.
DPRSMX=30000.
XHMNIG(8)=1.
XHMNIG(12)=1.
$
```

(2) HECTR 6-Compartment Model

```
!$$$$$$$$$$$$$$$$$$$$$$$$$$$$$$$$$$$$$$$$$$$$$$$$$$$$$$$$$$$$$$$$$$$$$$$$
!       ICE CONDENSER INPUT DECK
!$$$$$$$$$$$$$$$$$$$$$$$$$$$$$$$$$$$$$$$$$$$$$$$$$$$$$$$$$$$$$$$$$$$$$$$$
ICE CONDENSER CONTAINMENT$

THIS IS THE INPUT DECK FOR ICE CONDENSER STANDARD PROBLEM.
DATA ARE REDUCED FROM THE HECTR 16 COMPARTMENT MODEL.
6 VOLUMES, 1-D ICE BED ARE TREATED IN THIS CASE.
LOWER BOUND FAILURE PRESSURE (65 PSIG / 448200 Pa)
PART II: EX-VESSEL H2 PRODUCTION
ICE-CONDENSER BECOMES COMPARTMENT 6


6  ! NUMBER OF COMPARTMENTS EXCLUDING ICE REGION
!
! FOR EACH COMPARTMENT: THE VOLUME, ELEVATION, FLAME PROPAGATION
! LENGTH, NUMBER OF SURFACES, AND INTEGERS SPECIFYING WHICH SUMP
! TO DUMP EXCESS WATER (FROM SUPERSATURATION) INTO AND WHICH SUMP
! THE SPRAYS FALL INTO.
!
! WHERE SIMILAR NUMBERED COMPARTMENTS OCCUR ,E.G. C2 - C5,
! THEY ARE SPECIFIED BY COUNTING CLOCKWISE FROM THE REFUELING
! CANAL.
!
```

```
C1 - REACTOR CAVITY
382.89      0.        10.0     2      1      1
C2 - LOWER COMPARTMENT
5839.99     16.23     17.5     6      2      2
C3 - ANNULUS
2658.96     10.56     13.3     2      2      2
C4 - UPPER PLENUM
1330.00     37.60     9.00     1      3      3
C5 - UPPER COMPARTMENT
17355.73    38.39     17.5     4      4      4
C6 - ICE COMPARTMENT
3654.50     27.69     14.53    2      2      2
! FOR EACH SUMP, SUMP NUMBER, MAXIMUM VOLUME, SUMP NUMBER THAT
! THIS SUMP OVERFLOWS TO
!
1 396.00   2   ! SUMP IN REACTOR CAVITY
2 1450.0   1   ! LOWER COMPARTMENT SUMP
3 16.493   2   ! LOWER PLENUM FLOOR (2 IN. DEPTH)
4 1300.0   0   ! REFUELING CANAL SUMP
$
!
! FOR EACH SURFACE: TYPE OF SURFACE, MASS OF SURFACE, AREA OF
! SURFACE, CHARACTERISTIC LENGTH, SPECIFIC HEAT, EMISSIVITY,
! INTEGER INDICATING WHICH SUMP THE CONDENSATE GOES INTO.  FOR
! SLABS (STYPE = 1), THE NUMBER OF LAYERS IN THE SURFACE, AND FOR
! EACH, THE THICKNESS, THERMAL DIFFUSIVITY, AND THERMAL
! CONDUCTIVITY.  FINALLY, THE NODING INFORMATION AND BOUNDARY
! CONDITIONS ARE SPECIFIED (0'S INDICATE THE CODE WILL DETERMINE
! THE VALUES INTERNALLY). NOTE THAT SOME OF THE NUMBERS SET TO 1.
! ARE NOT USED FOR THAT SURFACE TYPE.
!
! REACTOR CAVITY - C1 - SURFACE 1 - 2
!
SUMP 1
3  1.311E4    59.20     5.18  1.0      0.94    1
RC CONCRETE
1  1.    234.86    5.18  854.15  0.9     1
1
1.524    7.18E-7   1.453
0  0.    0.        0.
!
! LOWER COMPARTMENT- C2 - SURFACES 3 - 8
!
LC STEEL
1  1.    3000.0    2.     1.0      0.9     2
1
0.0690   1.28E-5   47.25
0  0.    0.0       0.0
!
```

```
LC CONCRETE
1  1.    3569.0    4.     1.0      0.9     2
1
0.10     5.8E-7    1.453
0  0.    0.0       0.0
!
LC SUMP
3  1.175E6    353.00    10.67 1.        0.94    2
!
LC - LP STEEL WALL
1  1.    280.00    3.     1.0      0.9     3
1
0.013    1.28E-5   47.25
0  0.    0.0       0.0
!
LC - IC SUPPORT STRUCTURE
1  1.    2660.0    0.2    1.0      0.9     3
1
0.0081   1.28E-5   47.25
0  0.    0.0       0.0
!
LC - LP FLOOR/SUMP
3  3.940E3    310.00    4.0    1.       0.94    3
!
! ANNULUS AROUND LOWER COMPARTMENT - C3 - SURFACES 9 - 10
!
AN STEEL
1  1.    1834.0    4.     1.       0.9     2
1
0.0310   1.28E-5   47.25
0  0.    0.0       0.0
!
AN CONCRETE
1  1.    3257.0    4.     1.       0.9     2
1
0.4480   5.80E-7   1.454
0  0.    0.0       0.0
!
! UPPER PLENUM - C4 - SURFACE 11
!
UP - STEEL
1  1.    1000.     5.     1.       0.9     3
1
0.013    1.28E-5   47.25
0  0.    0.0       0.0
!
! UPPER COMPARTMENT - C5 - SURFACES 12 - 15
!
```

```
UC - DOME
1  1.    1762.0    8.     1.       0.9     4
1
0.0127   1.28E-5   47.25
0  0.    5.0       300.0
!
UC - CONCRETE
1  1.    2937.48   10.    1.       0.9     4
1
0.910    5.80E-7   1.454
0  0.    0.0       0.0
!
UC EQUIPMENT - STEEL
1  1.    2000.     1.     1.       0.9     4
1
0.013    1.28E-5   47.25
0  0.    0.0       0.0
!
UC - REFUELING CANAL SUMP
3  1.261E6  67.75     6.     1.0      0.94    4
!
!
! ICE COMPARTMENT - C6 - SURFACES 16 - 17
IC WALL+STRUCTURE
2  2.000E5    2058.00    14.53    485.7    0.9    2
!
IC BASKET
2  1.470E5    9920.00    14.53    460.5    0.9    2
!
$ NO CONTAINMENT LEAKS
!
! FLOW JUNCTION DATA: COMPARTMENT ID'S, TYPE OF CONNECTION, FLOW
! AREA, LOSS COEFFICIENT, L/A RATIO, RELATIVE POSITION OF
! COMPARTMENTS, AND JUNCTION ELEVATION. COMPARTMENT ID OF 0 INDICATES
! THE ICE CONDENSER.  JUNCTIONS WITHIN THE ICE CONDENSER ARE SET UP
! INTERNALLY.  ADDITIONAL INFORMATION IS PROVIDED FOR JUNCTION TYPES
! 3 AND 4.
!
1    2    1    4.952     3.     2.445    1    2.984
1    2    1    1.031     10.    11.74    1    0.6675
2    3    1    27.70     10.    0.545    0    10.60
2    6    1    91.88     1.0    0.164    1    20.42
6    4    1    1.858     3.0    4.921    1    35.052
6    4    3    91.30     1.0    0.100    1    35.052
0.   263.4     37910.    1.55
4    5    1    186.0     1.     0.081    1    40.16
5    2    4    0.204     10.    1.0     -1    7.864
2    750.
5    3    1    0.0022    10.    12690.  -1   10.60
$
```

```
!
! ICE CONDENSER INPUT
!
$ ICE CONDENSER IS REPRESENTED AS COMPARTMENT 6
!
$ NO SUPPRESSION POOL
!
! FAN DATA
! TEMP. AND PRESS. SETPOINTS, DELAY TIME, AND TIME TO TURN OFF. HIGH
! VALUE FOR TEMP. SETPOINT INDICATES THAT VALUE WON'T BE USED.
10000.  121590.0   600.0  1.E10
! COMPARTMENT ID'S, FLOW RATE (- INDICATES USE OF HEAD CURVE),
! SHUTOFF
! HEAD (PA), EFFICIENCY, RELATIVE POSITION OF COMPARTMENTS.
5   3  -35.540  1327.3575  1.  -1
2   3   1.1685  1327.3575  1.   0
5   3   0.9439  1327.3575  1.  -1
$ END OF FANS TABLE
$ END OF FANS INPUT
$ NO FAN COOLERS
!
! RADIATIVE BEAM LENGTHS - UPPER RIGHT HALF OF MATRIX IS INPUT.
! ICE SURFACES ARE NOT INCLUDED HERE. (THEY ARE DONE INTERNALLY)
!
! BEAM LENGTHS
!
   2*4.8480        15*0.0
     4.8480        15*0.0
   6*2.241683      9*0.0
   5*2.241683      9*0.0
   4*2.241683      9*0.0
   3*2.241683      9*0.0
   2*2.241683      9*0.0
   2.241683        9*0.0
   1.882381        1.882381        7*0.0
   1.882381        7*0.0
   4.788000        6*0.0
   9.903546        9.903546        9.903546        9.903546        2*0.0
   9.903546        9.903546        9.903546        2*0.0
   9.903546        9.903546        2*0.0
   9.903546        2*0.0
   2*1.0984
   1.098400
!
! VIEW FACTORS
!
  0.2013          0.7987          15*0.0
  0.7987          15*0.0
```

```
  0.2949272       0.3508651       3.4703106E-02  2.7526543E-02
   0.2615022       3.0475816E-02  9*0.0
  0.3508651       3.4703109E-02  2.7526544E-02  0.2615021
   3.0475818E-02  9*0.0
  3.4703109E-02   2.7526544E-02  0.2615022      3.0475816E-02  9*0.0
  2.7526543E-02   0.2615022      3.0475816E-02  9*0.0
  0.2615022       3.0475819E-02  9*0.0
  3.0475795E-02   9*0.0
  0.3602436       0.6397564      7*0.0
  0.6397564       7*0.0
  1.000000        6*0.0
  0.2603724       0.4340742      0.2955419      1.0011482E-02  2*0.0
  0.4340742       0.2955419      1.0011482E-02  2*0.0
  0.2955419       1.0011483E-02  2*0.0
  1.0011435E-02   2*0.0
  0.1718000       0.8282000
  0.8282000
!
! SPRAY INPUT
! NUMBER OF COMPARTMENTS WITH SPRAYS, AND ID OF THOSE
! COMPARTMENTS. SPRAY TEMP DURING INJECTION PHASE, FLOW RATE
! (M**3/S), NUMBER OF DROP SIZES, FREQUENCY AND DIAMETER
! (MICRONS) FOR EACH DROP SIZE.
1
5   313.56   0.593   2
0.95  309
0.05  810
! SPRAY CARRYOVER
$ NO CARRYOVER
! COMPARTMENT ID AND SPRAY FALL HEIGHT FOR THAT COMPARTMENT.
5   28.61
$
! TEMPERATURE AND PRESSURE SETPOINTS, DELAY TIME FOR SPRAYS,
! TIME THAT SPRAYS REMAIN OPERATIVE AFTER INITIATION.
! HIGH TEMPERATURE INDICATES THAT NUMBER WON'T BE USED.
10000.  120727.2   30.   1.E10
! INJECTION TIME, RATED SPRAY FLOW RATE (KG/S), HEAT EXCHANGER
! RATED EFFECTIVENESS (W/K), SECONDARY SIDE INLET TEMP, RATED
! SECONDARY SIDE FLOW RATE (KG/S), SUMP THAT WATER IS DRAWN FROM.
! (FROM MARCH-HECTR REPORT) 2000.   587.   3.74E6   301.5   7.55E2
$ NO SPRAY RECIRCULATION (S2HF ACCIDENT SCENERIO)
$
! ************************************************************
! ENTER INITIAL CONDITIONS AND ACCIDENT SCENARIO INFORMATION
! ************************************************************
! SIMULATION TIME
50000.
!
```

```
! COMPARTMENT INITIAL CONDITIONS: TEMP; PARTIAL PRESSURES OF
! STEAM, NITROGEN, OXYGEN, HYDROGEN, CARBON MONOXIDE,
! CARBON DIOXIDE ; CONVECTIVE VELOCITY.
!
! C1 - CAVITY
482.33  38479.  101756.  22710.  6582.  0.  711.  0.3
! C2 - LOWER COMP
367.02  37990.  101968.  22757.  6590.  0.  712.  0.3
! C3 - ANNULUS
355.19  37768.  101960.  22754.  6589.  0.  712.  0.3
! C4 - UPPER PLENUM
367.91  38151.  101878.  22735.  6584.  0.  711.  0.3
! C5 - UPPER COMPARTMENT
358.57  38783.  101363.  22622.  6550.  0.  707.  0.3
! ICE COMPARTMENT
367.66  38105.  101912.  22744.  6586.  0.  712.  0.3
!
! SOURCE TERMS
!
$ STEAM SOURCE FROM EXTERNAL TABLE
$ NO NITROGEN SOURCES
$ NO OXYGEN SOURCES
$ HYDROGEN SOURCE FROM EXTERNAL TABLE
$ CO SOURCE FROM EXTERNAL TABLE
$ CO2 SOURCE FROM EXTERNAL TABLE
$ NO SUMP WATER REMOVAL
$ NO ENERGY SOURCES
!
! CONTINUOUS BURNING
!
1
1.0E-2  1.0E4  0.005  1.00  2000.0  1.0
$ END OF CONTINUOUS BURNING INPUT
!
! INITIAL SURFACE TEMPERATURES
!
! C1  RC
347.91
570.17
! C2  LC
354.73
347.42
339.04
354.73
354.73
328.52
! C3  AN
345.00
342.92
```

```
! C4  UP
354.73
! C5  UC
347.44
320.78
349.16
315.53
! C6  IC
2*357.00
!
! NAMELIST INPUT
!
SPRAYS = OFF
FANS = ON
TIMZER=15043.62
PCHMAX=1000.
DTMPMX=50.
DPRSMX=30000.
$
```

(3) HECTR/MAAP 6-Compartment Model

```
!$$$$$$$$$$$$$$$$$$$$$$$$$$$$$$$$$$$$$$$$$$$$$$$$$$$$$$$$$$$$$$$$$$$$$$$$
!       ICE CONDENSER INPUT DECK
!$$$$$$$$$$$$$$$$$$$$$$$$$$$$$$$$$$$$$$$$$$$$$$$$$$$$$$$$$$$$$$$$$$$$$$$$
ICE CONDENSER CONTAINMENT$

THIS IS THE INPUT DECK FOR ICE CONDENSER STANDARD PROBLEM.
DATA ARE REDUCED FROM THE MAAP 6 COMPARTMENT MODEL.
6 VOLUMES, 1-D ICE BED ARE TREATED IN THIS CASE.
LOWER BOUND FAILURE PRESSURE (65 PSIG / 448200 Pa)
PART II: EX-VESSEL H2 PRODUCTION


6  ! NUMBER OF COMPARTMENTS EXCLUDING ICE REGION
!
! FOR EACH COMPARTMENT: THE VOLUME, ELEVATION, FLAME PROPAGATION
! LENGTH, NUMBER OF SURFACES, AND INTEGERS SPECIFYING WHICH SUMP
! TO DUMP EXCESS WATER (FROM SUPERSATURATION) INTO AND WHICH SUMP
! THE SPRAYS FALL INTO.
!
! WHERE SIMILAR NUMBERED COMPARTMENTS OCCUR ,E.G. C2 - C5,
! THEY ARE SPECIFIED BY COUNTING CLOCKWISE FROM THE REFUELING
! CANAL.
!
```

```
C1 - REACTOR CAVITY
405.98      0.      7.04     2      1      1
C2 - LOWER COMPARTMENT
7004.56     20.16   6.86     5      2      2
C3 - ANNULUS
2658.74     12.88   3.20     2      3      3
C4 - UPPER PLENUM
1330.89     37.58   1.37     0      2      2
C5 - UPPER COMPARTMENT
17173.45    35.22   16.12    4      4      4
C6 - ICE REGION (NO ICE, ONLY WALL + BASKET)
3654.5      27.69   14.53    2      2      2
! FOR EACH SUMP, SUMP NUMBER, MAXIMUM VOLUME, SUMP NUMBER THAT
! THIS SUMP OVERFLOWS TO
!
1 419.09  2  ! SUMP IN REACTOR CAVITY
2 1509.13 3  ! LOWER COMPARTMENT SUMP
3 1797.52 2  ! ANNULUS SUMP (13.2 FT. DEPTH)
4 1300.0  0  ! REFUELING CANAL SUMP
$
!
! FOR EACH SURFACE: TYPE OF SURFACE, MASS OF SURFACE, AREA OF
! SURFACE, CHARACTERISTIC LENGTH, SPECIFIC HEAT, EMISSIVITY,
! INTEGER INDICATING WHICH SUMP THE CONDENSATE GOES INTO.  FOR
! SLABS (STYPE = 1), THE NUMBER OF LAYERS IN THE SURFACE, AND FOR
! EACH, THE THICKNESS, THERMAL DIFFUSIVITY, AND THERMAL
! CONDUCTIVITY.  FINALLY, THE NODING INFORMATION AND BOUNDARY
! CONDITIONS ARE SPECIFIED (0'S INDICATE THE CODE WILL DETERMINE
! THE VALUES INTERNALLY). NOTE THAT SOME OF THE NUMBERS SET TO 1.
! ARE NOT USED FOR THAT SURFACE TYPE.
!
! REACTOR CAVITY - C1 - SURFACE 1 - 2
!
SUMP 1
3  1.311E4   60.29    5.18  1.0     0.94   1
RC CONCRETE
1  1.   234.86   5.18  854.15  0.9    1
1
1.524   7.18E-7  1.453
0  0.   0.       0.
!
! LOWER COMPARTMENT- C2 - SURFACES 3 - 8
!
LC STEEL
2   1.60E6   2780.12    2.   460.5   0.9    2
!
LC OUTER WALL - CONCRETE
1  1.   962.20   4.    854.15  0.9    2
1
0.9144  7.18E-7  1.453
0  0.   0.0      0.0
```

```
!
LC INTERIOR WALL - CONCRETE
1  1.    330.90    4.     854.15  0.9     2
1
1.8166  7.18E-7  1.453
0  0.    0.0       0.0
!
LC FLOOR - CONCRETE
1  1.    502.66    4.     854.15  0.9     2
1
3.6576  7.18E-7  1.453
0  0.    0.0       0.0
LC SUMP
3  1.179E6    502.66    4.     1.       0.94    2
!
! ANNULUS AROUND LOWER COMPARTMENT - C3 - SURFACES 8 - 9
!
A LINER CONCRETE
1  1.    1027.14   4.     854.15  0.9     3
2
0.0296  1.28E-5  47.25
0.9144  7.18E-7  1.453
0  0.    3.5033    310.78
!
A SUMP
3  3.037E3    446.77    4.     1.       0.94    3
!
! UPPER COMPARTMENTS - C5 - SURFACES 10 - 13
!
UC OUTER WALL - LINER CONCRETE
1  1.    1929.97   5.     854.15  0.9     4
2
0.0124  1.28E-5  47.25
0.9144  7.18E-7  1.453
0  0.    3.5033    310.78
!
UC DECK - CONCRETE
1  1.    1830.19   5.     854.15  0.9     4
1
0.7620  7.18E-7  1.453
0  0.    0.0       0.0
!B
UC EQUIPMENT - STEEL
2  1.052E5    1064.13    5.     460.5     0.9     4
!
UC SUMP
3  1.261E6   51.8863   5.     1.0      0.94    4
!
```

```
! ICE COMPARTMENT - C6 - SURFACES 14 - 15
IC WALL+STRUCTURE
2  2.000E5   2058.00   14.53   485.7   0.9   2
!
IC BASKET
2  1.470E5   9920.00   14.53   460.5   0.9   2
!
$ NO CONTAINMENT LEAKS
!
! FLOW JUNCTION DATA: COMPARTMENT ID'S, TYPE OF CONNECTION, FLOW
! AREA, LOSS COEFFICIENT, L/A RATIO, RELATIVE POSITION OF
! COMPARTMENTS, AND JUNCTION ELEVATION. COMPARTMENT ID OF 0 INDICATES
! THE ICE CONDENSER.  JUNCTIONS WITHIN THE ICE CONDENSER ARE SET UP
! INTERNALLY.  ADDITIONAL INFORMATION IS PROVIDED FOR JUNCTION TYPES
! 3 AND 4.
!
1   2   1   4.952    3.    2.445   1   2.984
1   2   1   1.031    10.   11.74   1   0.6675
2   3   1   27.69    1.0   0.550   0   10.60
2   6   1   101.08   1.0   0.151   1   20.50
6   4   1   0.1011   10.   97.40   1   35.052
6   4   3   186.09   1.0   0.053   1   35.052
0.  263.4   37910.  1.55
4   5   1   186.09   1.    0.095   1   40.12
5   2   4   0.223    10.   185.9   -1  7.864
2   750.
5   3   1   0.0022   10.   2277.   -1  10.60
$
!
! ICE CONDENSER INPUT
!
$ ICE CONDENSER IS INPUT AS A SEPARATE COMPARTMENT
!
$ NO SUPPRESSION POOL
!
! FAN DATA
! TEMP. AND PRESS. SETPOINTS, DELAY TIME, AND TIME TO TURN OFF. HIGH
! VALUE FOR TEMP. SETPOINT INDICATES THAT VALUE WON'T BE USED.
10000.  0.0   0.167      1.E10
! COMPARTMENT ID'S, FLOW RATE (- INDICATES USE OF HEAD CURVE),
! SHUTOFF
! HEAD (PA), EFFICIENCY, RELATIVE POSITION OF COMPARTMENTS.
5   3  37.753    1327.3575  1.  -1
$ END OF FANS TABLE
$ END OF FANS INPUT
$ NO FAN COOLERS
!
! RADIATIVE BEAM LENGTHS - UPPER RIGHT HALF OF MATRIX IS INPUT.
! ICE SURFACES ARE NOT INCLUDED HERE. (THEY ARE DONE INTERNALLY)
```

```
!
! BEAM LENGTHS
!
   5.111720        5.111720        13*0.0
   5.111720        13*0.0
   5.801047        5.801047        5.801047        5.801047        5.801047
   8*0.0
   5.801047        5.801047        5.801047        5.801047        8*0.0
   5.801047        5.801047        5.801047        8*0.0
   5.801047        5.801047        8*0.0
   5.801047        8*0.0
   6.501352        6.501352        6*0.0
   6.501352        6*0.0
   13.60971        13.60971        13.60971        13.60971        2*0.0
   13.60971        13.60971        13.60971        2*0.0
   13.60971        13.60971        2*0.0
   13.60971        2*0.0
   0.940400        0.940400
   0.940400
!
! VIEW FACTORS
!
  0.2042690       0.7957310       13*0.0
  0.7957310       13*0.0
  0.5474251       0.1894639       6.5156519E-02   9.8977268E-02
   9.8977268E-02  8*0.0
  0.1894639       6.5156512E-02   9.8977260E-02   9.8977260E-02   8*0.0
  6.5156542E-02   9.8977298E-02   9.8977298E-02   8*0.0
  9.8977245E-02   9.8977245E-02   8*0.0
  9.8977245E-02   8*0.0
  0.6968811       0.3031189       6*0.0
  0.3031189       6*0.0
  0.3957958       0.3753330       0.2182304       1.0640776E-02   2*0.0
  0.3753330       0.2182304       1.0640777E-02   2*0.0
  0.2182304       1.0640775E-02   2*0.0
  1.0640800E-02   2*0.0
  0.1718000       0.8282000
  0.8282000
!
! SPRAY INPUT
! NUMBER OF COMPARTMENTS WITH SPRAYS, AND ID OF THOSE
! COMPARTMENTS. SPRAY TEMP DURING INJECTION PHASE, FLOW RATE
! (M**3/S), NUMBER OF DROP SIZES, FREQUENCY AND DIAMETER
! (MICRONS) FOR EACH DROP SIZE.
1
5   313.56   0.593   1
1.00  700
! SPRAY CARRYOVER
$ NO CARRYOVER
```

```
! COMPARTMENT ID AND SPRAY FALL HEIGHT FOR THAT COMPARTMENT.
5   28.61
$
! TEMPERATURE AND PRESSURE SETPOINTS, DELAY TIME FOR SPRAYS,
! TIME THAT SPRAYS REMAIN OPERATIVE AFTER INITIATION.
! HIGH TEMPERATURE INDICATES THAT NUMBER WON'T BE USED.
10000.  120727.2   0.01611   1.E10
! INJECTION TIME, RATED SPRAY FLOW RATE (KG/S), HEAT EXCHANGER
! RATED EFFECTIVENESS (W/K), SECONDARY SIDE INLET TEMP, RATED
! SECONDARY SIDE FLOW RATE (KG/S), SUMP THAT WATER IS DRAWN FROM.
! (FROM MARCH-HECTR REPORT) 2000.   587.   3.74E6   301.5   7.55E2   2
$ NO SPRAY RECIRCULATION (S2HF ACCIDENT SCENERIO)
$
! ***********************************************************
! ENTER INITIAL CONDITIONS AND ACCIDENT SCENARIO INFORMATION
! ***********************************************************
! SIMULATION TIME (END TIME = 20 HRS. OR 72000 SEC)
50000.
!
! COMPARTMENT INITIAL CONDITIONS: TEMP; PARTIAL PRESSURES OF
! STEAM, NITROGEN, OXYGEN, HYDROGEN, CARBON MONOXIDE,
! CARBON DIOXIDE ; CONVECTIVE VELOCITY.
!
! C1 - CAVITY
482.33  38479.  101756.  22710.  6582.  0.  711.  0.3
! C2 - LOWER COMP
367.02  37990.  101968.  22757.  6590.  0.  712.  0.3
! C3 - ANNULUS
355.19  37768.  101960.  22754.  6589.  0.  712.  0.3
! C4 - UPPER PLENUM
367.91  38151.  101878.  22735.  6584.  0.  711.  0.3
! C5 - UPPER COMPARTMENT
358.57  38783.  101363.  22622.  6550.  0.  707.  0.3
! C6 - ICE COMPARTMENT
367.66  38105.  101912.  22744.  6586.  0.  712.  0.3
!
! SOURCE TERM
!
$ STEAM SOURCE FROM EXTERNAL TABLE
$ NO NITROGEN SOURCES
$ NO OXYGEN SOURCES
$ HYDROGEN SOURCE FROM EXTERNAL TABLE
$ CO SOURCE FROM EXTERNAL TABLE
$ CO2 SOURCE FROM EXTERNAL TABLE
$ NO SUMP WATER REMOVAL
$ NO ENERGY SOURCES
!
! CONTINUOUS BURNING
!
```

```
1
1.0E-2  1.0E4  0.005  1.00  2000.0  1.0
$ END OF CONTINUOUS BURNING INPUT
!
! INITIAL SURFACE TEMPERATURES
!
! C1  RC
347.91
570.17
! C2  LC
354.73
347.42
347.69
338.16
339.04
! C3  AN
342.92
356.23
! C5  UC
347.44
320.78
349.16
315.53
! C6 IC
2*357.00
!
! NAMELIST INPUT
!
SPRAYS = OFF
FANS = ON
TIMZER=15043.62
PCHMAX=1000.
DTMPMX=50.
DPRSMX=30000.
$
```

DISTRIBUTION:

E. S. Beckjord, NRC/RES
V. Benaroya, NRC/NRR
B. Burson, NRC/RES
W. R. Butler, NRC/NRR
F. Costanzi, NRC/RES
W. S. Farmer, NRC/RES
M. Fleischman, NRC/RES
C. N. Kelber, NRC/RES
G. W. Knighton, NRC/NRR
J. T. Larkins, NRC/NRR
T. Lee, NRC/RES
R. Meyer, NRC/RES
J. Mitchell, NRC/RES
C. W. Nilsen, NRC/RES
A. NotaFrancesco, NRC/NRR
R. Palla, NRC/NRR
K. I. Parczewski, NRC/NRR
Z. Rosctoczy, NRC/NRR
D. F. Ross, NRC/RES
B. W. Sheron, NRC/RES
T. P. Speis, NRC/RES
T. M. Su, NRC/NRR
J. Telford, NRC/RES
C. G. Tinkler, NRC/NRR
P. Worthington, NRC/RES
R. W. Wright, NRC/RES
D. D. Yue, NRC/NRR
N. Zuber, NRC/RES

U.S. Department of Energy
R. W. Barber
Office of Nuclear Safety Coordination
Washington, DC 20545

U. S. Department of Energy (2)
Albuquerque Operations Office
Attn: J. R. Roeder, Director
Transportation Safeguards
J. A. Morley, Director
Energy Research Technology
For: R. N. Holton
C. B. Quinn
P.O. Box 5400
Albuquerque, NM 87185

Acurex Corporation
485 Clyde Avenue
Mountain View, CA 94042

American Electric Power Service Corp.
Room 1158-D
Attn: K. Vehstedt
2 Broadway
New York, NY 10004

Applied Sciences Association, Inc.
Attn: D. Swanson
P. O. Box 2687
Palos Verdes Pen., CA 90274

Argonne National Laboratory (5)
Attn: R. Anderson
D. Armstrong
L. Baker, Jr.
Dae Cho
B. Spencer
9700 South Cass Avenue
Argonne, IL 60439

Prof. S. G. Bankoff
Northwestern University
Chemical Engineering Department
Evanston, IL 60201

Battelle Columbus Laboratory (2)
Attn: P. Cybulskis
R. Denning
505 King Avenue
Columbus, OH 43201

Battelle Pacific Northwest Laboratory (2)
Attn: M. Freshley
G. R. Bloom
P.O. Box 999
Richland, WA 99352

Bechtel Power Corporation (2)
Attn: D. Ashton
D. Patton
15740 Shady Grove Road
Gaithersburg, MD 20877

Dr. Brinka, Director
Test Operations
D 9500/B 33008
P.O. Box 13222
Sacramento, CA 95813

Brookhaven National Laboratory (4)
Attn: R. A. Bari
T. Ginsburg
G. Greene
T. Pratt
Upton, NY 11973

Cleveland Electric Illuminating Co.
Perry Nuclear Plant
Attn: R. Stratman
10 Center Road
North Perry, OH 44081

Combustion Engineering Incorporated
Attn: J. D. Boyajian
1000 Prospect Hill Road
Windsor, CT 06095

Lynn Connor
Document Search NRC
P.O. Box 7
Cabin John, MD 20818

Dr. Michael Cook
Morton Thiokol
Ventron Group
150 Andover Street
Danvers, MA 01923

Donald C. Cook Nuclear Station
Indiana & Michigan Electric Company
Attn: D. Nelson
P.O. Box 458
Bridgman, MI 49106

Prof. M. L. Corradini
University of Wisconsin
Nuclear Engineering Department
1500 Johnson Drive
Madison, WI 53706

Duke Power Company (2)
Attn: F. G. Hudson
A. L. Sudduth
P.O. Box 3189
Charlotte, NC 28242

A. Pete Dzmura
NE 43
U.S. DOE
Washington, DC 20545

EG&G Idaho (3)
Willow Creek Building, W-3
Attn: D. Croucher
R. Hobbins
Server Sadik
P.O. Box 1625
Idaho Falls, ID 83415

Electric Power Research Institute (5)
Attn: J. Haugh
W. Loewenstein
B. R. Sehgal
G. Thomas
R. Vogel
3412 Hillview Avenue
Palo Alto, CA 94303

Factory Mutual Research Corporation
Attn: R. Zalosh
P.O. Box 688
Norwood, MA 02062

Fauske & Associates (2)
Attn: R. Henry
M. Plys
16W070 West 83rd Street
Burr Ridge, IL 60521

GPU Nuclear
Attn: J. E. Flaherty
100 Interpace Parkway
Parsippany, NJ 07054

General Electric Corporation
Attn: K. W. Holtzclaw
175 Curtner Avenue
Mail Code N 1C157
San Jose, CA 95125

General Electric Corporation
Advanced Reactor Systems Dept.
Attn: M. I. Temme, Manager
Probabilistic Risk Assessment
P.O. Box 3508
Sunnyvale, CA 94088

General Physics Corporation
Attn: C. Kupiec
1000 Century Plaza
Columbia, MD 21044

General Public Utilities
Three Mile Island Nuclear Station
Attn: N. Brown
P.O. Box 480
Middletown, PA 17057

Dr. Dennis Hacking
Enercon Services
520 West Broadway
P.O. Box 2050
Broken Arrow, OK 74013

Jim O. Henrie
Westinghouse Hanford Division
P.O. Box 1970
Richland, Washington 99352

Indiana and Michigan Electric Company
Attn: J. Dickson
P.O. Box 458
Bridgman, MI 49106

Institute of Nuclear Power Operation (3)
Attn: Henry Piper
S. Visner
E. Zebroski
1100 Circle 795 Parkway, Suite 1500
Atlanta, GA 30339

International Technology Corporation
Attn: Mario H. Fontana
575 Oak Ridge Turnpike
Oak Ridge, TN 37830

Lt. Kevin Klonoski
6595 Shuttle Test Group
Vandenberg Air Force Base
Vandenberg AFB, CA 93437

Knolls Atomic Power Lab (2)
Attn: Albert J. Kausch
R. L. Matthews
General Electric Company
Box 1072
Schnectady, NY 12301

Professor C. K. Law
University of California
Department of Mechanical Engineering
Davis, CA 95616

Robert Lipp
Westinghouse Hanford
838 West Octave
Pasco, WA 99301

Los Alamos National Laboratory (8)
Attn: W. R. Bohl
F. J. Edeskuty
R. Gido
J. Carson Mark
G. Schott
H. Sullivan
J. Travis
K. D. Willaimson, Jr.
P.O. Box 1663
Los Alamos, NM 87545

Massachusetts Institute of Technology
Attn: N. C. Rasmussen
Nuclear Engineering Department
Cambridge,, MA 02139

University of Michigan
Attn: Prof. M. Sichel
Department of Aerospace Engineering
Ann Arbor, MI 47109

University of Michigan
Nuclear Engineering Department
Ann Arbor, MI 48104

Miller & White P.C.
Attn: John White, Patent Attorney
Anthony J. Zelano, Patent Attorney
503 Crystal Mall, Building 1
1911 Jefferson Davis Highway
Arlington, VA 22202

Mississippi Power & Light
Attn: S. H. Hobbs
P. O. Box 1640
Jackson, MS 39205

NUS Corporation
Attn: R. Sherry
4 Research Place
Rockville, MD 20850

Oak Ridge National Laboratory (2)
Attn: A. P. Malinauskas
T. Kress
NRC Programs
P.O. Box X, Bldg. 4500S
Oak Ridge, TN 37831

Pennsylvania Power & Light
Attn: R. DeVore
Susquehanna SES
P. O. Box 467
Berwick, PA 18603

Power Authority State of NY (2)
Attn: R. E. Deem
S. S. Iyer
10 Columbus Circle
New York, NY 10019

Dr. J. E. Shepherd
Rensselaer Polytechnic Institute
Troy, NY 12180-3590

Andrew F. Rutkiewic
E. F. DuPont
Marshall Laboratory
P.O. Box 3886
Philadelphia, PA 19146

Pam Bennett, Div. 6517 (15)
Sandia National Laboratories
P.O. Box 5800
Albuquerque, NM 87185

Bill Seddon
Atomic Energy of Canada
Research Company
Chalk River Nuclear Laboratories
CANADA K0J 1J0

Dpak Shah, Sr. Dev. Eng.
Honeywell, Inc.
MN63-B170
Corporation Systems Dev. Division
1000 Boone Avenue North
Golden Valley, MN 55427

Stone & Webster Engineering Corp. (2)
Attn: G. Brown
E. A. Warman
245 Summer Street/9
Boston, MA 02143

Stratton & Associates, Inc.
Attn: W. Stratton
2 Acoma Lane
Los Alamos, NM 87544

Dr. Roger Strehlow
505 South Pine Street
Champaign, IL 61820

Steve Sweargin
Omaha Public Power District
Jones Street Station
O.H.P.D.
1623 Harney Street
Omaha, NE 68102

Technology for Energy Corporation (2)
Attn: J. Carter
E. L. Fuller
10770 Dutchtown Road
Knoxville, TN 37922

Texas A & M University
Nuclear Engineering Dept.
College Station, TX 77843

Prof. T. G. Theofanous
Chemical and Nuclear Engineering Dept.
University of California
Santa Barbara, CA 93106

Thompson Associates (2)
Attn: Timothy Woolf
639 Massachusetts Avenue
Third Floor
Cambridge, MA 02139

TVA
Attn: Wang Lau
400 Commerce
W9C157-CD
Knoxville, TN 37902

UCLA
Nuclear Energy Laboratory (2)
Attn: Prof. I. Catton
Prof. D. Okrent
405 Hilgard Avenue
Los Angeles, CA 90024

Virginia Electric & Power Company (3)
Attn: A. Hogg
E. L. Vilson
A. K. White
Northanna Power Station
P.O. Box 402
Mineral, VA 23117

Virginia Electric & Power Company
Attn: R. Garner
P.O. Box 26666
James River Plaza
Richmond, VA 23261

Danialle Weaver
Nucleonics Week
1120 Vermont Avenue N.W.
Suite 1200
Washington, DC 20005

Bill West
Bettis Atomic Power Laboratory
P.O. Box 79
West Mifflin, PA 15122

Westinghouse Corporation (3)
Attn: N. Liparulo
J. Olhoeft
V. Srinivas
P.O. Box 355
Pittsburgh, PA 15230

Westinghouse Electric Corporation (2)
Bettis Atomic Power Laboratory
Attn: Donald R. Connors
Charles Quinn
P.O. Box 79
West Mifflin, PA 15122

Westinghouse Electric Corporation
Attn: P. Lain
Monroeville Nuclear Center
Monroeville, PA 15146

Westinghouse Hanford Company (3)
Attn: G. R. Bloom
L. Mulstein
R. D. Peak
P.O. Box 1970
Richland, VA 99352

Lt. Sherman Westvig
Building 8500
Vandenberg Air Force Base
Vandenberg AFB, CA 93437

Keith Williams
Tayco Engineering, Inc.
P.O. Box 19
Long Beach, CA 90802

Zion Nuclear Power Station
Commonwealth Edison Company
Attn: C. Schultz
Shiloh Blvd. and Lake Michigan
Zion, IL 60099

Belgonucleaire S.A.
Attn: H. Bairiot
Rue de Champ de Mars 25
B-1050 Brussels
BELGIUM

Professor Lue Gillon
University of Louvain la Neuve
Batiment Cyclotron
B1348 Louvain La Neuve
BELGIUM

Director of Research, Science & Education
CEC
Attn: B. Tolley
Rue De La Loi 200
1049 Brussels
BELGIUM

Atomic Energy Ltd. (4)
Whiteshell Nuclear Research Establishment
Attn: D. Liu
C. Chan
K. Tennankore
D. Wren
Pinawa, Manitoba
CANADA

Atomic Energy Canada Ltd.
Attn: P. Fehrenbach
Bill Seddon
Chalk River, Ontario
CANADA KOJ 1JO

Defense Research Establishment Suffield
Attn: Dr. Ingar O. Moen
Ralston, Alberta TOJ 2NO
CANADA

McGill University (3)
Attn: Prof. John H. S. Lee
315 Querbes
Outremont, Quebec H2V 3W1
CANADA

Professor Karl T. Chuang
University of Alberta
Edmonton, Alberta, T6G 2E1
CANADA

CEA
Attn: M. Georges Berthoud
B.P. No. 85X-Centre de
F-38041 Grenoble Cedex
FRANCE

Battelle Institut E. V. (4)
Attn: Dr. Werner Baukal
Werner Geiger
Dr. Guenter Langer
Dr. Manfred Schildknecht
Am Roemerhof 35
6000 Frankfurt am Main 90
FEDERAL REPUBLIC OF GERMANY

Gesellschaft für Reaktorsicherheit (GRS)
Postfach 101650
Glockengasse 2
5000 Koeln 1
FEDERAL REPUBLIC OF GERMANY

Gesellschaft für Reaktorsicherheit (2)
Attn: Dr. E. F. Hicken
Dr. H. L. Jahn
8046 Garching
Forschungsgelande
FEDERAL REPUBLIC OF GERMANY

Universität Heidelberg
Attn: Juergen Warnatz
Heidelberg
FEDERAL REPUBLIC OF GERMANY

Institute für Kernenergetik und
Energiesysteme (2)
Attn: M. Buerger
G. Froehlich
H. Unger
University of Stuttgart
Stuttgart
FEDERAL REPUBLIC OF GERMANY

Kernforschungszentrum Karlsruhe (4)
Attn: Dr. S. Hagen
Dr. Heusener
Dr. Kessler
Dr. M. Reimann
Postfach 3640
7500 Karlsruhe
FEDERAL REPUBLIC OF GERMANY

Kraftwerk Union (2)
Attn: Dr. M. Peehs
Dr. K. Hassman
Hammerbacherstrasse 12 & 14
Postfach 3220
D-8520 Erlangen 2
FEDERAL REPUBLIC OF GERMANY

Lehrgebiet für Mechanik der
RWTH Aachen
Attn: Prof. Dr. Ing. N. Peters
Templergraben 55
D5100 Aachen
FEDERAL REPUBLIC OF GERMANY

Technische Universität München
Attn: Dr. H. Karwat
8046 Garching
FEDERAL REPUBLIC OF GERMANY

Propulsion and Combustion
Dept. of Aeronautical Engineering
Attn: Alon Gany, D.Sc.
Technion, Haifa 32000
ISRAEL

CNEN NUCLIT
Attn: A. Morici
Rome
ITALY

ENEA Nuclear Energ Alt Disp (2)
Attn: P. L. Ficara
G. Petrangeli
Via V. Brancati
00144 Roma
ITALY

ISPRA
Commission of the European Communities
Attn: Dr. Heinz Kottowski
C.P. No. 1, I-21020 Ispra (Varese)
ITALY

Universita Degli Studi Di Pisa
Dipartmento Di Costruzioni
Attn: M. Carcassi
Meccahniche E. Nucleari
Facolta Di Ingegneria
Via Diotisalvi 2
56100 Pisa
ITALY

Japan Atomic Energy Research Institute
Attn: Dr. K. Soda, Manager
Chemical Engineering Safety Laboratory
Dept. of Nuclear Fuel Safety
Tokai-mura, Naku-gun Ibaraki-ken
319-11
JAPAN

Japan Atomic Energy Research Institute
Attn: Dr. T. Fujishiro, Manager
Dept. of Fuel Safety Research
Tokai-mura, Naka-gun, Ibaraki-ken
319-11
JAPAN

Japan Atomic Energy Research Institute
Attn: Mr. Kazuo Sato, Director
Dept. of Reactor Safety Research
Tokai-mura, Naka-gun Ibaraki-ken
319-11
JAPAN

Power Reactor Nuclear Fuel
Development Corp. (PNC)
Attn: Dr. Watanabe
FBR Project
9-13, 1-Chome, Akasaka
Minato-ku, Tokyo
JAPAN

Korea Advanced Energy Research
Institute
Attn: H. R. Jun
P.O. Box 7
Daeduk Danji, Chungnam
KOREA

Netherlands Energy Research Foundation
Attn: K. J. Brinkmann
P.O. Box 1
1755ZG Petten NH
NETHERLANDS

Royal Institute of Technology
Attn: Prof. Kurt M. Becker
Dept. of Nuclear Reactor Engineering
Stockholm S-10044
SWEDEN

Statens Karnkraftinspektion
Attn: Wiktor Frid
P.O. Box 27106
S-10252 Stockholm
SWEDEN

Studsvik Energiteknik AB
Attn: K. Johansson
S-611 82 Nykoping
SWEDEN

Swedish State Power Board
S-162 Fach 87 Vallingby
SWEDEN

Swedish State Power Board
Attn: Eric Ahlstroem
181-OCH Vaermeteknik
SWEDEN

D. Ulrich
SULZER Bros. Ltd.
TMV-0460
CH-8401 WINTERTHUR
SWITZERLAND

AERE Harwell
Attn: J. R. Matthews, TPD
Didcot
Oxfordshire OX11 ORA
UNITED KINGDOM

Berkeley Nuclear Laboratory (3)
Attn: J. E. Antill
S. J. Board
N. Buttery
Berkeley GL 139PB
Gloucestershire
UNITED KINGDOM

British Nuclear Fuels, Ltd.
Attn: W. G Cunliffe
Building 396
Springfield Works
Salwick, Preston
Lancs
UNITED KINGDOM

Imperial College of Science and Technology
Attn: Dr. A. D. Gosman
Dept. of Mechanical Engineering
Exhibition Road
London SW7 2BX
UNITED KINGDOM

National Nuclear Corp. Ltd.
Attn: R. May
Cambridge Road
Whetestone, Leicester, LE8 3LH
UNITED KINGDOM

Simon Engineering Laboratory (2)
University of Manchester
Attn: Prof. W. B. Hall
S. Garnett
M139PL
UNITED KINGDOM

Anthony R. Taig
GDCD/CEGB
Barnwood, Gloucester
Gloucestershire
UNITED KINGDOM

UKAEA Safety & Reliability Directorate (5)
Attn: J. G. Collier
J. H. Gittus
S. F. Hall
M. R. Hayns
C. Wheatley
Wigshaw lane, Culcheth
Warrington WA3 4NE
Cheshire
UNITED KINGDOM

UKAEA, Culham Laboratory (4)
Attn: F. Briscoe
Ian Cook
D. Fletcher
B. D. Turland
Abingdon
Oxfordshire OX14 3DB
UNITED KINGDOM

UKAEA AEE Winfrith (4)
Attn: M. Bird
T. Butland
R. Potter
A. Wickett
Dorchester
Dorset DT2 8DH
UNITED KINGDOM

University of Aston in Birmingham (2)
Dept. of Chem.
Attn: A. T. Chamberlain
F. M. Page
Gosta Green, Birmingham B47ET
UNITED KINGDOM

Sandia Distribution:
1510 J. W. Nunziato
1512 J. C. Cummings
1530 L. W. Davison
1555 C. C. Wong (3)
3141 S. A. Landenberger (5)
3151 W. I. Klein
4030 J. D. Corey
4050 K. Olsen
6400 D. J. McCloskey
6410 D. A. Dahlgren
6412 A. L. Camp
6418 J. E. Kelly
6418 S. E. Dingman
6510 J. V. Walker
6422 D. A. Powers
6425 S. S. Dosanjh
6429 K. D. Bergeron
6500 A. W. Snyder
6517 M. Berman (5)
6517 D. F. Beck
6517 J. E. Dec
6517 L. S. Nelson
6517 M. P. Sherman
6517 S. E. Slezak
6517 D. W. Stamps (7)
6517 S. R. Tieszen
8524 J. A. Wackerly